Stress-induced accumulation of heme oxygenase-1 in *Xenopus laevis* A6 kidney epithelial cells

by

Ena Music

A thesis
presented to the University of Waterloo
in fulfillment of the
thesis requirement for the degree of
Master of Science
in
Biology

Waterloo, Ontario, Canada, 2014

Author's Declaration

I hereby declare that I am the sole author of this thesis. This is a true copy of the thesis, including any required final revisions, as accepted by my examiners. I understand that my thesis may be made electronically available to the public.

Abstract

Previous studies have examined stress-induced heme oxygenase-1 (HO-1) expression primarily in mammalian systems. The present study examines, for the first time in amphibians, the effect of heat shock, sodium arsenite, cadmium chloride, and the proteasomal inhibitor MG132 on HO-1 accumulation in *Xenopus laevis* A6 kidney epithelial cells. Western blot analysis revealed that exposure of A6 cells to a range of heat shock temperatures (30-35 °C), which induced HSP30 accumulation, did not induce HO-1 accumulation. In contrast, cells treated with sodium arsenite (5-50 μM), cadmium chloride (50-200 μM) or MG132 (5-30 μM) exhibited a dose- and time-dependent accumulation of HO-1. Additionally, immunocytochemical analysis revealed that HO-1 and HSP30 accumulation occurred in a granular pattern primarily in the cytoplasm in cells treated with sodium arsenite, cadmium chloride, or MG132. In cells recovering from sodium arsenite or cadmium chloride treatment, HO-1 and HSP30 accumulation initially increased to a maximum at 12 h and 24 h recovery, respectively, followed by a 50% reduction at 48 h. This initial increase in the relative levels of stress proteins was likely the result of new synthesis as it was inhibited by cycloheximide. In comparison, cells recovering from MG132 treatment displayed reduced but prolonged accumulation of HO-1 and HSP30. Interestingly, cells treated with low concentrations (10 μM) of sodium arsenite or MG132 but not cadmium chloride in combination with a mild 30 °C heat shock had enhanced accumulation of HO-1 and HSP30 accumulation compared to either of the stressors individually. This study has shown for the first time in amphibians that HO-1 accumulation is induced in response to metals and proteasomal inhibitors, suggesting that it may play a role in mediating the cellular stress response in *X. laevis*.

Acknowledgements

This thesis is the final result of two years of research, reading, and a lot of writing, none of which would have been possible without my supervisor Dr. John Heikkila. Thank you for your guidance, patience, for sharing your knowledge with me and, above all, thank you for this great opportunity. I would also like to thank my committee members, Dr. Moira Glerum and Dr. Mungo Marsden, for reading my thesis with a critical eye and giving valuable feedback. Thank you to my fellow lab members, Imran and Saad, for being my mentors, and my cheer squad on days when experiments weren't going so well. On the non-academic side, I would like to thank my friends and family, who have kindly put up with all my talk of heat shock proteins and frog cells (to the point where "How are you?" started to get followed up with "And how are the cells doing?"). Thank you for your support, advice, and kind words. I could not have done this without all of you.

Table of Contents

List of Figures

List of Tables

List of abbreviations

ANOVA	analysis of variance
AP-1	activator protein
APS	ammonium persulfate
As	sodium arsenite
ATP	adenosine triphosphate
Bach1	bric-a-brac and cap'n'collar homology
BCA	bicinchoninic acid
BCIP	5-bromo-4-chloro-3-indolyl phosphate
BSA	bovine serum albumin
BR	bilirubin
BV	biliverdin
BVR	biliverdin reductase
C	control
Cd	cadmium chloride
CdRE	cadmium response element
cGMP	cyclic guanosine monophosphate
CHX	cycloheximide
CO	carbon monoxide
Cu	copper sulfate
DAPI	4,6-diamidino-2-phenylindole
DMSO	dimethylsulphoxide
E protein	ubiquitin activating enzyme
EDTA	ethylene-diamine-tetraacetic acid
EGTA	ethylene glycol tetraacetic acid
ER	endoplasmic reticulum
Fe	iron sulfate
FBS	fetal bovine serum
HBSS	Hank's balanced salt solution
HeLa	*Homo sapiens* cervix adenocarcinoma
HEPES	4-(2-hydroxyethyl)-1-piperazineethanesulfonic acid
HO	heme oxygenase
HSE	heat shock element
HSF	heat shock factor
HL60	*Homo sapiens* promyeloblast
HSP	heat shock protein
Hsp	heat shock protein gene or mRNA
HSR	heat shock response
Keap1	Kelch-like erythroid-cell derived protein with cap'n'collar homology-associated protein1
L-15	Leibovitz-15
LSCM	laser scanning confocal microscopy

MAPK	mitogen activated protein kinase
MARE	Maf recognition element
MG132	carbobenzoxy-L-leucyl-L-leucyl-L-leucinal
NADPH	nicotinamide adenine dinucleotide phosphate
NBT	4-nitro blue tetrazolium
NF-E2	nuclear factor-erythroid 2
NF-κB	nuclear factor-κB
NO	nitric oxide
Pb	lead nitrate
PBS	phosphate buffered saline
ROS	reactive oxygen species
SDS	sodium dodecyl sulfate
SDS-PAGE	sodium dodecyl sulfate-polyacrylamide gel electrophoresis
sGC	soluble guanylyl cyclase
SHSP	small heat shock protein
STRE/ARE	stress response element / antioxidant response element
TBS-T	Tris buffered saline solution – Tween20
TEMED	tetra-methyl-ethylene-diamine
TNFα	tumour necrosis factor alpha
TRITC	rhodamine-tetramethylrhodamine-5-isothiocyanate phalloidin
UPS	ubiquitin proteasome system
Zn	zinc sulfate

1. Introduction

Organisms routinely face stressful stimuli that pose a threat to their survival. The effects that these stressors have on cells at the molecular level can disrupt the structure of protein, resulting in unfolded proteins that form aggregates (Morimoto, 1998). Damaged proteins and protein aggregates are detrimental to cell survival. As proteostasis is essential to proper cellular functioning, two protective mechanisms have evolved: the heat shock response and the ubiquitin-proteasome protein degradation pathway. Furthermore, stressful stimuli may result in the formation of reactive oxygen species (ROS), resulting in oxidative stress, another cytotoxic condition (Fauconneau et al., 2002). Oxidative stress is combated by an array of antioxidant enzymes, and heme oxygenase-1 (HO-1) is recognized as an antioxidant defence protein (Uppu et al., 2010).

1.1. Heat Shock Proteins (HSPs)

Heat shock proteins (HSPs), also known as stress proteins, are molecular chaperones, some of which are expressed under stress conditions, while others may be constitutively expressed (Morimoto, 1998; 2008; Mymrikov et al., 2011). They are grouped into at least six families based on size including HSP110, HSP90, HSP70, HSP60, HSP40, and the small HSPs (sHSPs; Katschinski, 2004). HSPs are generally highly conserved, and have been found in organisms ranging from bacteria to humans (Kregel, 2002). Under stressful conditions, stress-inducible HSPs prevent the aggregation of unfolded proteins. Additionally, they contribute to protein refolding once the stress is alleviated, and are involved in the degradation of proteins damaged beyond repair (Morimoto, 1998; 2008). In addition to their activities under stress conditions, they also play a role in both development and normal cell

function. HSPs that are constitutively expressed are involved in protein synthesis and folding (Hendrick and Hartl, 1993). Some HSPs prevent aggregation of unfolded proteins by binding to their hydrophobic regions and maintaining their solubility in the cell (Becker and Craig, 1994).

1.2. Small HSPs

There is documentation of the existence of small heat shock proteins (sHSPs) in bacteria, plants, nematodes, insects, crustaceans, amphibians and mammals (Allen et al., 1992; Wotton et al., 1996; Boston et al., 1996; Waters et al., 1996; Linder et al., 1996; Michaud et al., 1997; Liang et al., 1997; Ohan et al., 1998a; MacRae, 2000; Sun and MacRae, 2005; Heikkila, 2010). SHSPs bind improperly folded proteins and transfer them to ATP-dependent chaperones such as HSP70, for refolding or for degradation by the proteasome (Mymrikov et al., 2011). SHSPs range from 12 to 43 kDa in size and are not highly conserved except for an 80-100 amino acid long α-crystallin domain (MacRae, 2000; Van Montfort et al., 2001; Acunzo et al., 2012; Garrido et al., 2012). This domain, which is made up of 6-8 β-strands, is found in the lens proteins αA-crystallin and αB-crystallin (Katschinski, 2004).

SHSPs can form multimeric complexes up to 1 MDa, which appear to be essential for their chaperone activity (Ohan et al., 1998, Heikkila, 2003; Sun & MacRae, 2005). Research suggests that sHSPs may be involved in actin capping and decapping, apoptosis prevention, modulation of redox parameters, cellular differentiation and the acquisition of thermotolerance (Arrigo et al., 1998; MacRae, 2000; Van Montfort et al., 2001; Heikkila et al., 2004; Garrido et al., 2012). They are induced in cells by a range of stresses including

heavy metals, sodium arsenite, proteasomal inhibitors and heat shock (MacRae, 2000; Gellalchew & Heikkila, 2005; Akerfelt et al., 2007). Once expression is induced, the multimeric sHSP complexes prevent detrimental protein aggregation by binding to unfolded proteins and keeping them in a soluble state (Heikkila, 2004; Garrido et al., 2012). Protein aggregation, which can be lethal to a cell, has been implicated in many diseases including Alzheimer's and Parkinson's, in which protein aggregates are associated with the pathology of the disease (Calabrese et al., 2003; 2008; Garrido et al., 2012). Furthermore, they have also been implicated in other conditions including cataracts and muscular dystrophy (Sun and MacRae, 2005; Mymrikov et al., 2011).

1.3. Heat shock response

The heat shock response (HSR) was discovered in 1962 in *Drosophila* and has been extensively studied in both prokaryotes and eukaryotes (Ritossa, 1962; Parsell and Lindquist, 2003). The HSR leads to the upregulation of HSP accumulation to protect cells from proteotoxic stress (Morimoto, 2008). The HSR is activated when unfolded proteins accumulate in response to heat, heavy metals, oxidants, and other stressors (Akerfelt et al., 2007; Morimoto, 2008).

1.4. Stress-induced regulation of *hsp* gene expression

Stress-induced regulation of *hsp* gene expression is mainly regulated at the transcriptional level, although there is also evidence for regulation of the level of mRNA stability and translation (Kim and Jang, 2002; Heikkila et al., 2007). Constitutive or stress-inducible transcription of *hsp* genes involves the binding of heat shock factor (HSF) to the

heat shock element (HSE) found in their promoters (Voellmy, 2004). Four HSFs have been discovered to date, including HSF1, HSF2, and HSF4 in mammals, and the avian-specific HSF3 (Voellmy, 2004; Yamamoto et al., 2009). HSF2 is activated during animal development, while HSF3 is involved in stress-induced *hsp* gene expression in birds (Rallu et al., 1997; Voellmy, 2004). HSF4 expression has been observed in the human heart, brain, skeletal muscle, and pancreas (Nakai et al., 1996).

HSF1, the HSF family member responsible for activating the HSR in higher organisms, is activated by a variety of stressors including thermal shock, proteasomal inhibitors, and heavy metals (Morimoto, 1998; Voellmy, 2004; Tonkiss and Calderwood, 2005). Under non-stress conditions, HSF1 persists as a cytosolic monomer that is bound to HSP90 (Fig. 1). When a cell is subjected to proteotoxic stress such that there is an increase in unfolded protein, HSP90 is recruited to inhibit their aggregation. This permits HSF1 to form trimers (Voellmy, 2004). The HSF1 trimer is hyperphosphorylated at serine and threonine residues, and subsequently translocated to the nucleus, where it binds to the heat shock element (HSE) in the 5' promoter region of the *hsp* genes to initiate transcription by RNA polymerase II (Voellmy, 2004; Tonkiss and Calderwood, 2005). These stress-inducible HSPs prevent unfolded proteins from forming damaging aggregates, and also assist in refolding once cellular conditions return to normal.

1.5. Heme oxygenase

Heme oxygenase (HO) catalyzes the degradation of pro-oxidant heme to iron, carbon monoxide, and bilirverdin by cleaving the α-methene carbon bridge of heme (Fig. 2; Uppu et al., 2010). Biliverdin is subsequently reduced to bilirubin by biliverdin reductase. There are

Figure 1. Stress-induced activation of the heat shock response (HSR). External stress (indicated by the lightning bolt) can cause native proteins within the cell to unfold. HSP90, which is bound to HSF1 under normal conditions, is recruited to prevent the aggregation of unfolded proteins. The unbound HSF1 monomers trimerize and translocate to the nucleus. The phosphorylated HSF1 trimer binds to the heat shock element within the 5' promoter of *hsp* genes, which initiates transcription by RNA polymerase II. Newly translated stress-induced HSPs bind to unfolded protein to assist in the prevention of protein aggregation.

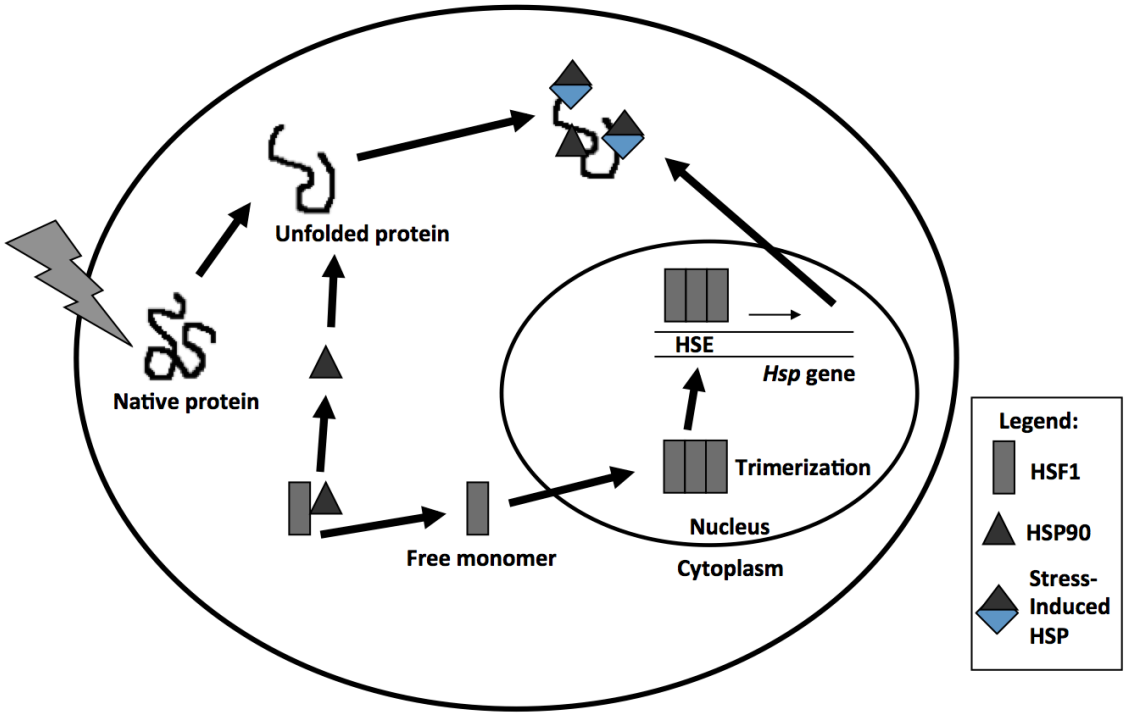
Unfolded protein
Native protein
HSE
Hsp gene
Trimerization
Nucleus
Free monomer
Cytoplasm
Legend:
HSF1
HSP90
Stress-Induced HSP

Figure 2. Enzymatic activity of heme oxygenase. Heme oxygenase catalyzes the breakdown of heme into equimolar amounts of iron, carbon monoxide, and biliverdin. Biliverdin is then converted to bilirubin through the action of biliverdin reductase. Additionally, two molecules of NADPH and three oxygen molecules are required, and two NADP+ and three water molecules are released (adapted from Kirkby and Adin, 2006).

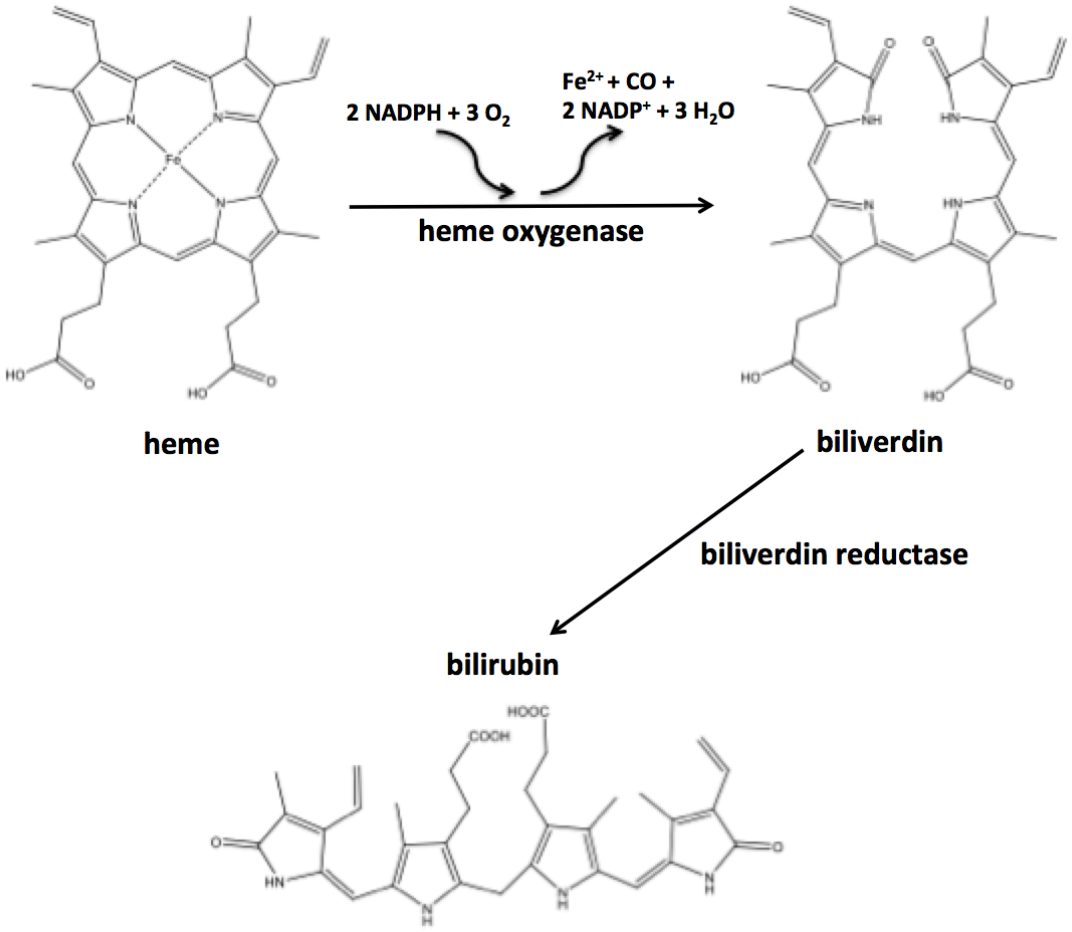
2 NADPH + 3 O2
Fe2+ + CO +
2 NADP+ + 3 H2O
heme oxygenase
heme
biliverdin
biliverdin reductase
bilirubin

three HO isoforms that have been discovered, which are named HO-1, HO-2, and HO-3. The HO-1 and HO-2 proteins that had already been sequenced were found to share an amino acid percent identity of 43% (Maines, 1997). HO-2 and HO-3 are much more similar, sharing 90% of the same amino acids.

HO-1, the focus of this research, is the inducible isozyme (Ryter et al., 1999). It is a 32 kDa protein which is expressed in kidney, liver, and is found in greatest amounts in the spleen as this is where senescent erythrocytes are sequestered and hemoglobin is degraded (Raju et al., 1997). HO-2 is a constitutive 36 kDa protein that is not stress-inducible (Lee et al, 1996). It is generally found in the brain, endothelium, and testes. Unlike HO-1, which is induced by a wide array of stressors, HO-2 was induced only by adrenal glucocorticoids (Maines, 1997). The 33 kDa HO-3 isoform, which is similar to HO-2, has low enzyme activity although its mRNA was detected in many organs (McCoubrey et al., 1997). It is thought to play a role in heme sensing and binding (Immenschuh and Ramadori, 2000). It was detected in the brain, heart, testes, liver, kidney, and spleen (Siow et al., 1999).

1.6. Heme oxygenase-1

1.6.1. *Ho-1* gene regulation

Ho-1 gene expression is controlled mainly at the transcriptional level (Shibahara et al., 1978; Ryter et al., 2006). The *ho-1* gene has a wide variety of inducer-responsive elements such as the stress response element (StRE; also called antioxidant response element [ARE]), cadmium response element (CdRE) and heat shock element (HSE; Choi and Alam, 1996; Lee et al., 1996). These elements are found in the 5' region, where there are two inducible enhancers, E1 and E2, as well as a promoter (Choi and Alam, 1996; Alam et al.,

2000). Several protein families were implicated in *ho-1* gene activation including nuclear factor-κB (NF-κB), nuclear factor-erythroid 2 (NF-E2), activator protein-1 (AP-1) and heat shock factor (HSF; Alam & Cook, 2007). Consensus sequences to which AP-1, NF- κB, and HSF1 bind were identified in the promoter region of *ho-1* genes (Choi and Alam, 1996; Maines, 1997; Hartsfield et al., 1998; Hartsfield et al., 1999).

In mammalian systems, a variety of inducers were shown to induce HO-1 accumulation via Nrf2, including curcumin, MG132, sodium arsenite, and cadmium (Alam et al., 2000; Wu et al., 2004; Yamamoto et al., 2010; Wang et al., 2013). Nrf2, a NF-E2 family member, is a transcription factor that is inactivated when bound to Kelch-like erythroid-cell-derived protein with cap'n'collar homology-associated protein 1 (Keap1). In response to redox-dependent stimuli, Cys273 and Cys288 of Keap1 are modified. This causes the dissociation of Nrf2, which then translocates to the nucleus. Nrf2 forms a heterodimer with Maf protein and they bind to Maf recognition elements (MARE) to induce the expression of antioxidant genes (Fig. 3; Balogun et al., 2003; Li et al., 2008b). Additionally, inactivation of bric-a-brac and cap'n'collar homology (Bach1) protein, a thiol-rich transcriptional repressor, is required for Nrf2 to induce HO-1. Bach1 forms a heterodimer with a small Maf protein and binds to DNA at ARE-like enhancers until it is inactivated by pro-oxidants (Reichard et al., 2007). Additionally, Bach1 can be inactivated through direct binding with heme (Ogawa et al., 2001). Another protein implicated in HO-1 induction is p38 MAPK, which was found to induce Nrf2 translocation (Balogun et al., 2003; Gong et al., 2004). Curcumin was determined to activate the HO-1 gene through regulation of transcription factor Nrf2 and the NF- κB pathway, while MG132 and cadmium act through the p38 MAPK pathway (Alam et

Figure 3. Regulation of HO-1 gene by Nuclear factor-erythroid 2-related factor 2 (Nrf2). Nrf2 is the transcription factor that is responsible for the induction of the HO-1 gene. When there is a lack of external stressors, Nrf2 is bound to Kelch-like erythroid-cell-derived protein with CNC homology (ECH)-associated protein 1 (Keap1), which sequesters it in the cytoplasm. Bach1, a repressor, forms a heterodimer with a Maf transcription factor, and the complex binds to Maf recognition elements (MARE; an antioxidant response element or ARE) to prevent transcription of the gene. When cells are exposed to stress, Bach1 is exported from the nucleus, the Nrf2-Keap1 heterodimer dissociates, Nrf2 is imported into the nucleus. It binds to MAREs within the HO-1 gene and activates transcription (adapted from Naito et al., 2011).

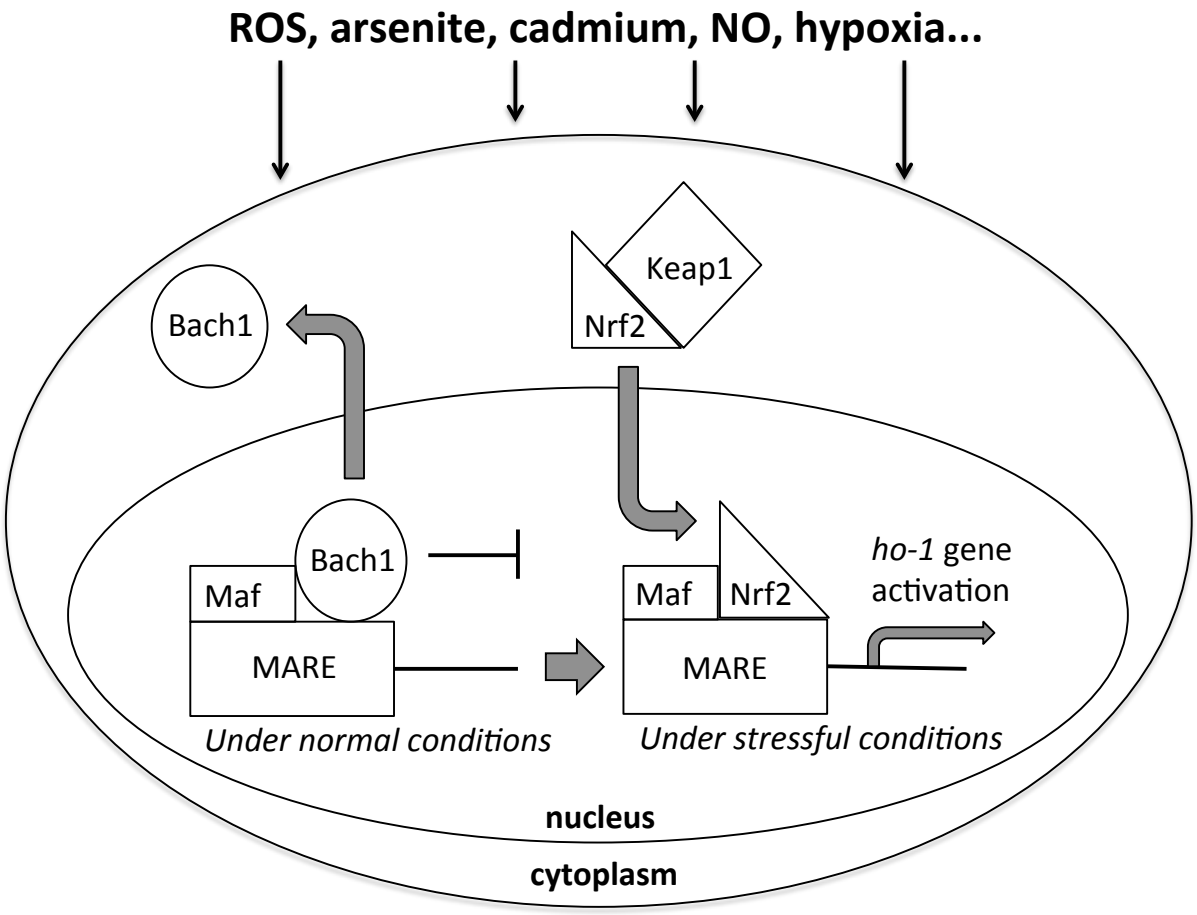
ROS, arsenite, cadmium, NO, hypoxia...
Keap1
Nrf2
Bach1
Bach1
Maf
MARE
Maf
Nrf2
MARE
ho-1 gene
activation
Under normal conditions
Under stressful conditions
nucleus
cytoplasm

al., 2000; Hill-Kapturczak et al., 2001; Balogun et al., 2003; Wu et al., 2004; Gonzalez-Reyes et al., 2013). Cadmium and MG132 induction of HO-1 also involves MARE/Nrf2 (Alam et al., 2000; Cui et al., 2013). Arsenite also induces HO-1 through Nrf2 and the p38 pathway (Elbirt et al., 1998; Lau et al., 2012).

1.6.2 HO-1 function

Heme oxygenase-1 (HO-1; also known as HSP32) was first identified in 1968 by Tenhunen et al. HO-1 catalyzes the catabolism of heme to iron, carbon monoxide, and biliverdin, which is then converted to bilirubin. This requires NADPH molecules, which are provided by NADPH-cytochrome P450 reductase. Heme, when it is not bound to hemoproteins, is able to promote deleterious iron-dependent reactions, which can generate ROS and lead to membrane lipid peroxidation (Ewing and Maines, 1997; Ryter and Tyrell, 2000).

Studies with HO-1 null or deficient organisms demonstrate that HO-1 is critical for organisms. HO-$1^{-/-}$ mice that were exposed to endotoxin exhibited higher mortality rates than wild type mice (Poss and Tonegawa, 1997). The only known case of HO-1 deficiency in humans was characterized by growth retardation, hemolytic anemia, endothelial damage, iron deposition, as well as increased vulnerability to oxidative stress-related injury (Yachie et al., 1999).

HO-1 plays a protective role against diverse stressors, likely through the effects of its catalytic by-products, which are free iron, carbon monoxide, and bilirubin via the action of biliverdin reductase on biliverdin (Fig. 4). Free iron leads to the expression of ferritin, the protein that sequesters Fe^{2+}. This protects the cells from the adverse effects of free iron. In

Figure 4. Heme degradation pathway and the effects of its degradative products. Through the action of stress-inducible HO-1 and constitutive HO-2, heme is degraded to biliverdin (BV), iron, and carbon monoxide (CO). Biliverdin reductase (BVR) catalyses the conversion of biliverdin to bilirubin (BR). Bilirubin, a potent free radical scavenger, contributes to a decrease in reactive oxygen species (ROS) and nitric oxide (NO). Iron induces the expression of ferritin, which sequesters it to reduce the toxic effects of free iron, although iron may still contribute to an increase in ROS. CO inhibits apoptosis, proliferation, and is anti-inflammatory. CO also increases levels of sGC, which causes protective vascular relaxation through its effect on cGMP (adapted from Kim et al., 2011).

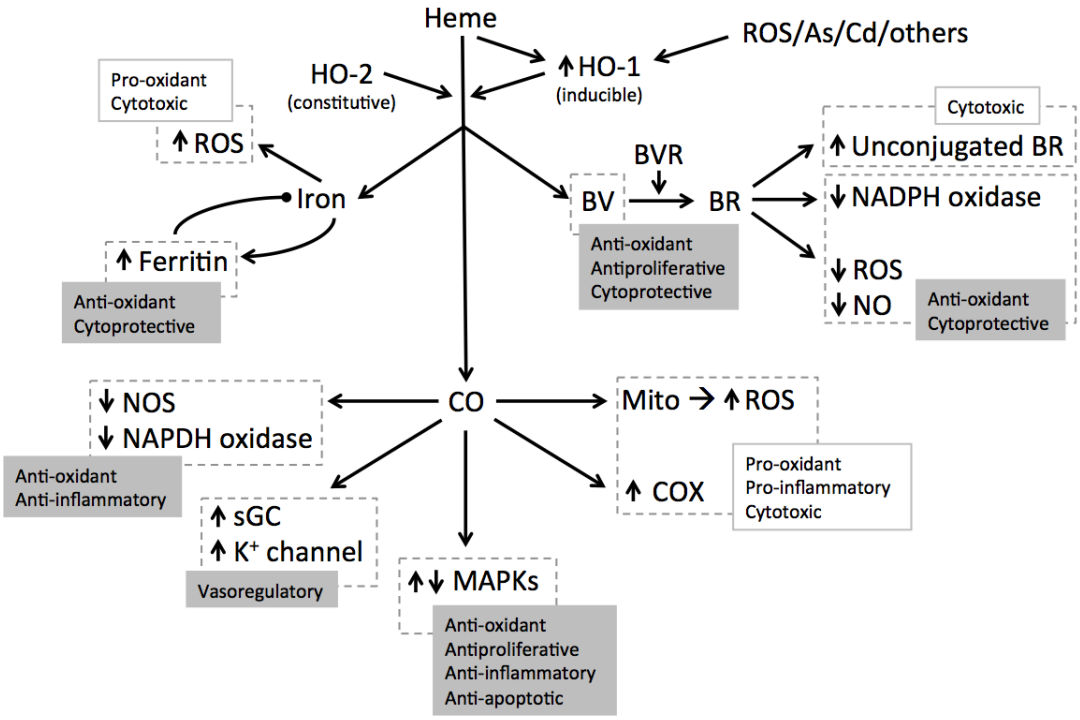
Heme
ROS/As/Cd/others
HO-2
(constitutive)
↑HO-1
(inducible)
Pro-oxidant
Cytotoxic
↑ROS
Iron
BVR
BV
BR
Cytotoxic
↑Unconjugated BR
↓NADPH oxidase
↓ROS
↓NO
Anti-oxidant
Cytoprotective
Anti-oxidant
Antiproliferative
Cytoprotective
↑Ferritin
Anti-oxidant
Cytoprotective
CO
↓NOS
↓NAPDH oxidase
Anti-oxidant
Anti-inflammatory
Mito → ↑ROS
↑ COX
Pro-oxidant
Pro-inflammatory
Cytotoxic
↑ sGC
↑ K+ channel
Vasoregulatory
↑↓ MAPKs
Anti-oxidant
Antiproliferative
Anti-inflammatory
Anti-apoptotic

addition to the action of ferritin, intracellular iron is also removed by an ATPase pump (Ferris et al., 1999). Bilirubin is a potent antioxidant through its scavenging of reactive oxygen species (ROS; Morita et al., 1997). Carbon monoxide, although most often thought of as toxic, confers a protective effect in lower doses than that which lead to carbon monoxide poisoning. On an organismal level, carbon monoxide is a second messenger that also contributes to vascular function through its regulating action on vascular tone (Morita et al., 1997). It also suppresses production of tumour necrosis factor alpha (TNFα), as part of its anti-inflammatory effect. Carbon monoxide may also inhibit the release of mitochondrial cytochrome c, which is an apoptosis signal. This may explain why HO-1 was reported to protect endothelial cells from apoptosis (Siow et al., 1999). Additionally, HO-1 was induced by agents that cause oxidative stress including sodium arsenite, UV radiation, hyperoxia, and glutathione depletion. This suggests that HO-1 is important in the cellular defense mechanism against oxidative and inflammatory damage (Keyse and Tyrrell, 1989; Elbirt et al., 1998; Oguro et al., 1998, Otterbein et al., 1999).

1.6.3. Stressed-induced HO-1 accumulation

HO-1, the enzyme that breaks down heme, is induced by its substrate (Yoshida et al., 1988). HO-1 is also induced by oxidative stress in rat, cow, and fish cells (Turner et al., 1999; Motterlini et al., 2000; Wang et al., 2008). Hyperthermia or heat shock as an inducer of HO-1 was demonstrated *in vivo* in a variety of rat organs, European sea bass liver, mouse Sertoli cells, human fibroblasts, and in certain rat and human hepatoma cells (Taketani et al., 1988; Keyse and Tyrrell, 1989; Mitani et al., 1990; Raju and Maines, 1994; Lee et al., 1996; Hachfi et al., 2012; Li et al., 2014). Conversely, HO-1 was not induced by heat shock in

human alveolar macrophages, an erythroblastic cell line, fibroblasts, two hepatoma cell lines, glioma, HeLa, or HL60 cells (Yoshida et al., 1988; Keyse and Tyrrell, 1989; Taketani et al., 1989; Mitani et al., 1990; Okinaga et al., 1996). Interestingly, HO-1 expression in spleen and kidney of European sea bass decreased after heat shock (Hachfi et al., 2012). The mechanisms involved in the responses of different cells or tissues to heat shock with respect to HO-1 accumulation is not known at present.

Many disease states have been observed to involve the induction of HO-1. These include neurological diseases such as Alzheimer's, Huntington's, and Parkinson's (Smith et al., 1994; Schipper et al., 1998; Pappolla et al., 1998). Additionally, HO-1 is associated with the pathogenesis of diverse pulmonary diseases such as emphysema and adult respiratory distress syndrome (Lee et al., 1996). Furthermore, it was detected in high levels in prostate and brain cancer tumours, where HO-1 appears to have a cytoprotective effect (Maines and Abrahamsson, 1996; Hara et al., 1996; Fang et al., 2004). Interestingly, in the presence of an oxidative chemotherapeutic agent, tumour cells with blocked HO-1 expression exhibited a high rate of cell death (Fang et al., 2004). This may have been due to the prevention of the antioxidant effect that HO-1 activity confers in cells. Finally, inhibition of HO-1 may be beneficial in treating cancer as HO-1 catalytic by-products were found to have an anti-apoptotic and angiogenic effect, contributing to better vascularisation of tumours (Brouard et al., 2000; Deshane et al., 2007).

Diseases such as Alzheimer's disease and Parkinson's disease have been linked to impaired proteasome function (Ross and Pickart, 2004; Morimoto, 2008). The proteasomal inhibitors MG132 and lactacystin were found to induce HO-1 protein and mRNA, respectively, in astrocytes of mesencephalic cell cultures (Yamamoto et al., 2010). MG132

also induced HO-1 accumulation in murine macrophages (Wu et al., 2004). Curcumin, a component of the spice turmeric and a demonstrated proteasomal inhibitor, induced HO-1 accumulation in rat endothelial cells (Khan and Heikkila, 2011; Wang et al., 2013). Cadmium and arsenite have been established as inducers of HO-1 in avian and mammalian systems, and cadmium-induced HO-1 accumulation has also been demonstrated in fish and soybean plants (Taketani et al., 1989; Elbirt et al., 1998; Alam et al., 2000; Balestrasse et al., 2006; Søfteland et al., 2010; Williams and Gallagher, 2013).

1.7. Chemical stressors

1.7.1. Sodium arsenite

Sodium arsenite is a toxic compound found in ground water that comes from natural sources such as mineral leaching from weathered rocks and soils (Del Razo et al., 2001). Additionally, industrial sources contribute to the presence of sodium arsenite in water. At the organismal level, this chemical was shown to be associated with an increased risk of renal, hepatic and cardiovascular cancers (Del Razo et al., 2001). At the cellular level, it can cause metabolic abnormalities, apoptosis, cell cycle arrest and cytoskeletal damage, inhibition of the production of cytoskeleton proteins as well as the production of free radicals and reactive oxygen species (ROS; Chou, 1989; Liu et al., 2001; Bode and Dong, 2002; Del Razo et al., 2001; Li & Chou, 1992). Furthermore, arsenite was reported to increase caspase-3 activity, the enzyme associated with the apoptotic pathway (Liu et al., 2001). Other research found that arsenite induced DNA-damage/repair-related gene expression, which contributed to its action as a toxicant (Liu et al., 2001). Finally, arsenite was reported to induce the accumulation of HO-1, HSP70, and HSP90 in cultured cells including human skin fibroblasts

and rat hepatocytes (Keyse & Tyrrell, 1989; Bauman et al., 1993). In our laboratory, it was demonstrated that sodium arsenite induces *hsp* gene expression (Ohan et al., 1998; Gauley and Heikkila, 2006; Young et al., 2009). Sodium arsenite's effect on the ubiquitin-proteasome system (UPS) has been studied mainly in mammalian systems, where it was determined to inhibit proteasomal activity due to an increase in ubiquitinated protein, and a decrease in the chymotrypsin-like activity of the 20S core (Kirkpatrick, 2003; Tsou et al., 2005; Medina-Diaz et al., 2009). Studies have demonstrated that HSF1 trimerization was not directly caused by arsenite, suggesting an indirect activation mechanism that has not yet been elucidated (Zhong et al., 1998).

The toxicity of arsenic depends on its oxidation state and composition. Inorganic arsenicals, especially trivalent inorganic arsenic species like sodium arsenite, have been demonstrated to be the most toxic forms (Del Razo et al., 2001). Uptake of trivalent arsenic into the cell involves the phosphate transport system and aquaglyceroporins (Bhattacharjee et al., 2009). *X. laevis* oocytes microinjected with the aquaporins AQP7 or AQP9 cDNA demonstrated that both transport trivalent arsenite (Liu et al., 2002). Arsenic's toxicity is thought to arise partially from its ability to substitute for phosphate, as this would affect vital processes including DNA and ATP synthesis (Del Razo et al, 2001). Furthermore, arsenite has a high affinity for sulfhydryl groups within proteins, which is reported to be one mechanism of its toxicity (Chen et al., 1998; Liu et al., 2001; Del Razo et al., 2001).

1.7.2. Cadmium chloride

Cadmium is a toxic heavy metal, which has been labeled a category one human carcinogen due to its implication in various cancers including kidney, lung, pancreas, and

prostate (Waisberg et al., 2003). It accumulates mainly within the liver, kidney, and reproductive tissues (Bonham et al., 2003; Barbier et al., 2004; Loumbourdis, 2005; Mendez-Mouchet et al., 2006; Armenta and Rios, 2007). Its accumulation in water from anthropogenic sources leads to the accumulation of cadmium in humans and other organisms. Sources of cadmium include tobacco smoke, contaminated food, air pollution, and certain fertilizers (Waisberg et al., 2003). Cadmium enters cells through divalent metal transport 1 (DMT1) and also enhances the expression of the transporter (Gu et al., 2009). For aquatic organisms, cadmium can enter through the skin and gills. Exposure has been noted to result in developmental abnormalities, and protein denaturation or damage (Pedersen and Bjerregaard, 2000; Fort et al., 2001; Waisberg et al., 2003).

Cadmium toxicity has been associated with a number of damaging mechanisms at the cellular level, including the ability to cause the dysregulation of gene expression, damage DNA and inhibit its repair. In addition, it can cause apoptosis and induce oxidative stress (Waisberg et al., 2003; Mouchet et al., 2007; Mendez-Arementa and Rios, 2007; Blechinger et al., 2007). Heavy metals can induce oxidative stress through the production of toxic hydroxyl radicals created by Fenton reactions after interactions with cysteine thiol groups (Jozefczak et al., 2012). Cadmium leads to the formation of denatured proteins by reacting with thiol groups or substituting for zinc in zinc proteins (Waisberg et al., 2003; Galazyn-Sidorczuk et al., 2009). Cadmium disrupts E-cadherin mediated cell adhesion, cellular calcium pathways, and proteasomal activity (Joseph et al., 2001; Waisberg et al., 2003; Yu et al., 2008). Additionally, cadmium induces the activation of protein kinases, which leads to increased protein phosphorylation and expression of proto-oncogene transcription factors.

Through these mechanisms, cadmium causes abnormal levels of cell growth and proliferation (Waisberg et al., 2003).

Previously, cadmium chloride was demonstrated to induce the accumulation of both HSP30 and HSP70 in *Xenopus laevis* A6 cells (Woolfson and Heikkila, 2009). Cadmium chloride has additionally been reported to affect proteasome activity in a wide variety of systems including bivalves and human, rat, and mouse cell lines (Thevenod and Friedmann, 1999; Figueiredo-Pereira and Cohen, 1999; Othumpangat et al., 2005; McDonagh and Sheehan, 2006; Chora et al., 2008; Li et al., 2008a, Yu et al., 2008; McDonagh, 2009; Yu et al., 2011).

1.8. Protein degradation

1.8.1. Ubiquitin proteasome system

Proteins are degraded through two main pathways in eukaryotes. The lysosomal degradation pathway hydrolyses extracellular proteins, and is less involved in the degradation of cellular protein (Lee and Goldberg, 1998; Morimoto, 2008). The other pathway is the ubiquitin-proteasome system (UPS), which plays a major role in the degradation of cellular protein through ATP-dependent hydrolysis. The UPS has been studied for several decades (Hershko et al., 1980; Ciechanover et al., 1980; Wilkinson et al, 1980; Hough et al., 1987). This system is found in both the cytoplasm and nucleus, and is responsible for the removal of the majority of damaged proteins, up to 90% of all cellular proteins (Lee and Goldberg, 1998; Awasthi and Wagner, 2005). Figure 5 shows the two-step process involved in the pathway. Initially, proteins are targeted for degradation by ubiquitination, after which they are degraded by the 26S proteasome (Yang et al., 2008). Ubiquitin is a small protein that

Figure 5. Mechanism of protein degradation by the ubiquitin-proteasome system (UPS). Proteins are targeted for degradation through the addition of ubiquitin molecules by ubiquitinating enzymes in an ATP-dependent process. Polyubiquitinated proteins are recognized by the 26S proteasome's 19S regulatory particle. Proteins are degraded by chymotrypsin-like, trypsin-like and peptidyl-glutamyl peptide-hydrolyzing enzymes, to small peptides within the 20S core. Some peptides may be further degraded into individual amino acids, or else transported to the cell surface for antigen presentation (adapted from Lee and Goldberg, 1998).

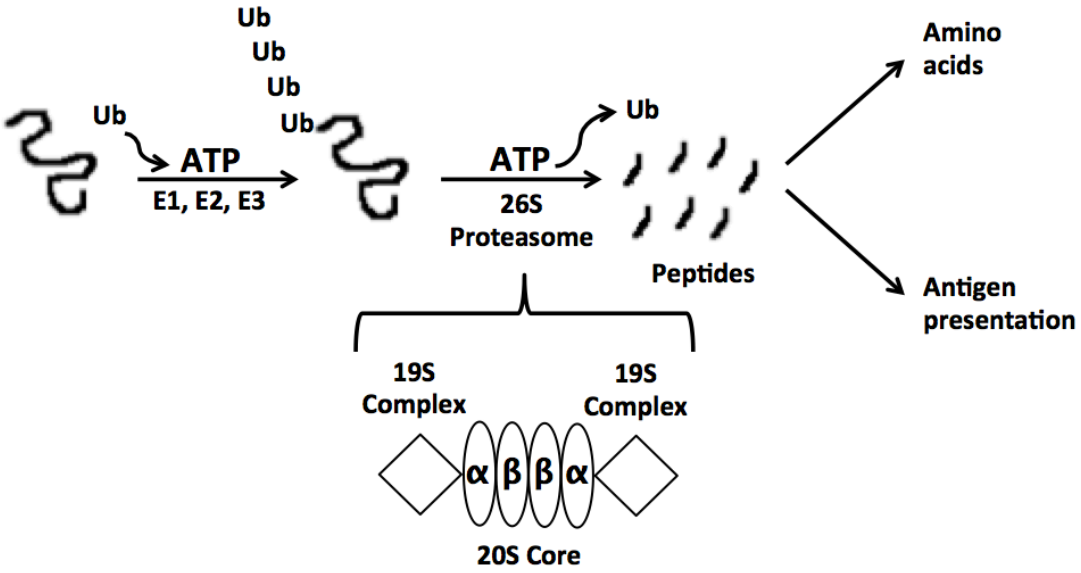
Ub
Ub
Ub
Ub
Ub
ATP
E1, E2, E3
ATP
26S
Proteasome
Ub
Peptides
Amino
acids
Antigen
presentation
19S
Complex
19S
Complex
α
β
β
α
20S Core

forms an isopeptide bond between its carboxy terminus and a lysine residue on the target protein. The process of ubiquitination involves several enzymes, which are named E1, E2, E3, and E4. Ubiquitination is activated by E1 through the ATP-dependent process of adenylation, and the creation of a thiol-ester bond at the carboxy terminus. Ubiquitin is transferred to a lysine residue on the target protein by E2 and E3, which is a ubiquitin ligase. E4 assists in the polyubiquitination of these lysine residues (Hershko and Ciechanover, 1998; Koegl et al., 1999). Finally, the polyubiquitinated protein is delivered to the proteasome. The 26S proteasome includes the 20S proteolytic core flanked by two 19S regulatory regions. The 20S core is comprised of two non-catalytic α rings and two catalytic β rings. The α subunit structure allows for the entry of polypeptides, and the β subunits include several proteolytic sites which work to degrade protein (Lee and Goldberg, 1998). These proteolytic sites have chymotrypsin-like, trypsin-like, and caspase-like activity (Lee and Goldberg, 1998). Peptides may be broken down further into amino acids by exopeptidases, while other peptides are used in antigen presentation after being transported to the endoplasmic reticulum lumen.

1.8.2. Proteasomal inhibition and effect on HSPs

The rate of protein breakdown in the cell decreases upon inhibition of the proteasome. This leads to the accumulation of proteins. Damaged proteins that accumulate can form aggregates, and apoptosis may be induced (Yang et al., 2008). A plethora of illnesses have been linked to the impairment of the UPS, including Alzheimer's, Parkinson's, and Huntington's diseases (Masliah et al., 2000; Ross and Pickart, 2004). Proteasomal inhibition has also been demonstrated to increase *hsp* gene expression in *Xenopus laevis* and other eukaryotic organisms (Bush et al., 1997; Stangl et al., 2002; Pritts et al., 2002; Le Goff et al.,

2004; Awasthi and Wagner, 2005; Lundgren et al., 2005; Noonan et al., 2007; Young and Heikkila, 2010; Walcott and Heikkila, 2010; Khan and Heikkila, 2011). Researchers studying this system can employ any of several known chemical inhibitors of proteasome activity, including carbobenzoxy-L-leucyl-L-leucyl-L-leucinal (MG132), lactacystin, curcumin, celastrol, and withaferin A (Wu et al., 2004; Yamamoto et al., 2010; Young and Heikkila, 2010; Walcott and Heikkila, 2010; Khan and Heikkila, 2011; Khan et al., 2012; Park and Kim, 2012). MG132, lactacystin and curcumin have all been demonstrated to induce HO-1 accumulation (Yamamoto et al., 2010; Wang et al., 2013).

1.9. *Xenopus laevis* as a model organism

Xenopus laevis, which is known as the South African clawed frog, has been used as a model research organism for decades. The oocytes, eggs and embryos of this aquatic frog are large and thus are ideal for microinjection studies (Guille, 1999; Heikkila et al., 2006). There is an extensive amount of information available about *Xenopus* at both the cellular and molecular level. Cellular and molecular data from *Xenopus* are often applicable to human cells. The specific cell line used for the research presented in this thesis is the A6 kidney epithelial cell line, for which there is an ever-increasing collection of data. This cell line was isolated from the renal proximal tubules of adult male *Xenopus* over 4 decades ago (Rafferty & Sherwin, 1969). A6 cells are hardy, have a doubling time of about 22 hours, and can exceed 100 generations *in vitro* (Rafferty, 1975). It has been used as a model system for the study of constitutive and stress-inducible *hsp* gene expression and function for more than three decades (Heikkila, 2010).

1.10. *Hsp30* gene expression and function in *Xenopus laevis*

The regulation of stress-induced HSP30 accumulation has been extensively studied in *Xenopus* A6 cells (Heikkila, 2010). Multiple *hsp30* genes were isolated from *Xenopus laevis* including *hsp30A*, which has an insertional mutation, and *hsp30B*, which is a pseudogene (Bienz, 1984). However, our laboratory isolated another gene cluster that included the *hsp30C* and *D* genes, which encode two functional 24 kDa proteins (Krone et al., 1992). Both *hsp30C* and *D* genes have a functional HSE in their 5' promoter region. Studies with recombinant HSP30C and D demonstrated that they can act as molecular chaperones by inhibiting heat-induced aggregation of client proteins as well as maintaining them in a folding-competent state (Fernando and Heikkila, 2000; Abdulle et al., 2002; Fernando et al., 2003; Heikkila, 2010). During *Xenopus* development, the *hsp30* gene family is not heat-inducible until the late neurula/early tailbud stage, while *hsp110, hsp90, hsp70 and hsp47* genes were stress-inducible at the midblastula stage. HSP30 was detected constitutively in the cement gland where it has been hypothesized to function in the prevention of apoptosis (Lang et al., 1999; Heikkila, 2004).

In *Xenopus* A6 kidney epithelial cells, various chemical stressors induced HSP30 accumulation including sodium arsenite, cadmium chloride, and heat shock (Gellalchew and Heikkila, 2005; Voyer & Heikkila, 2008; Woolfson and Heikkila, 2009). Recently, it was reported that proteasomal inhibitors such as lactacystin, MG132, and curcumin also induced HSP30 accumulation (Young and Heikkila, 2010; Khan and Heikkila, 2011).

1.11. *Ho-1* gene expression in *Xenopus laevis*

Information about the expression and function of the *ho-1* gene in *Xenopus* is limited to a single report (Shi et al., 2008). In this study, cDNA data were obtained from GenBank, and it was determined that the percent identity of *Xenopus* with human and mouse amino acid sequences was 61% and 58%, respectively. Ho-1 mRNA was detected in oocytes and during early embryogenesis from the 1-cell stage to tadpole. Ho-1 mRNA was found to accumulate in the dorsal region once embryos reached the neurula stage, an expression pattern that was similar to heme synthases. However, this study did not examine HO-1 protein levels or the effect of various stressors.

1.12. Objectives

Most of the knowledge regarding HO-1 accumulation and function has been derived from mammalian research systems. There is a general lack of information on stressor-induced HO-1 accumulation in poikilothermic vertebrates. The present study will examine stress-induced HO-1 accumulation for the first time in an amphibian cell line. The cell line used throughout this research is *Xenopus laevis* A6 kidney epithelial cells. The accumulation of HO-1 has been implicated in a variety of diseases associated with oxidative stress including but not limited to Alzheimer's disease, diabetes, atherosclerosis, cancer, and myocardial infarction (Takahashi et al., 2000; Juan et al., 2001; Turkseven et al., 2005; Liu et al., 2005; Was et al., 2006). Furthermore, some neurological disorders are associated with inhibition of the proteasome, which was found to induce HO-1 accumulation. To better elucidate HO-1's role in cellular and organismal health, studies with agents that induce oxidative stress and/or proteasomal inhibition will be carried out. Furthermore, the use of a

mild heat shock in conjunction with these chemicals stressors parallels the current issue of climate change faced by aquatic organisms such as amphibians. Aquatic amphibians are quite susceptible to the deleterious effects of toxicants such as sodium arsenite and cadmium chloride. Given that there is a global rise in temperature in recent history, it is worth examining whether higher temperatures in conjunction with these toxicants may exacerbate living organisms further. Finally, if HO-1 is induced by these chemicals in amphibians, then the relative levels of this stress-induced protein could act as a biomarker for environmental contamination by cadmium chloride, sodium arsenite or other chemicals.

The objectives of this research are as follows:

- To examine the effect of different heat shock temperatures and selected heavy metals on HO-1 accumulation
- To determine the effect of various concentrations of sodium arsenite, cadmium chloride, and MG132 on HO-1 and HSP30 protein accumulation
- To monitor the temporal pattern of HO-1 and HSP30 accumulation in cells treated with sodium arsenite, cadmium chloride, and MG132
- To compare the intracellular localization of HO-1 and HSP30 in cells subjected to heat shock, sodium arsenite, cadmium chloride, and MG132 treatment
- To investigate the pattern of HO-1 and HSP30 accumulation during recovery from sodium arsenite, cadmium chloride, and MG132 stress
- To examine the effect of mild thermal stress on sodium arsenite-, cadmium chloride-, and MG132-induced HO-1 and HSP30 accumulation

2. Materials and Methods

2.1. Maintenance and treatment of *Xenopus laevis* A6 kidney epithelial cells

Xenopus laevis A6 kidney epithelial cells were obtained from the American Type Culture Collection (CCL-102; Rockville, MD). Cells were cultured in 70% Leibovitz (L)-15 media (Sigma-Aldrich, Oakville, ON) and supplemented with 10% fetal bovine serum (FBS; Sigma-Aldrich) and 100 units/mL penicillin (Sigma-Aldrich), 100 μg/mL streptomycin (Sigma-Aldrich) at 22 °C in T75 cm^2 BD Falcon tissue culture flasks (VWR International, Mississauga, ON). Cells that became confluent were passaged by aspirating old media and rinsing with 1 mL versene (0.02% (w/v) KCl, 0.8% (w/v) NaCl, 0.02% (w/v) KH_2PO4, 0.115% (w/v) Na_2HPO_4, 0.02% (w/v) Na_2EDTA), succeeded by a 1 min treatment with 2 mL versene to chelate metal ions. Following aspiration of versene, 1 mL of 1X trypsin (Sigma-Aldrich) dissolved in 100% Hank's balanced salt solution (HBSS; Sigma-Aldrich) was added to the flask for 1 min to promote detachment of cells from the flask surface. Trypsin was partially removed, and cells were then resuspended in fresh media and divided evenly into new culture flasks at a ratio of 1:3 or 1:4, depending on the initial state of confluency.

Flasks of cells that had achieved 80-90% confluency were used for experiments. Initial heat shock treatments were carried out for 2 h in water baths set to different temperatures, namely, 30, 33 and 35 °C, followed by a 2 h recovery at 22 °C. A 100 mM stock solution of sodium arsenite (As; Sigma-Alrich) was used to create a working solution of 1 mM. Cadmium chloride (Sigma-Aldrich) treatments were carried out with 1 mM or 100 mM solutions as deemed appropriate for dispensing accurate volumes. MG132 (Sigma-Aldrich) was dissolved in dimethylsulphoxide (Sigma-Aldrich) to create a 5 mg/mL stock solution. Lead(II) nitrate, copper(II) sulphate, zinc sulphate, and iron sulphate (all Sigma-

Aldrich) were dissolved in sterile water, to working concentrations of 1, 10, 10, and 100 mM, respectively. Cells were incubated in 10 mL of complete media and treated with 5-50 μM preparations of sodium arsenite, 10-200 μM cadmium chloride, or 5-30 μM MG132 at 22 °C. These treatments ranged in time from 0 to 24 h. Lead nitrate, copper sulphate, zinc nitrate, and iron sulphate were used to treat cells at concentrations of 100, 200, and 500 μM. Recovery treatments involved 24 h of treatment with sodium arsenite or MG132, or 12 h treatment with cadmium chloride, followed by removal of media, rinsing of the flasks and incubation in fresh media for 0 to 48 h. Some cells recovering from sodium arsenite treatment were also incubated with 100 μM cycloheximide (CHX) for the duration of the recovery period at 22 °C. In experiments that combined a mild heat shock with chemical treatment, sodium arsenite, cadmium chloride, or MG132 were added to flasks of cells at the indicated concentrations and then incubated in a heated water bath at 30 °C for 12 h. Following treatment, media was removed, and cells were rinsed with 2 mL of 65% HBSS, followed by the addition of 1 mL 100% HBSS. Cells were removed from the flask by use of a cell scraper, and subsequently transferred to a 1.5 mL microcentrifuge tube. Cells were then pelleted by means of centrifugation for 1 min at 14000 rpm, after which the supernatant was removed. The pelleted cells were stored at -80 °C prior to protein isolation and quantification.

2.2. Protein isolation and quantification

Frozen cells were thawed on ice and then suspended in 250-350 μL lysis buffer (200 mM sucrose, 2 mM EGTA, 1 mM EDTA, 40 mM NaCl, 30 mM HEPES, pH 7.4) with 1% (w/v) SDS and 1% (w/v) protease inhibitor cocktail (Roche, Laval, QC) added. Samples were

then sonicated on ice using a sonic dismembranator (Model 100, Fisher Scientific, Waltham, MA) to deliver approximately 15 bursts followed by centrifugation at 14000 rpm for 30 min at 4 °C. After centrifugation, supernatant containing protein was transferred to 1.5 mL microcentrifuge tubes and stored at -20 °C until required.

Protein quantification was performed utilizing the bicinchoninic acid (BCA) method following the manufacturer's protocol (Pierce, Rockford, IL). Bovine serum albumin (BSA; Bioshop, Burlington, ON) was utilized to create a protein standard. BSA was diluted in distilled water, creating a range of concentrations from 0-2 mg/mL. Distilled water was likewise employed to dilute protein samples 1:2; 20 μL of sample and water were used. The BSA standards and protein samples were loaded in 10 μL volumes in triplicate into individual wells of a 96 well polystyrene plate. Subsequently, 80 μL of combined BCA reagent A and B (Pierce, 50:1) was added to each standard and protein sample well. The plate was incubated at 37 °C for 30 min. After incubation, the plate was allowed to cool at room temperature for 10 min prior to being monitored at 562 nm using a Versamax Tunable microplate reader (Molecular Devices, Sunnyvale, California) and Softmax Pro software. The BSA standards were used to create a standard curve that was then used to calculate sample concentrations. Samples containing 40 μg of protein were mixed with loading buffer [0.065 M Tris pH 6.8, 10% (v/v) glycerol, 2% (w/v) SDS, 5% (v/v) β-mercaptoethanol, 0.00125% (w/v) bromophenol blue]. If not used immediately, samples were maintained at -80 °C.

2.3. Immunoblot analysis

Protein separation employed sodium dodecyl sulphate-polyacrylamide gel electrophoresis (SDS-PAGE) as previously conducted in Khamis and Heikkila, 2013. Twelve percent polyacrylamide gels were used throughout this study. The vertical separating gel [12% (w/v) acrylamide, 0.32% (v/v) n'n'-bis methyl acrylamide, 0.375 M Tris pH 8.8, 1% (w/v) SDS, 0.2% (w/v) ammonium persulfate (APS), 0.14% (v/v) tetramethylethylenediamine (TEMED)] was prepared and allowed to polymerize for 25 min with 100% ethanol layered on top of it. Ethanol was subsequently poured off and the stacking gel [4% (v/v) acrylamide, 0.11% (v/v) n'n'-bis methylene acrylamide, 0.125 M Tris pH 6.8, 1% (w/v) SDS, 0.4% (w/v) APS, 0.21% (v/v) TEMED] was poured on top of the separating gel. Combs were then inserted and the gel was allowed to polymerize for 25 min. Protein samples in loading buffer were thawed on ice, boiled for 10 min, briefly centrifuged and then loaded onto the gels. Gels were electrophoresed with 1X running buffer (25 mM Tris, 0.2 M glycine, 1 mM SDS) at 90 V for approximately 20 min, after which time the voltage was increased to 160 V until the samples reached the bottom of the gel.

Transfer of electrophoresed protein from the gel to a nitrocellulose membrane employed a Trans Blot Semi-dry transfer system (BioRad). Nitrocellulose membranes and filter paper (both BioRad, Mississauga, ON) were cut into 5 x 8.5 cm pieces. The membranes were soaked in 20% transfer buffer (25 mM Tris, 192 mM glycine, 20% (v/v) methanol) for 30 min, and the gels were soaked in the same buffer for 15 minu. After electrophoresis, protein transfer from gel to nitrocellulose membrane was accomplished using a Trans Blot Semi-dry transfer system for 25 min at 20 V. Ponceau-S [0.19% (w/v) Ponceau-S, 5% (v/v) acetic acid; Sigma-Aldrich] staining of the membrane was performed for 5 min to determine

efficient transfer of all samples. The blot was then incubated with 5% blocking [20 mM Tris pH 7.5, 0.1% Tween 20 (Sigma), 300 mM NaCl, 5% (w/v) Carnation Instant Skim Milk Powder (Markham, ON)] for 1 h to prevent non-specific binding. Blocking solution was then poured off and membranes were subsequently incubated with rabbit anti-HO-1 antibody (1:500, Enzo Life Sciences, Farmingdale, NY), rabbit anti-*Xenopus* HSP30 antibody (1:1000), or rabbit anti-actin polyclonal antibody (1:200, Sigma-Aldrich) in blocking solution. Primary antibody was then removed and the membrane was briefly rinsed twice and subsequently immersed once for 15 min and twice for 10 min with Tris buffered saline solution with Tween-20 [TBS-T; 2 mM Tris pH 7.5, 0.1% Tween-20 (Sigma-Aldrich), 30 mM NaCl]. Membranes were incubated for 1 h with AP-conjugated goat anti-rabbit secondary antibody (1:3000, BioRad) in blocking solution. After washing with TBS-T for 15 min once and 5 min twice, blots were incubated in an alkaline phosphatase detection buffer (50 mM Tris base, 50 mM NaCl, 25 mM $MgCl_2$, pH 9.5) with 0.3% 4-nitro blue tetrazolium (NBT; Roche) and 0.17% 5-bromo-4-chloro-3-indolyl phosphate, toluidine salt (BCIP; Roche) until bands were visible. The detection buffer was then poured off, and blots were rinsed with distilled water and scanned when dry.

2.4. Densitometry and statistical analysis

Image J software (Version 1.44; National Institute of Health; http://rsb.info.nih.gov/ij/) was used to perform densitometric analysis within the range of linearity on all blots, with experiments performed at least in triplicate. The average values obtained were graphed as a percentage of the maximum value of either HO-1 or HSP30 bands. Vertical error bars display the standard error of the mean. Statistical analysis was

performed on normalized data using a one-way analysis of variance (ANOVA) with a Tukey's post-test ($p<0.05$; indicated by *) to determine if statistically significant differences existed between samples.

2.5. Immunocytochemistry and laser scanning confocal microscopy (LSCM)

A6 cells were grown on flame-sterilized glass coverslips previously washed with a base solution [49.5% (v/v) ethanol, 0.22 M NaOH] in small jars (Thomas Scientific Apparatus, Philadelphia, PA) for 30 min and rinsed with distilled water for 3 h. Cells were cultured on coverslips in Petri dishes, which were kept at 22 °C for 24-48 h. The cells were then treated with heat shock and/or heavy metals followed by removal of L-15 media and two rinses with phosphate buffered saline (PBS; 11.37 M NaCl, 67 mM Na_2HPO_4, 26 mM KCl, 14.7 mM H_2PO_4, 1 mM $CaCl_2$, 0.5 mM $MgCl_2$, pH 7.4). Fixation was carried out with 3.7% paraformaldehyde in PBS (BDH Inc., Toronto, ON) for 15 min. Cells were rinsed three times for 5 min with PBS and then with 0.3% Triton X-100 (Sigma-Aldrich) for 10 min to permeabilize cells followed by three washes with PBS. A6 cells were incubated 1 h or at 4 °C overnight with 3.7% (w/v) filtered bovine serum albumin (BSA) fraction V in PBS (Fischer Scientific). Cells were then incubated with either affinity-purified rabbit anti-*Xenopus* HSP30 (1:500) or anti-HO-1 (1:200) antibody in 3.7% BSA for 1 h. Cells were washed with PBS three times for 2 min. The remainder of the steps were done in the dark. Indirect labeling was carried out for 30 minutes with fluorescent-conjugated goat anti-rabbit Alexa Fluor 488 (Invitrogen Molecular Probes, Carlsbad, CA) in BSA at a 1:2000 dilution. After washing with PBS three times for 3 min, cells were incubated with rhodamine-tetramethylrhodamine-5-isothiocyanate phalloidin (TRITC; 1:100; Invitrogen Molecular Probes) for 15 min to visualize the actin cytoskeleton. After washing three times with PBS, coverslips were dried

and mounted on a microscope slide with Vectashield mounting medium (Vector Laboratories Inc., Burlingame, CA), which contained 4,6-diamidino-2-phenylindole (DAPI; Vector Laboratories Inc.) for the staining of nuclei. The slides were blotted dry and clear nail polish was used as an adhesive to bind coverslips to glass microscope slides. Slides were stored at 4 °C for a minimum of 1 h or until required. Cells were visualized using a Zeiss Axiovert 200 confocal microscope with Zen 2009 software (Carl Zeiss Canada Ltd., Mississauga, ON). Images were viewed with Zen 2009 Light Edition software.

3. Results

3.1. Characterization of heme oxygenase-1 (HO-1) protein in *Xenopus laevis*

Stress-inducible HO-1 protein accumulation and function has been documented primarily in mammalian experimental systems including human, pig, mouse, and rat (Alam et al., 2000; Balogun et al, 2003; Chen et al., 2011; Gonzales-Reyes et al., 2013). However, to the best of our knowledge, there have been no studies examining stress-induced HO-1 protein accumulation and function in *Xenopus* or other amphibians. The present study has compared the effect of heat shock, sodium arsenite, cadmium chloride, and MG132 on HO-1 accumulation in *X. laevis* A6 kidney epithelial cells by means of immunoblot and immunocytochemical analysis. HSP30, a small heat shock protein, was chosen as a comparison protein given the abundance of information on its accumulation in response to heat shock and chemical stressors (Heikkila, 2010).

The *Xenopus laevis* HO-1 amino acid (aa) sequence (Genbank accession number: NP_001089909) was originally derived from the nucleotide sequence of a HO-1 cDNA (NM_001096440.1) isolated from an oocyte cDNA library. *Xenopus* HO-1 is 291 aa in length and includes 8 heme binding pocket residues (Fig. 6). The heme ligand binding site is histidine in position 28. A comparison of the percent identity of the *Xenopus laevis* HO-1 aa sequence with the HO-1 aa sequence from other selected organisms and the constitutive HO-2 from *Xenopus laevis* is shown in Table 1. *Xenopus laevis* HO-1 shares 91% identity with *Xenopus tropicalis* HO-1. However, the percent identity with other organisms including chicken, duck, human, rat, mouse, alligator and zebrafish HO-1 ranged from 63 to 45%. However, when percent identity was determined for a particularly conserved region (P129-

Figure 6. Amino acid sequence of *Xenopus laevis* HO-1. The *Xenopus laevis* HO-1 protein (Genbank accession number: NP_001089909) is 291 amino acids long. The heme ligand binding site, a conserved histidine (H) residue, is indicated by an asterisk below the letter. The heme binding pocket residues are shown in a bold font and underlined. The HO-1 antibody (Enzo Life Sciences, BML-HC3001) used in this research was produced against a synthetic human HO-1 peptide. The corresponding *Xenopus* HO-1 amino acids (D15-H28) share 100% sequence identity with this peptide and are indicated by the horizontal bracket. The conserved region that was compared with other organisms for shared identity in Table 1 is indicated with a dashed bracket, spanning P129 to R186.

```
1   MDPSASQQYK STHEDLSEAL KEATKEVHVQ AENTEFMRNF
                                    *
41  QKGQVSLEEF KLVMSSLYFI YEALEEEINR NKDNPVFSPV

81  YFPLELHRKN ALEVDLEYFY GPQWRKKIIC PHSTKNYVDR

121 LHHVGQKEPE LLVSHAYTRY LGDLSGGQVL KKIAQKALQL

161 PASGEGLAFF TFDNVTNATK FKQLYRSRMN SIETDAYAKK

201 RILEEAKTAF LLNIKLFEEL QTLSLATSQN GNTRTEATEL

241 RSRGPKTENG RPTKTDNREN NSSSEEQPTT FLRWFLIAGC

281 ALITLMGLYI F
```

Table 1. A comparison of *Xenopus laevis* HO-1, HO-2, and selected HO-1 homologues from other organisms.

Protein / Species	% identity (complete amino acid sequence)	% identity (conserved region)
HO-1 / *Xenopus tropicalis*	91	100
HO-1 / *Gallus gallus*	63	91
HO-1 / *Anas platyrhynchos*	63	91
HO-1 / *Homo sapiens*	61	88
HO-1 / *Rattus norvegicus*	59	84
HO-1 / *Mus musculus*	59	84
HO-1 / *Alligator mississipiensis*	58	88
HO-2 / *Xenopus laevis*	53	74
HO-1 / *Danio rerio*	45	69

The sequences were obtained from the GenBank database (www.ncbi.nlm.nih.gov). The NCBI reference sequences of the proteins are: *Xenopus laevis* HO-1, NP_001089909; *Xenopus tropicalis* HO-1, XP_002934766; *Gallus gallus* HO-1, ADK26061; *Anas platyrhynchos* HO-1, XP_005015402; *Homo sapiens* HO-1, ADZ76424; *Rattus norvegicus* HO-1, NP_036712; *Mus musculus* HO-1, EDL10826; *Alligator mississipiensis* HO-1, XP_006261961; *Xenopus laevis* HO-2, NP_001085675, and *Danio rerio* HO-1, NP_001120988. The percent identity of a highly conserved region (residues P129 – R186 in *Xenopus laevis* HO-1) was also determined using these data. This domain is indicated with a dashed bracket in the previous figure.

R186), similarity to *Xenopus laevis* HO-1 was higher in all cases ranging from 69% identity with zebrafish HO-1 to 100% identity with *Xenopus tropicalis* HO-1. This region contains 4 of the 8 heme binding pocket residues and is indicated in Fig. 6 with a dashed bracket. *Xenopus laevis* constitutive HO-2 shared only 53% identity overall with HO-1 and 74% in the conserved region. Additionally, the size and theoretical pI of *Xenopus* laevis HO-1 were determined by the Compute pI/Mw tool (http://web.expasy.org/compute_pi/) to be 33.5 kDa and 6.7, respectively. This differs from human HO-1, which has a predicted pI of 7.9 and a size of 32.8 kDa.

Following the *in silico* analysis of *Xenopus* HO-1 and its analogues in other species, an effective antibody was required to perform immunoblot and immunocytochemistry analyses. No *Xenopus* anti-HO-1 antibody was available, but an antibody (Enzo Life Sciences, BML-HC3001) that was made against a synthetic peptide (DLSEALKEATKEVH) derived from a human HO-1 conserved sequence shared 100% identity with *Xenopus laevis* HO-1 (Figure 6). This region includes 3 of 8 heme binding pocket residues, as well as the heme ligand binding site. Previous studies employed this anti-HO-1 antibody in both Western blotting and immunocytochemistry in human cells (Hock et al., 2004; Hanneken et al., 2006). Thus, the anti-human HO-1 antibody was employed in our analyses of stress-induced HO-1 accumulation in *Xenopus laevis* A6 kidney epithelial cells.

3.2. Stress-induced accumulation of heme oxygenase-1 (HO-1) and HSP30

Initially, the effect of heat shock on HO-1 accumulation in A6 cells was examined by immunoblot analysis. Arsenite was employed as a positive control since previous studies

demonstrated that HO-1 accumulation was induced by sodium arsenite in rat, murine, and human cells (Li et al., 2001; Fauconneau et al., 2002; Gong et al., 2002). As shown in Figure 7A, arsenite treatment enhanced the relative level of HO-1 accumulation. However, at all heat shock temperatures (30, 33, and 35 °C) employed, enhanced HO-1 accumulation was not detected although HSP30 accumulation was induced. Densitometric analysis determined that at 30 °C and 35 °C, the relative levels of HSP30 were approximately 20% and 70% of the maximal value, which was observed at 33°C (Fig. 7B).

In preliminary studies, we examined the effect of different heavy metals such as cadmium chloride, copper sulphate, zinc sulphate, lead nitrate and iron sulphate for 24 h on HO-1 and HSP30 accumulation. In these studies, 20 μM sodium arsenite was used as a positive control (Fauconneau et al., 2002). Occasionally, a faint HO-1 band was observed in A6 cells maintained at 22 °C in the absence of metals. Concentrations of 100 and 200 μM cadmium chloride for 24 h induced both HO-1 and HSP30 accumulation, although a greater accumulation of HO-1 was observed at 100 μM (Fig. 8A). Copper sulphate and zinc sulphate did not induce either HO-1 or HSP30 accumulation at either of the two concentrations employed. However, an enhanced accumulation of HO-1 was observed with 200 μM iron sulphate treatment, while no HSP30 accumulation was observed (Fig. 8B). The effect of a higher 500 μM concentration of copper sulphate, iron sulphate, lead nitrate and zinc sulphate on HO-1 and HSP30 accumulation is shown in Figure 8C. At this concentration, iron induced a detectable level of HO-1 with lead nitrate exposure producing a slight HO-1 accumulation. None of these metals induced detectable HSP30 accumulation.

Figure 7. Heat shock-induced HSP30 accumulation. A) Cells were incubated at 30°C, 33°C, or 35°C for 2 h with a recovery time of 2 h at 22 °C. Some cells were also treated with 20 μM sodium arsenite (As) at 22 °C for 24 h. Cells were harvested and total protein was isolated and subjected to immunoblot analysis using anti-HO-1, anti-HSP30, and anti-actin antibodies as described in Materials and methods. These results are representative of 2 separate experiments.

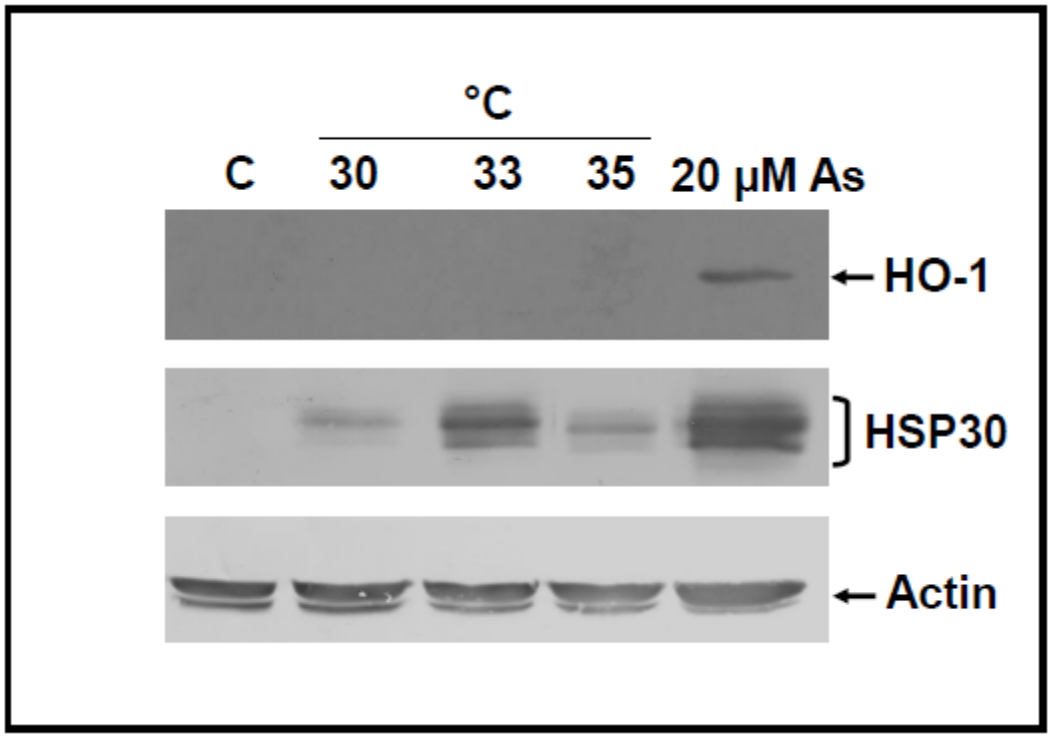
°C
C
30
33
35
20 μM As
HO-1
HSP30
Actin

Figure 8. Effect of different concentrations of various metals on HO-1 and HSP30 accumulation. A) Cells were incubated with or without 100 or 200 μM of Cd, Cu or Zn or 20 μM As at 22 °C for 24 h. After treatment, total protein was isolated and subjected to immunoblot analysis as detailed in Materials and methods. B) Cells were incubated with or without 100 or 200 μM of Fe or Pb or 20 μM As at 22 °C for 24 h. After treatment, total protein was isolated and subjected to immunoblot analysis as detailed in Materials and methods. These results are representative of 2 separate experiments. C) Cells were incubated with or without 100 or 500 μM of Cu, Fe, Pb or Zn or 20 μM As at 22 °C for 24 h. After treatment, total protein was isolated and subjected to immunoblot analysis as detailed in Materials and methods. These results are representative of 2 separate experiments.

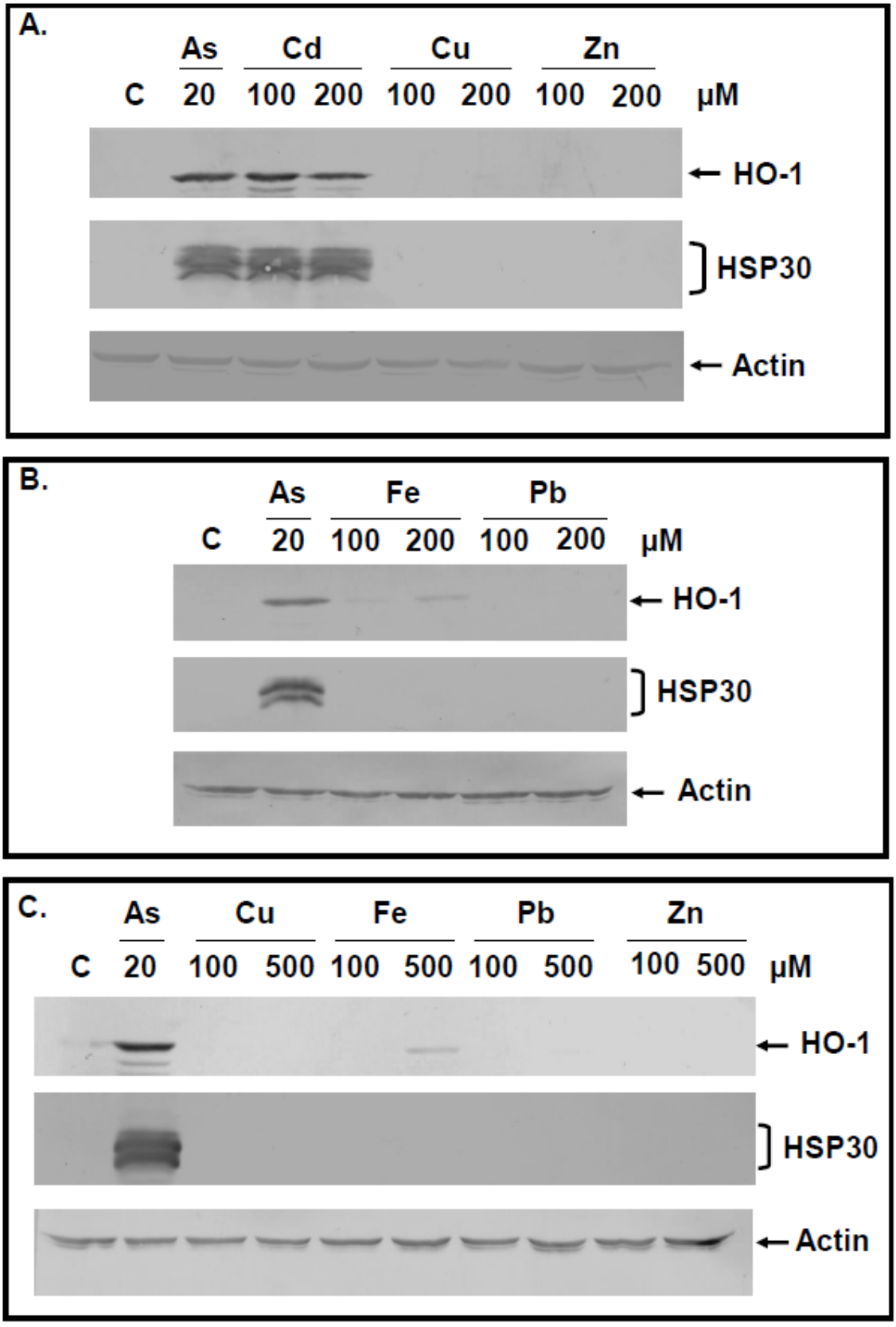
A.
As
Cd
Cu
Zn
C
20
100
200
100
200
100
200
μM
HO-1
HSP30
Actin
B.
As
Fe
Pb
C
20
100
200
100
200
μM
HO-1
HSP30
Actin
C.
As
Cu
Fe
Pb
Zn
C
20
100
500
100
500
100
500
100
500
μM
HO-1
HSP30
Actin

3.3. HO-1 and HSP30 accumulation is induced by sodium arsenite and cadmium chloride in a concentration- and time-dependent manner

After this initial survey of metal-induced HO-1 accumulation, further characterization employed sodium arsenite and cadmium chloride as both were found to strongly induce both HO-1 and HSP30. In an examination of the effect of different concentrations of sodium arsenite for 24 h on HO-1 accumulation in A6 cells, HO-1 was detectable at 5 μM sodium arsenite, peaked at 10 μM and then declined to slightly lower relative levels at 20, 30 and 50 μM (Fig. 9A). Densitometric analysis revealed that at 5 μM sodium arsenite HO-1 accumulation was 79% of maximal value (10 μM) and a reduction to 69, 69 and 56% at 20, 30 and 50 μM, respectively (Fig. 9B). Pretreatment of cells with cycloheximide, an inhibitor of protein synthesis prevented sodium arsenite-induced HO-1 and HSP30 accumulation indicating that the accumulations were the result of *de novo* synthesis (Fig. 10). Likewise, the transcriptional inhibitor actinomycin D inhibited the accumulation of HO-1 and HSP30 in response to sodium arsenite and cadmium chloride treatment (data not shown). In sodium arsenite-treated A6 cells, enhanced HSP30 accumulation was first observed at 10 μM with peak levels at 20 or 30 μM and a slight reduction at 50 μM. In time course studies with 30 μM sodium arsenite, HO-1 and HSP30 accumulation was first detectable at 8 h and increased in a time-dependent manner until the final time point, 48 h (Fig. 11A). Densitometric analysis revealed that at 8, 12, and 24 h, HO-1 signal intensities were approximately 12, 30, and 85% of maximum, respectively. A similar pattern was observed for HSP30, as the relative intensities at 8, 12, and 24 h were approximately 33, 40 and 79% of maximum (Fig. 11B).

Figure 9. Effect of different concentrations of sodium arsenite on HO-1 and HSP30 accumulation. A) Cells were incubated with 0, 5, 10, 20, 30, or 50 μM sodium arsenite (As) at 22 °C for 24 h. After treatment, total protein was isolated and subjected to immunoblot analysis as detailed in Materials and methods. B) Densitometric analysis of the band intensity for HO-1 (black; panel B) and HSP30 (grey; panel B) employed Image J software. The results were expressed as a percentage of the maximum band intensity acquired for each protein in each trial (10 μM for HO-1 and 30 μM for HSP30). Vertical error bars denote the standard error. A one-way ANOVA with a Tukey's Multiple Comparisons post-test was used to determine significance. Significant differences between the control cells and treated cells are indicated as * ($p < 0.05$). These results are representative of 3 separate experiments.

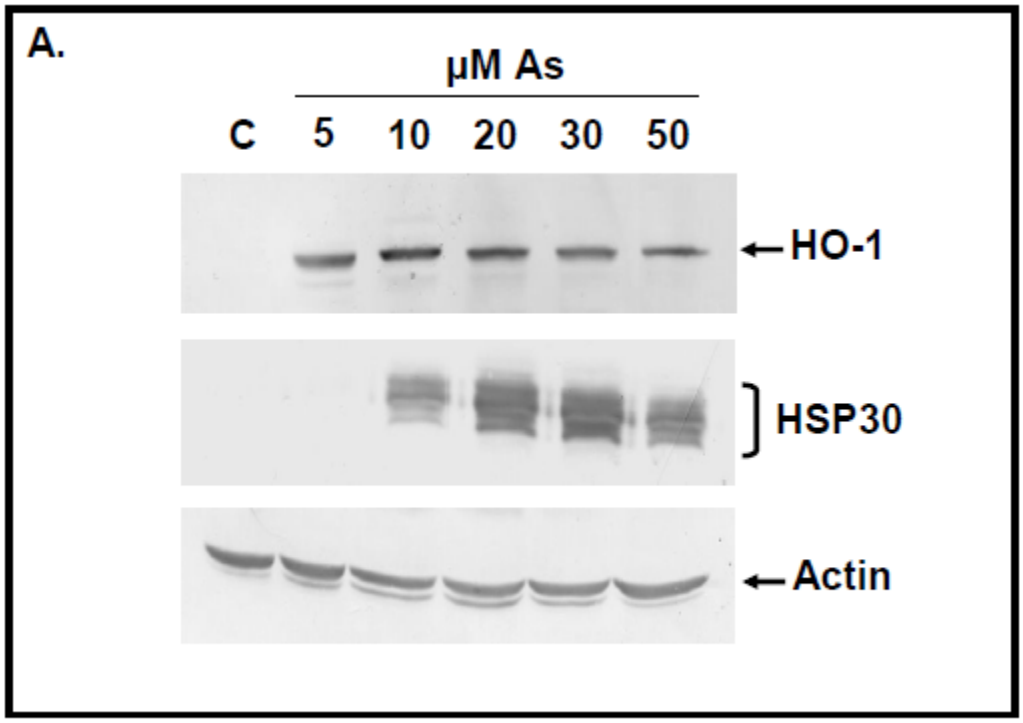
A.
μM As
C
5
10
20
30
50
HO-1
HSP30
Actin

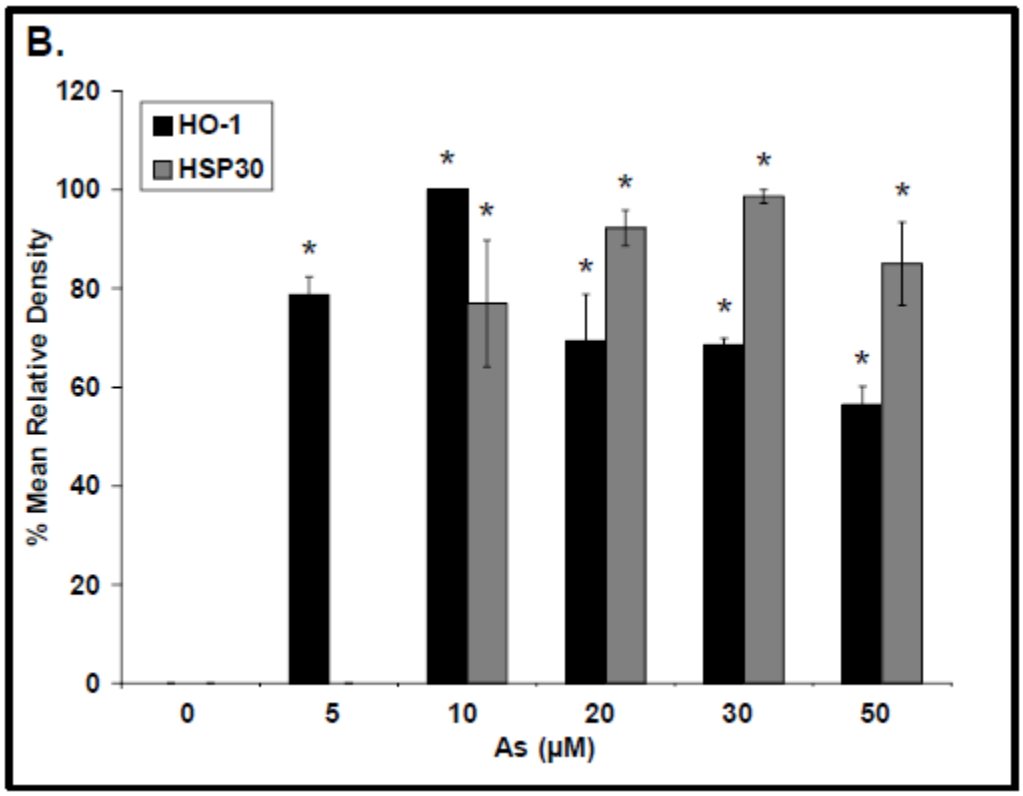
B.
HO-1
HSP30
% Mean Relative Density
120
100
80
60
40
20
0
0
5
10
20
30
50
As (μM)

Figure 10. Effect of cycloheximide on HO-1 and HSP30 accumulation in cells treated with sodium arsenite and cadmium chloride. A) Cells were incubated at 22 °C (C) or treated with 30 μM As for 24 h or 100 μM Cd for 12 h at 22 °C, with or without 6 h pre-treatment with 100 μM cycloheximide (CHX). After treatment, total protein was isolated and subjected to immunoblot analysis as detailed in Materials and methods.

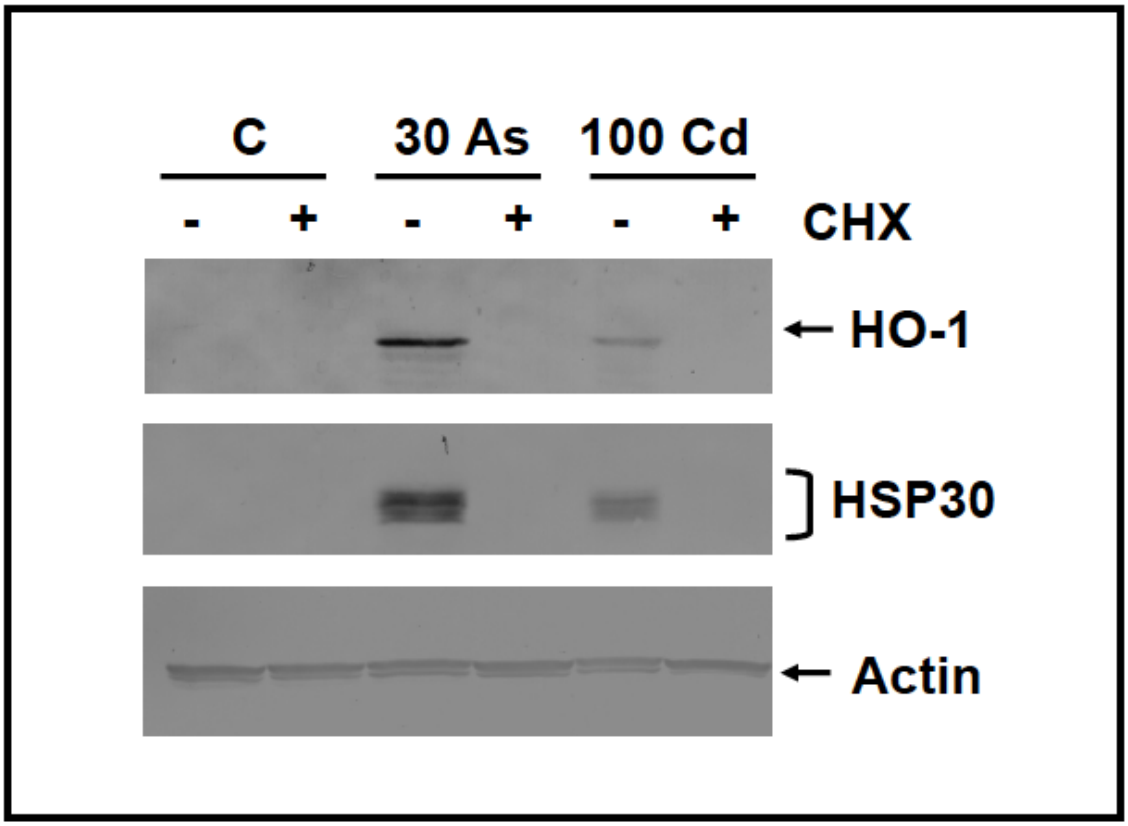
C
30 As
100 Cd
- + - + - +
CHX
← HO-1
HSP30
← Actin

Figure 11. Time course of sodium arsenite-induced HO-1 and HSP30 accumulation. A) Cells were incubated with 30 μM As at 22 °C for 0, 4, 8, 12, 24 or 48 h. After treatment, total protein was isolated and subjected to immunoblot analysis as detailed in Materials and methods. B) Densitometric analysis of the band intensity for HO-1 (black; panel B) and HSP30 (grey; panel B) utilized Image J software. The results were expressed as a percentage of the maximum band intensity acquired for each protein in each trial (48 h for both HO-1 and HSP30). Vertical error bars denote the standard error. A one-way ANOVA with a Tukey's Multiple Comparisons post-test was used to determine significance. Significant differences between the control cells and treated cells are indicated as * ($p < 0.05$). These results are representative of 3 separate experiments.

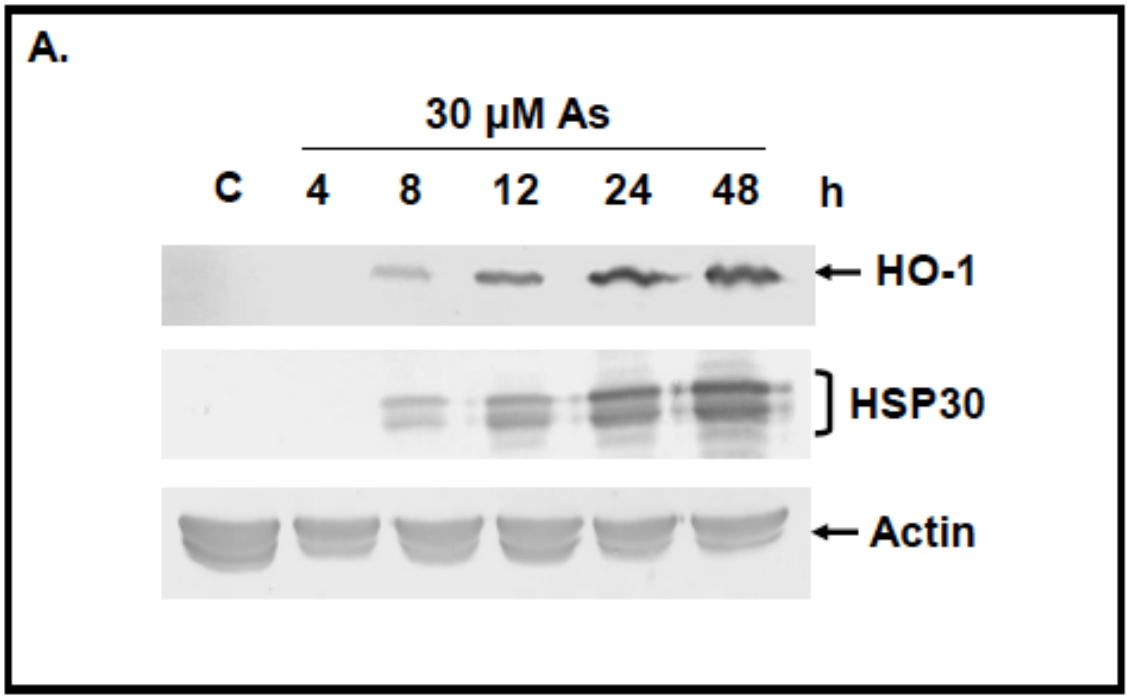
A.
30 μM As
C
4
8
12
24
48
h
HO-1
HSP30
Actin

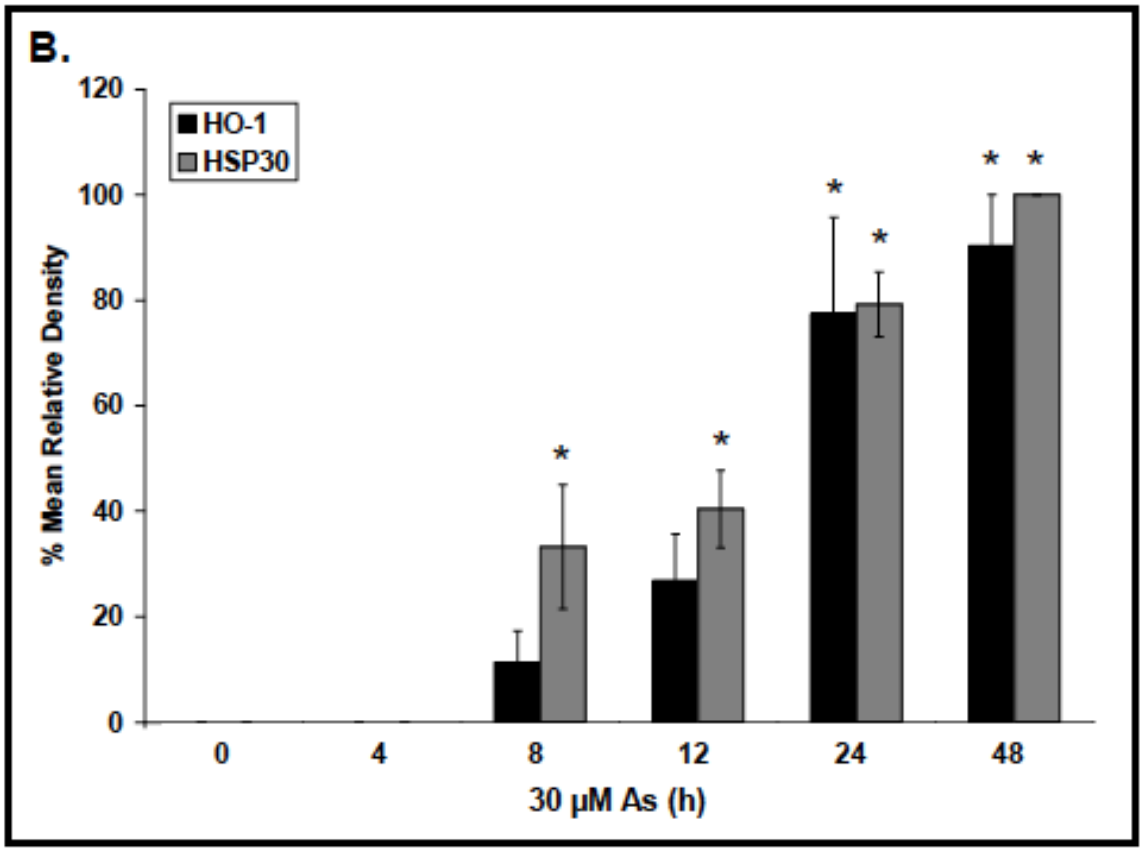
B.
HO-1
HSP30
% Mean Relative Density
120
100
80
60
40
20
0
0
4
8
12
24
48
30 μM As (h)
*

In a comparable analysis with cadmium chloride, both HO-1 and HSP30 accumulation was detectable at 50 μM cadmium chloride, peaked at 100 μM and then declined to slightly lower relative levels at 200 μM (Fig. 12A). Densitometric analysis determined that the relative level of HO-1 accumulation at 50 and 200 μM were 81 and 32% of maximal values, respectively, whereas HSP30 values at the same concentrations were 54 and 73%, respectively, of the maximum density (Fig. 12B). The cadmium chloride-induced accumulation of HO-1 and HSP30 was also inhibited by cycloheximide indicating that the enhanced accumulation was the result of *de novo* synthesis (Fig. 10). Additionally, in temporal studies with 100 μM cadmium chloride minimal relative levels of HO-1 and HSP30 accumulation were first detected at 8 h and then increased in a time dependent manner up to 48 h (Fig. 13A). Densitometric analysis revealed that the relative values of HO-1 accumulation at 8, 12, and 24 h were 7, 44 and 49%, respectively, of the maximum value. Treatments of 8, 12, and 24 h induced relative HSP30 accumulation of 25, 43, and 92%, respectively, compared to the 48 h treatment (Fig. 13B).

3.4. Localization of sodium arsenite- and cadmium chloride-induced HO-1 and HSP30

Immunocytochemistry and laser scanning confocal microscopy was used to examine the effect of heat shock, sodium arsenite, and cadmium chloride on HO-1 and HSP30 localization in *Xenopus* A6 cells. HO-1 was not detected under heat shock conditions (Fig. 14), whereas HSP30 was detected in approximately 85% of cells (Fig. 15). Of the cells treated with 10 μM sodium arsenite for 24 h, approximately 80% exhibited detectable HO-1 and HSP30 accumulation. Interestingly, in response to sodium arsenite stress, 20% of the cells displayed HO-1 accumulation in larger structures (yellow arrows). Cadmium chloride

Figure 12. Effect of different concentrations of cadmium chloride on HO-1 and HSP30 accumulation. A) Cells were incubated at 22 °C (C) or treated with 25, 50, 100, or 200 μM cadmium chloride (Cd) at 22 °C for 24 h. After treatment, total protein was isolated and subjected to immunoblot analysis as detailed in Materials and methods. B) Densitometric analysis of the band intensity for HO-1 (black; panel B) and HSP30 (grey; panel B) employed Image J software. The results were expressed as a percentage of the maximum band intensity acquired for each protein in each trial (100 μM for both HO-1 and HSP30). Vertical error bars denote the standard error. A one-way ANOVA with a Tukey's Multiple Comparisons post-test was used to determine significance. Significant differences between the control cells and treated cells are indicated as * ($p < 0.05$). The data are representative of 3 separate experiments.

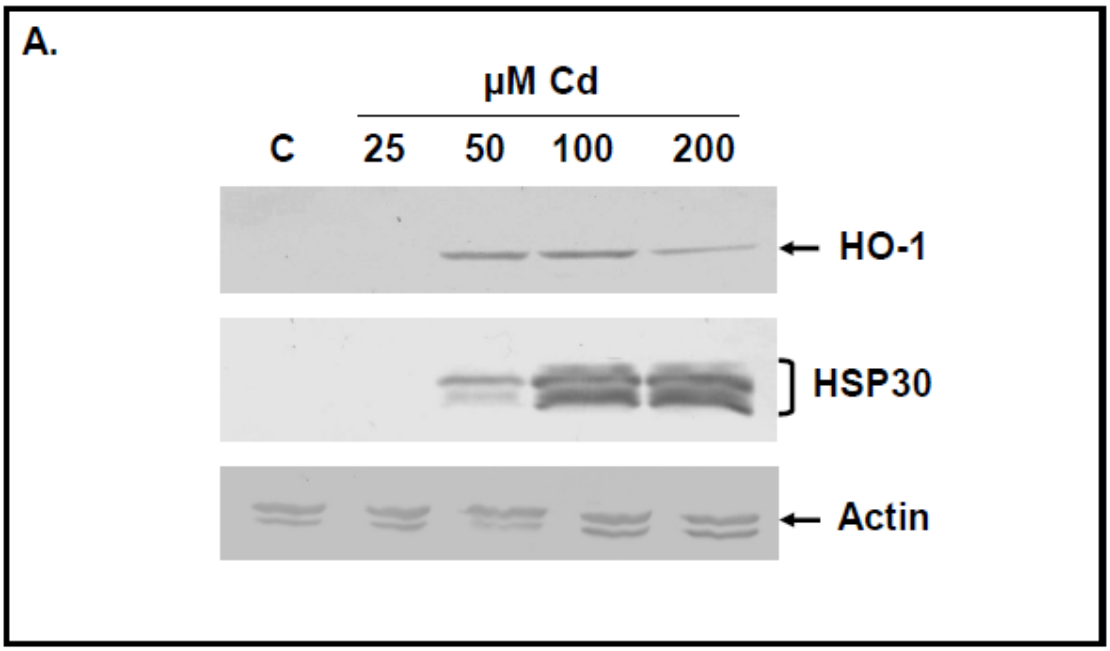
A.
μM Cd
C
25
50
100
200
HO-1
HSP30
Actin

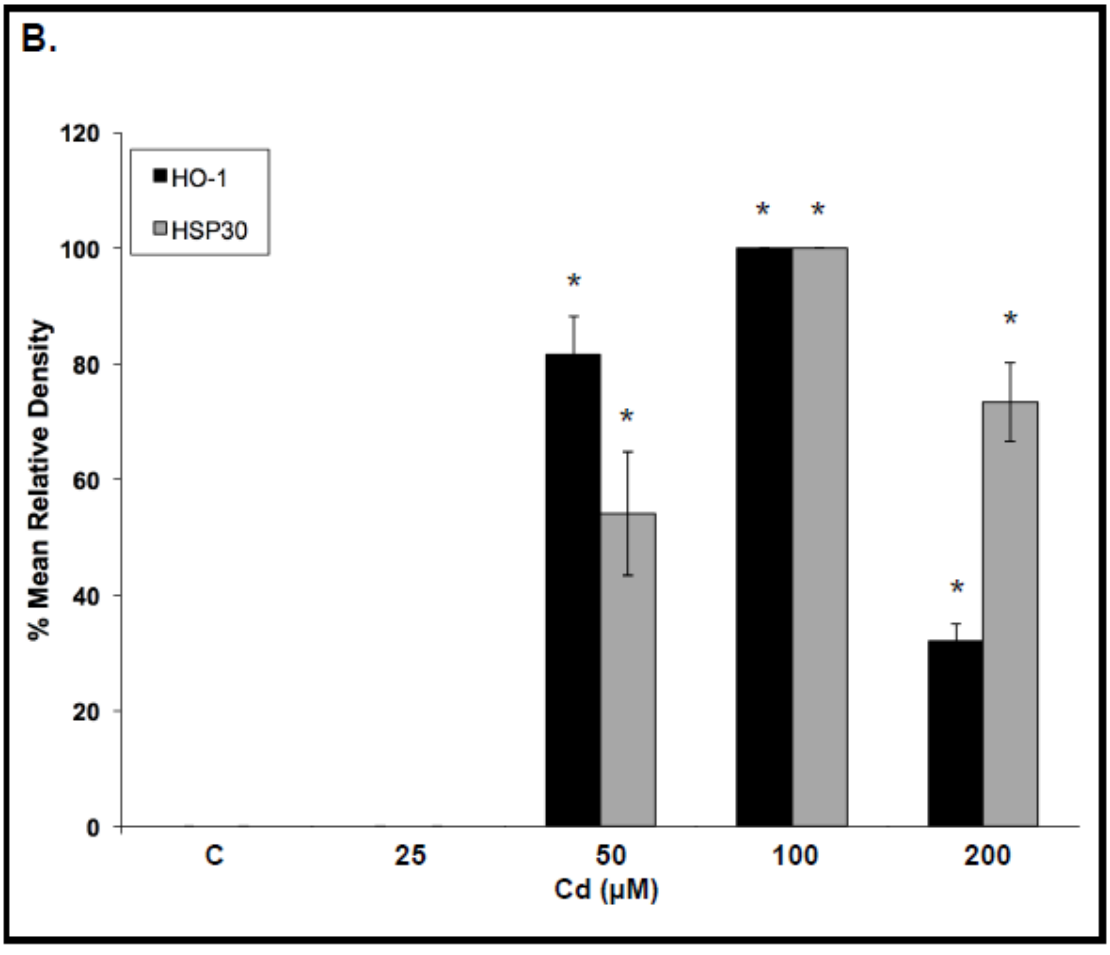
B.
HO-1
HSP30
% Mean Relative Density
120
100
80
60
40
20
0
C
25
50
100
200
Cd (μM)

Figure 13. Time course of cadmium chloride-induced HO-1 and HSP30 accumulation. A) Cells were incubated with 30 μM of cadmium chloride (Cd) at 22 °C for 0, 4, 8, 12, 24, or 48 h. After treatment, total protein was isolated and subjected to immunoblot analysis as detailed in Materials and methods. B) Densitometric analysis of the band intensity for HO-1 (black; panel B) and HSP30 (grey; panel B) was performed using Image J software. The results were expressed as a percentage of the maximum band intensity acquired for each protein in each trial (48 h for both HO-1 and HSP30). Vertical error bars denote the standard error. A one-way ANOVA with a Tukey's Multiple Comparisons post-test was used to determine significance. Significant differences between the control cells and treated cells are indicated as * ($p < 0.05$). The data are representative of 3 separate experiments.

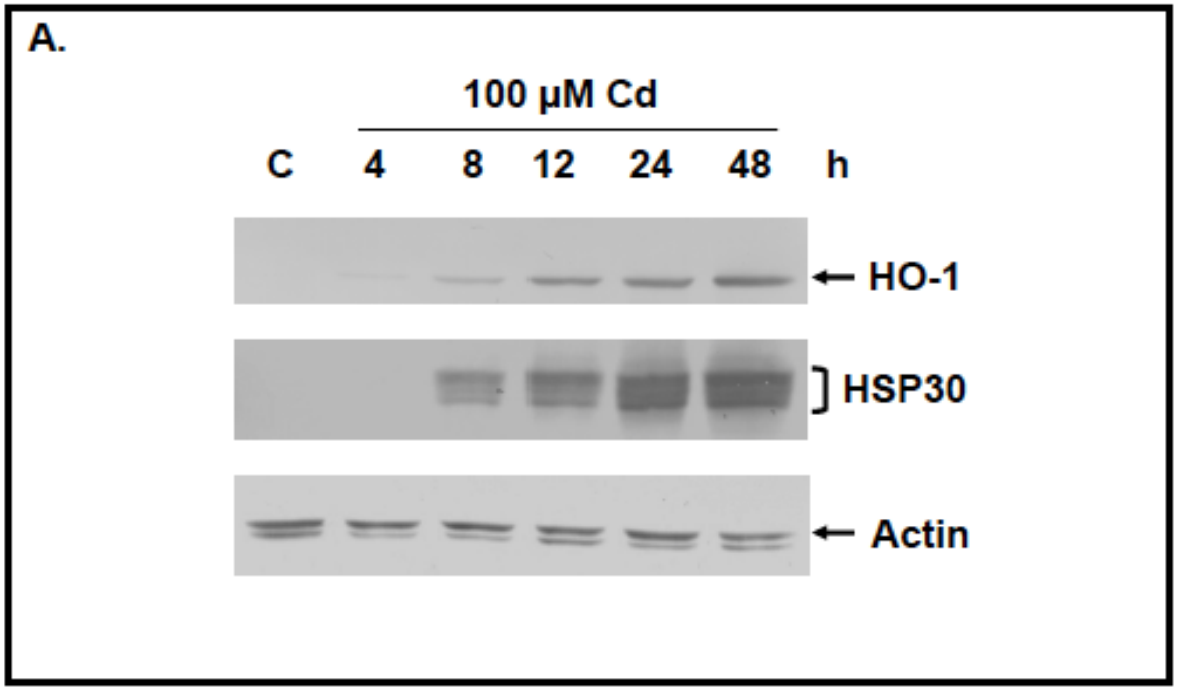
A.
100 μM Cd
C
4
8
12
24
48
h
HO-1
HSP30
Actin

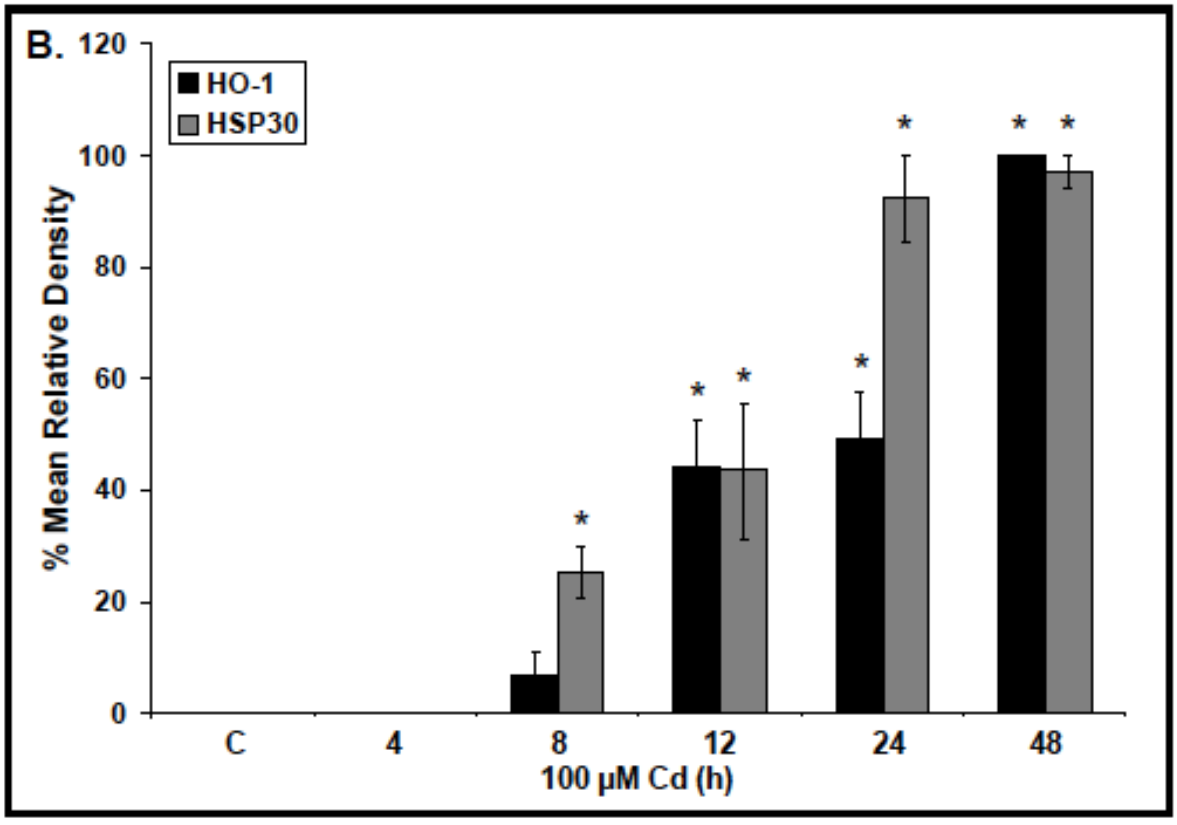
B.
HO-1
HSP30
% Mean Relative Density
120
100
80
60
40
20
0
C
4
8
12
24
48
100 μM Cd (h)

Figure 14. Effect of heat shock, sodium arsenite and cadmium chloride on the localization of HO-1 in A6 cells. Cells were cultured on base-washed glass coverslips, and then either maintained at 22 °C (C), heat shocked at 33 °C (HS) for 2 h with 2 h recovery, or treated with 10 μM sodium arsenite or 100 μM cadmium chloride for 24 h. Actin and nuclei staining were done directly with phalloidin conjugated to TRITC (red) and DAPI (blue), respectively. HO-1 was detected with rabbit anti-HO-1 antibody, and a secondary antibody conjugated to Alexa-488 (green). The columns, from left to right, show the fluorescence detection channels for actin, HO-1, and combined actin, nuclei (DAPI), and HO-1, respectively. The LSCM procedure was followed as outlined in the Materials and methods. White arrows indicate ruffling of F-actin cytoskeleton, observed in stressed cells. Yellow arrows indicate larger anti-HO-1 antibody staining structures. The 20 μm scale bars are indicated at the bottom right corner of each panel.

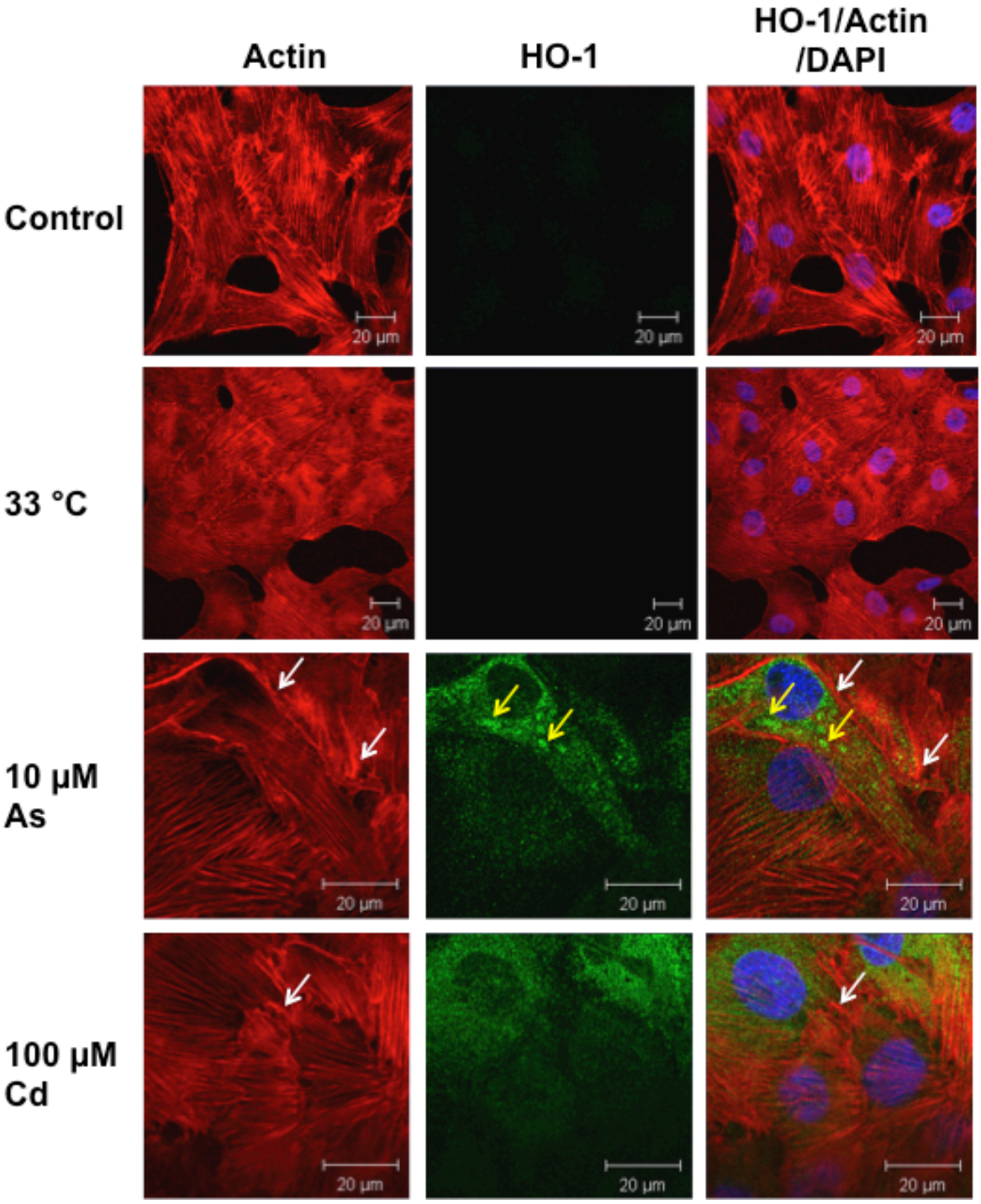
Actin
HO-1
HO-1/Actin
/DAPI
Control
33 °C
10 μM
As
100 μM
Cd
20 μm

Figure 15. Effect of heat shock, sodium arsenite and cadmium chloride on the localization of HSP30 in A6 cells. Cells were cultured on base-washed glass coverslips, and then either maintained at 22 °C (C), heat shocked at 33 °C (HS) for 2 h with 2 h recovery, or treated with 10 μM sodium arsenite or 100 μM cadmium chloride for 24 h. Actin and nuclei staining were done directly with phalloidin conjugated to TRITC (red) and DAPI (blue), respectively. HSP30 was detected with the polyclonal rabbit anti-HSP30 antibody, and a secondary antibody conjugated to Alexa-488 (green). The columns, from left to right, show the fluorescence detection channels for actin, HSP30, and combined actin, nuclei (DAPI), and HSP30, respectively. The LSCM procedure was followed as outlined in the Materials and methods. White arrows indicate ruffling of F-actin cytoskeleton, observed in stressed cells. The 20 μm scale bars are indicated at the bottom right corner of each panel.

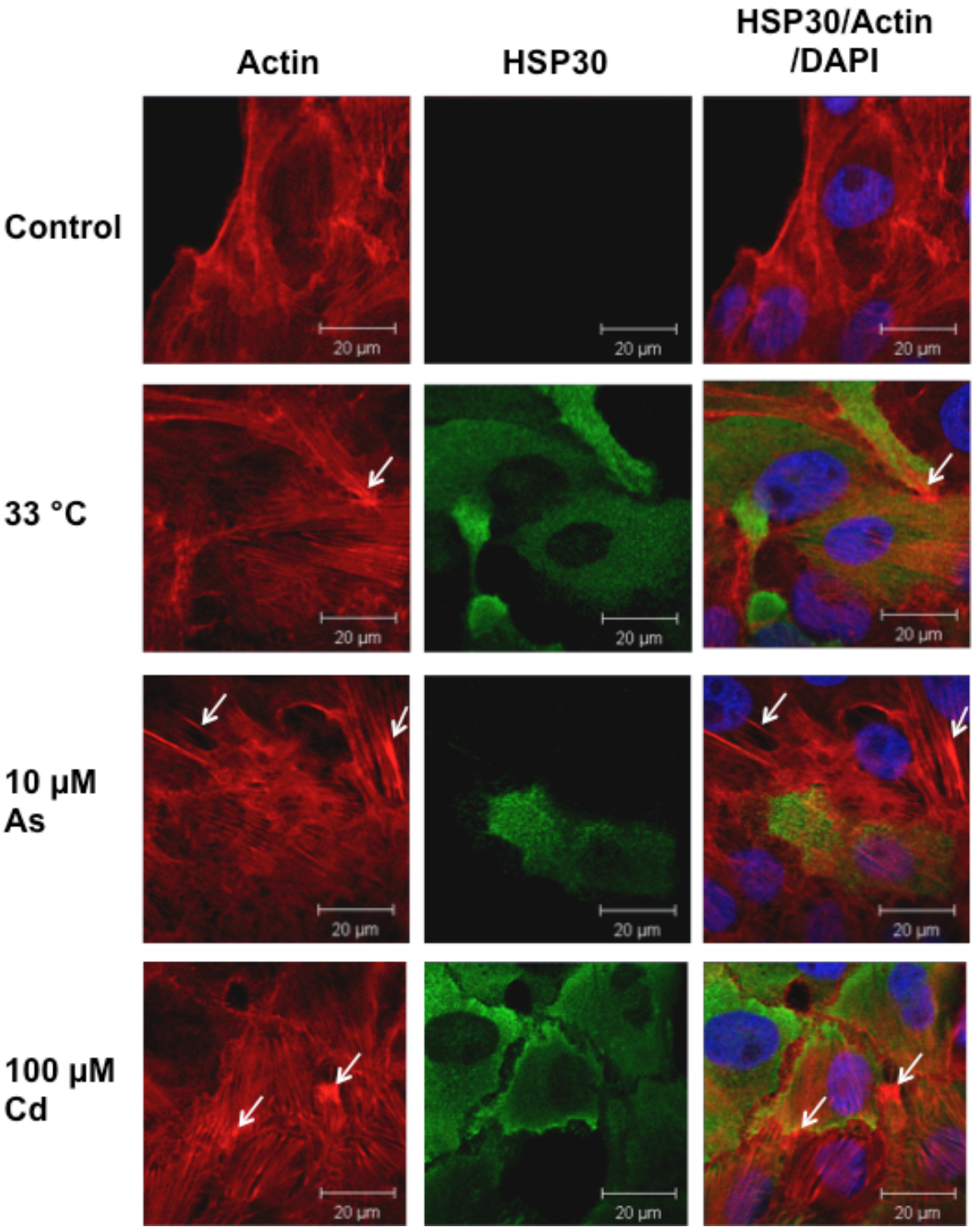
Actin
HSP30
HSP30/Actin /DAPI
Control
33 °C
10 µM As
100 µM Cd
20 µm

induced HO-1 and HSP30 accumulation was detected in approximately 80% of cells. The stressed A6 cells displayed stress fibers and an intact F-actin cytoskeleton, similar to control cell morphology. However, membrane ruffling (white arrows) was observed in cells that were heat shocked or treated with sodium arsenite or cadmium chloride.

3.5. HO-1 and HSP30 accumulation in cells recovering from sodium arsenite and cadmium chloride

The next phase of this study examined the relative levels of HO-1 and HSP30 accumulation during recovery from chemical treatments. A6 cells were subjected to a 24 h 30 μM sodium arsenite treatment followed by recovery in fresh media. Interestingly, the relative levels of HO-1 increased during recovery up to 12 h followed by a decrease at 24 h and a 4-fold reduction at 48 h (Fig. 16A). Similar results were observed for the relative levels of HSP30, with an increase in accumulation from 0 to 12 h recovery, followed by a decrease in HSP30 accumulation after 24 h of recovery, and a two-fold reduction at 48 h recovery compared to maximal values (Fig. 16B). In order to monitor the decay pattern of HO-1 during recovery after a 24 h sodium arsenite pretreatment in the absence of translation, cycloheximide (CHX), a protein synthesis inhibitor, was employed. As shown in Figure 17, preincubation of cells with 100 μM CHX for 6 h completely inhibited the sodium arsenite-induced transient accumulation of both HO-1 and HSP30 after 12 h of recovery such that the relative levels of these proteins decreased gradually over 48 h. Additionally, following recovery from 12 h of 100 μM cadmium chloride treatment, a transient increase in the relative levels of HO-1 and HSP30 was observed at 24 h recovery before decreasing to lower levels (Fig. 18). While it is likely that *de novo* synthesis is responsible for this transient

Figure 16. HO-1 and HSP30 accumulation during recovery from sodium arsenite treatment. A) Cells were maintained at 22 °C (C) or subjected to a 24 h 30 μM As treatment and then allowed to recover for 0 to 48 h in fresh media at 22 °C. After treatment, total protein was isolated and subjected to immunoblot analysis as detailed in Materials and methods. B) Densitometric analysis of the band intensity for HO-1 (black; panel B) and HSP30 (grey; panel B) employed Image J software. The results were expressed as a percentage of the maximum band intensity acquired with each protein in each trial (12 h recovery time point for HO-1 and HSP30). Vertical error bars denote the standard error. A one-way ANOVA with a Tukey's Multiple Comparisons post-test was used to determine significance. Significant differences between the control cells and treated cells are indicated as * ($p < 0.05$). The data are representative of 3 separate experiments.

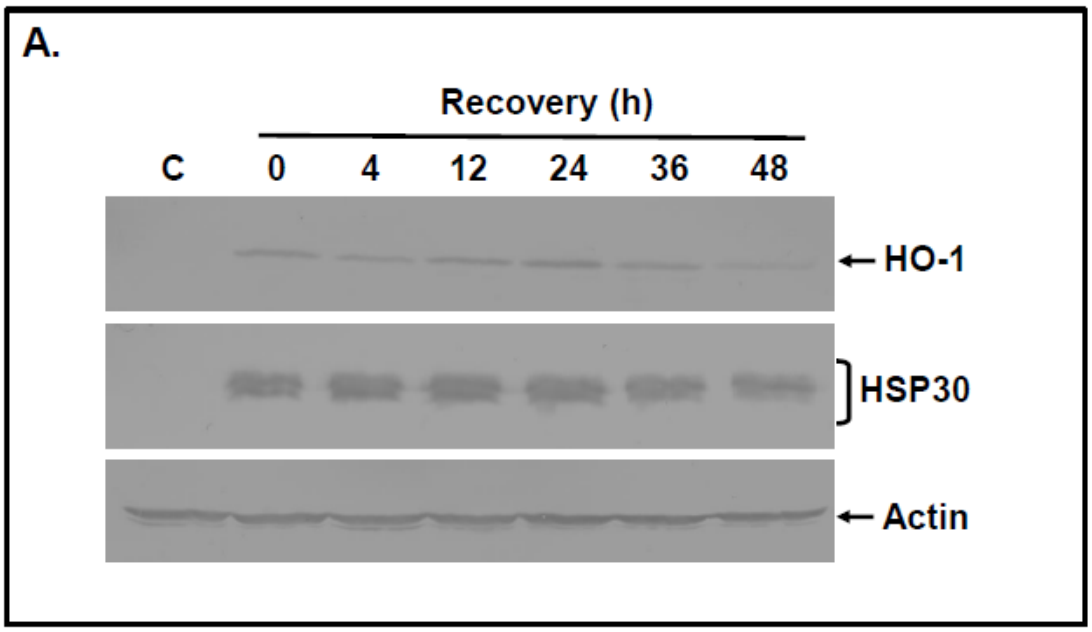
A.
Recovery (h)
C
0
4
12
24
36
48
HO-1
HSP30
Actin

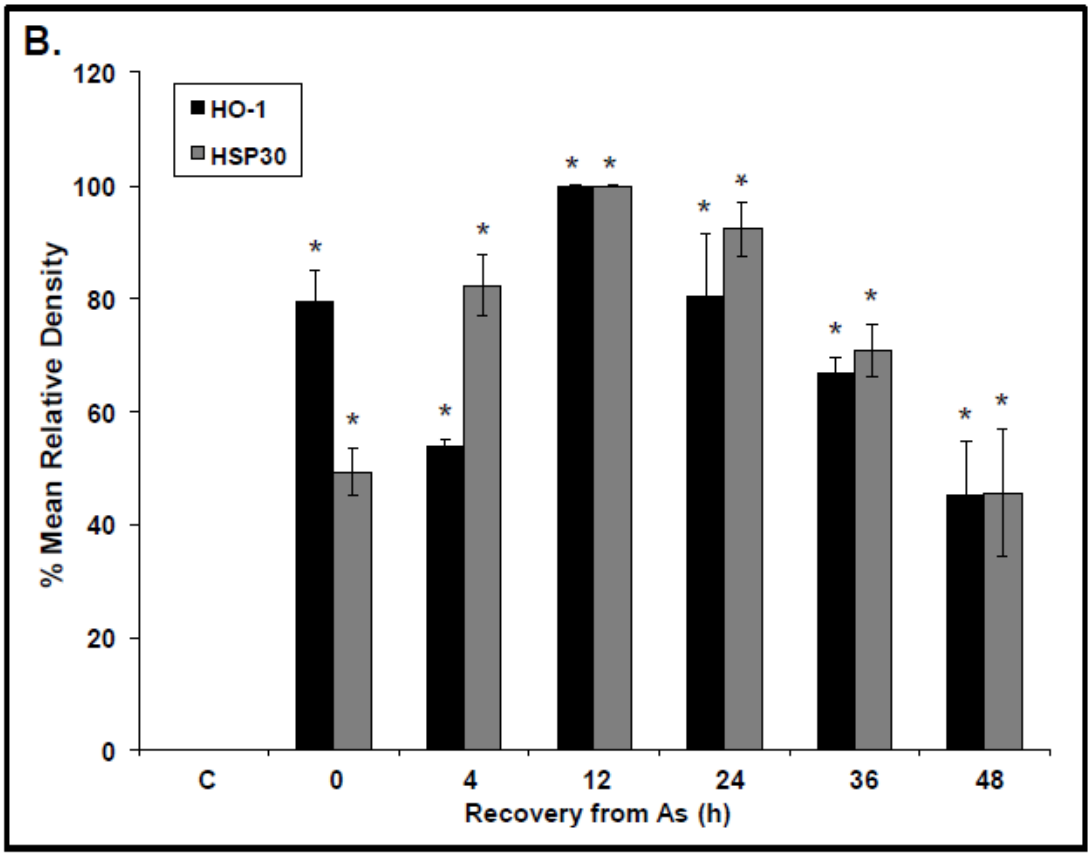
B.
HO-1
HSP30
% Mean Relative Density
120
100
80
60
40
20
0
C
0
4
12
24
36
48
Recovery from As (h)

Figure 17. Effect of cycloheximide on HO-1 and HSP30 accumulation during recovery from sodium arsenite. A) Cells were incubated at 22 °C (C) or treated with 30 μM As at 22 °C for 24 h. Media was then removed and flasks were rinsed once, and 100 μM cycloheximide (CHX) was added to the fresh media and cells were given 0 to 48 h recovery time. After treatment, total protein was isolated and subjected to immunoblot analysis as detailed in Materials and methods. B) Densitometric analysis of the band intensity for HO-1 (black; panel B) and HSP30 (grey; panel B) utilized Image J software. The results were expressed as a percentage of the maximum band intensity acquired for each protein in each trial (no recovery for HO-1 and 4 h recovery for HSP30). Vertical error bars denote the standard error. A one-way ANOVA with a Tukey's Multiple Comparisons post-test was used to determine significance. Significant differences between the control cells and treated cells are indicated as * ($p < 0.05$). The data are representative of 3 separate experiments.

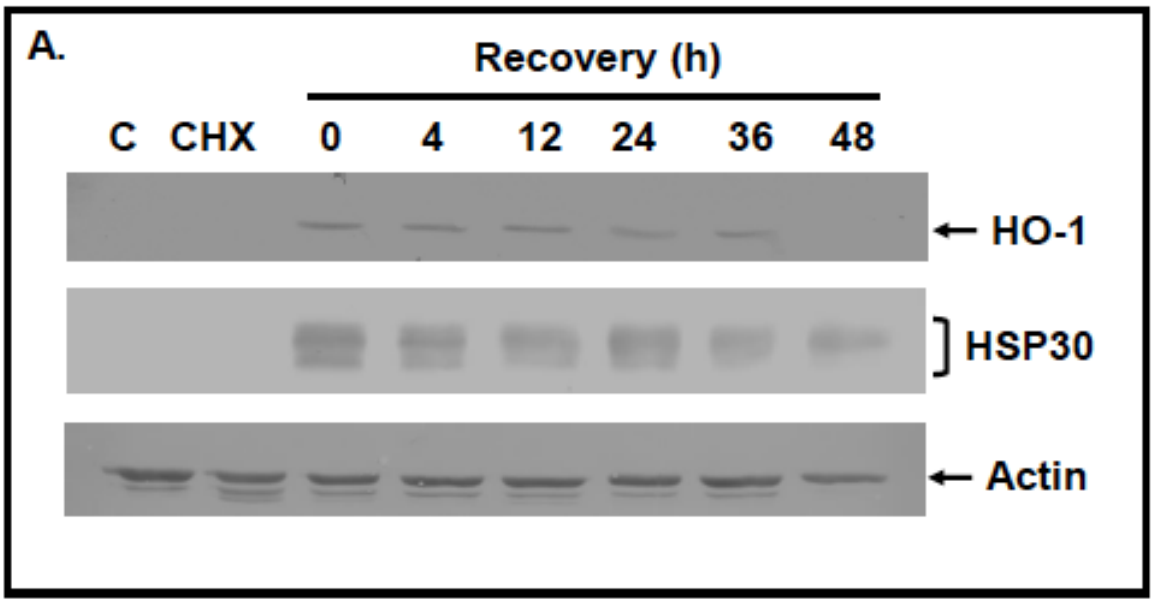
A.
Recovery (h)
C
CHX
0
4
12
24
36
48
HO-1
HSP30
Actin

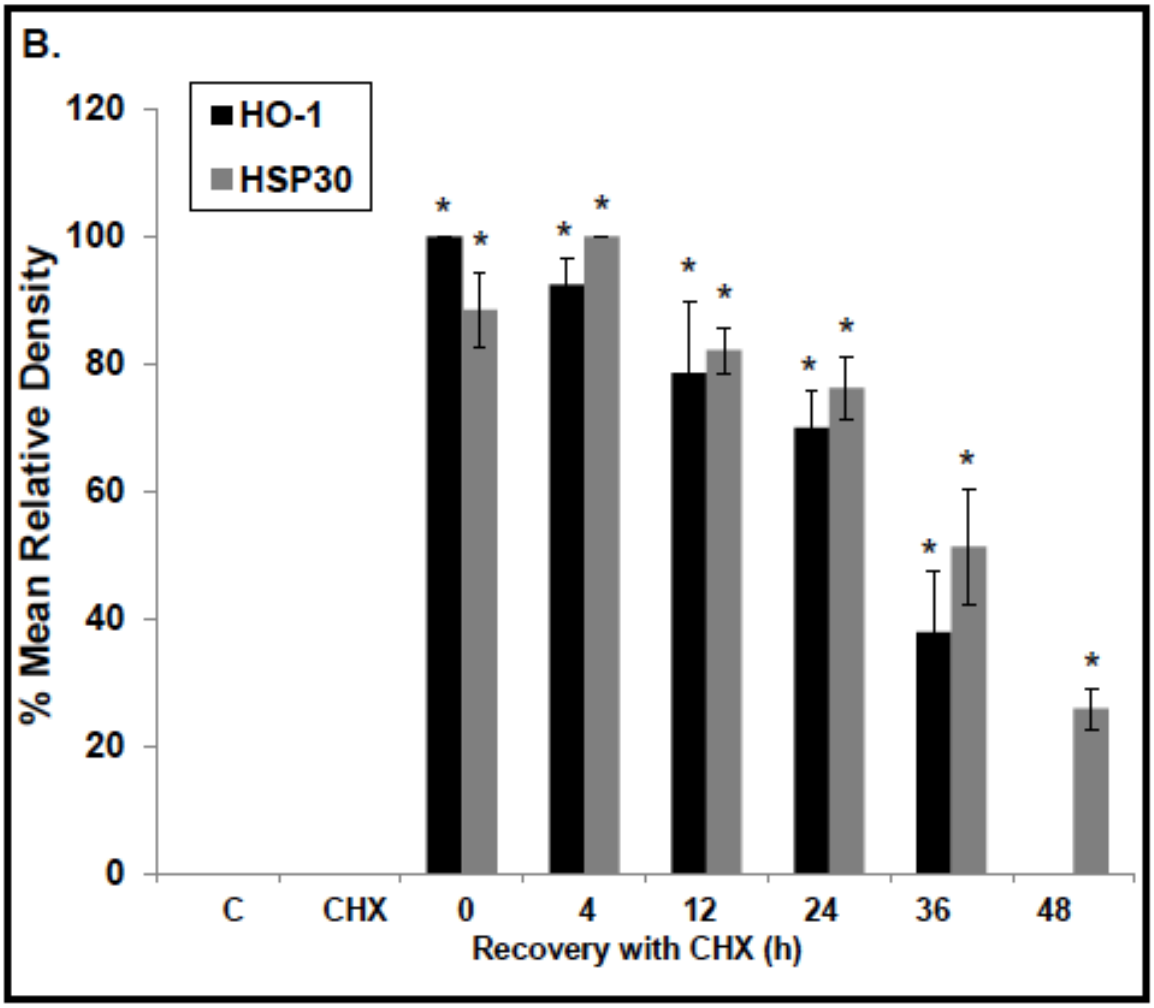
B.
HO-1
HSP30
% Mean Relative Density
120
100
80
60
40
20
0
C
CHX
0
4
12
24
36
48
Recovery with CHX (h)

Figure 18. HO-1 and HSP30 accumulation during recovery from cadmium chloride treatment. A) Cells were maintained at 22 °C (C) or subjected to a 12 h 100 μM Cd treatment and then allowed to recover for 0 to 48 h in fresh media at 22 °C. After treatment, total protein was isolated and subjected to immunoblot analysis as detailed in Materials and methods. Results are representative of two experiments.

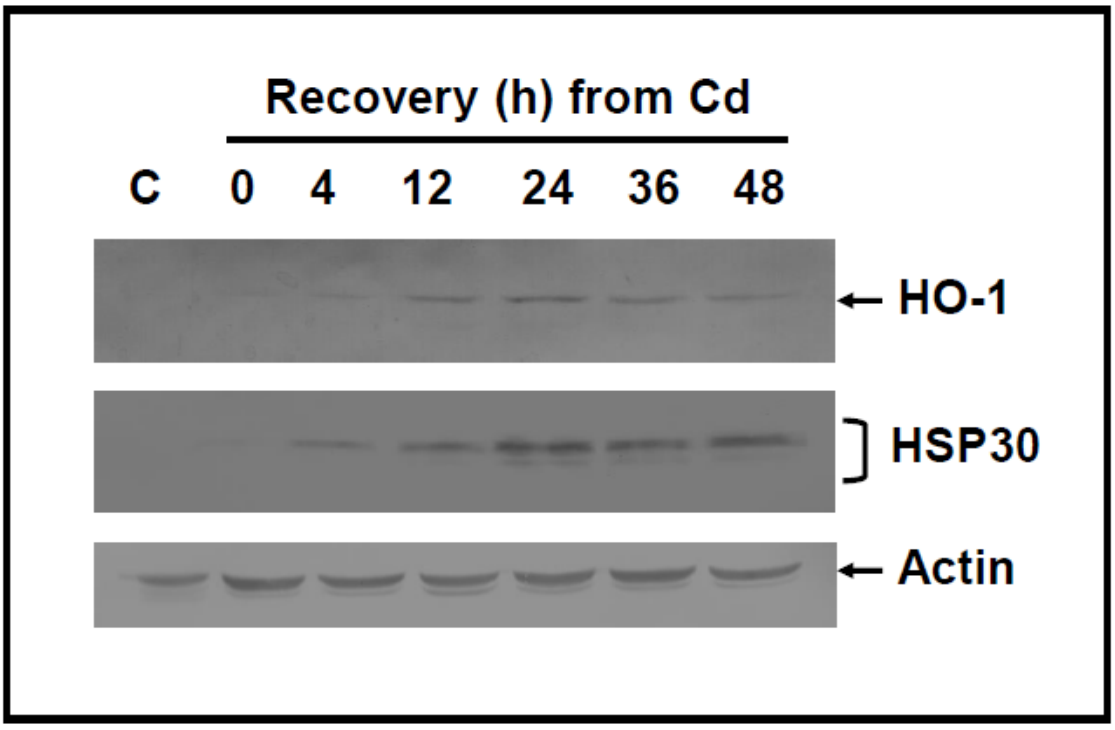
Recovery (h) from Cd
C
0
4
12
24
36
48
HO-1
HSP30
Actin

increase during recovery from cadmium chloride, CHX experiments should be carried out to verify this possibility.

3.6. Mild heat shock combined with chemical stressors increases accumulation of HO-1 and HSP30

In the next phase of this study, experiments were carried out to determine the effect of a mild heat shock in conjunction with either sodium arsenite or cadmium chloride treatment on HO-1 and HSP30 accumulation in A6 cells. Treatment of cells with a mild heat shock of 30 °C for 12 h did not result in detectable levels of HO-1 or HSP30 accumulation (Fig. 19A). Exposure of cells to 10 μM cadmium chloride or 10 μM sodium arsenite for 12 h, individually, resulted in HO-1 accumulation that was 3% and 30%, respectively, compared to maximum levels (Fig. 19B). HSP30 accumulation for these treatments was 0 and 10% compared to the maximum value, although occasionally HSP30 was weakly detected in response to cadmium treatment. The highest relative levels of HO-1 and HSP30 accumulation were detected when cells were subjected to a mild heat shock plus arsenite, which exhibited three-fold and 11-fold increases, respectively, compared to 10 μM sodium arsenite alone. Cadmium and arsenite were also applied concurrently. When the two chemicals were combined HO-1 and HSP30 accumulation were 56% and 16% of the maximum values, respectively.

3.7. MG132 induces HO-1 and HSP30 in a concentration- and time-dependent manner, and HO-1 and HSP30 accumulation in cells recovering from MG132 stress

An examination of the effect of MG132 on HO-1 and HSP30 accumulation revealed

Figure 19. Effect of sodium arsenite or cadmium chloride on HO-1 and HSP30 accumulation with or without a mild heat shock. A) Cells were maintained at 22 °C (C), or incubated with 10 μM As or 10 μM Cd at either 22 or 30 °C. After treatment, total protein was isolated and subjected to immunoblot analysis as detailed in Materials and methods. B) Densitometric analysis of the band intensity for HO-1 (black; panel B) and HSP30 (grey; panel B) utilized Image J software. The results were expressed as a percentage of the maximum band intensity acquired for each protein in each trial (10 μM As plus 30 °C for both HO-1 and HSP30). Vertical error bars denote the standard error. A one-way ANOVA with a Tukey's Multiple Comparisons post-test was used to determine significance. Significant differences between the control cells and treated cells are indicated as * ($p < 0.05$). The data are representative of 3 separate experiments.

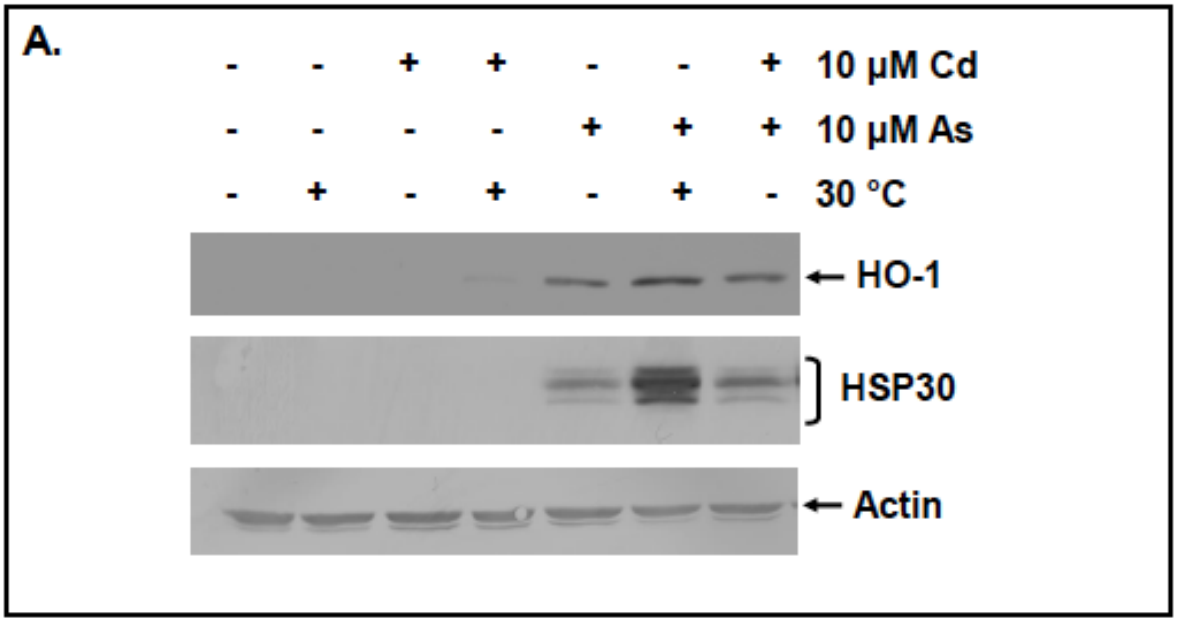
A.
- - + + - - + 10 μM Cd
- - - - + + + 10 μM As
- + - + - + - 30 °C
HO-1
HSP30
Actin

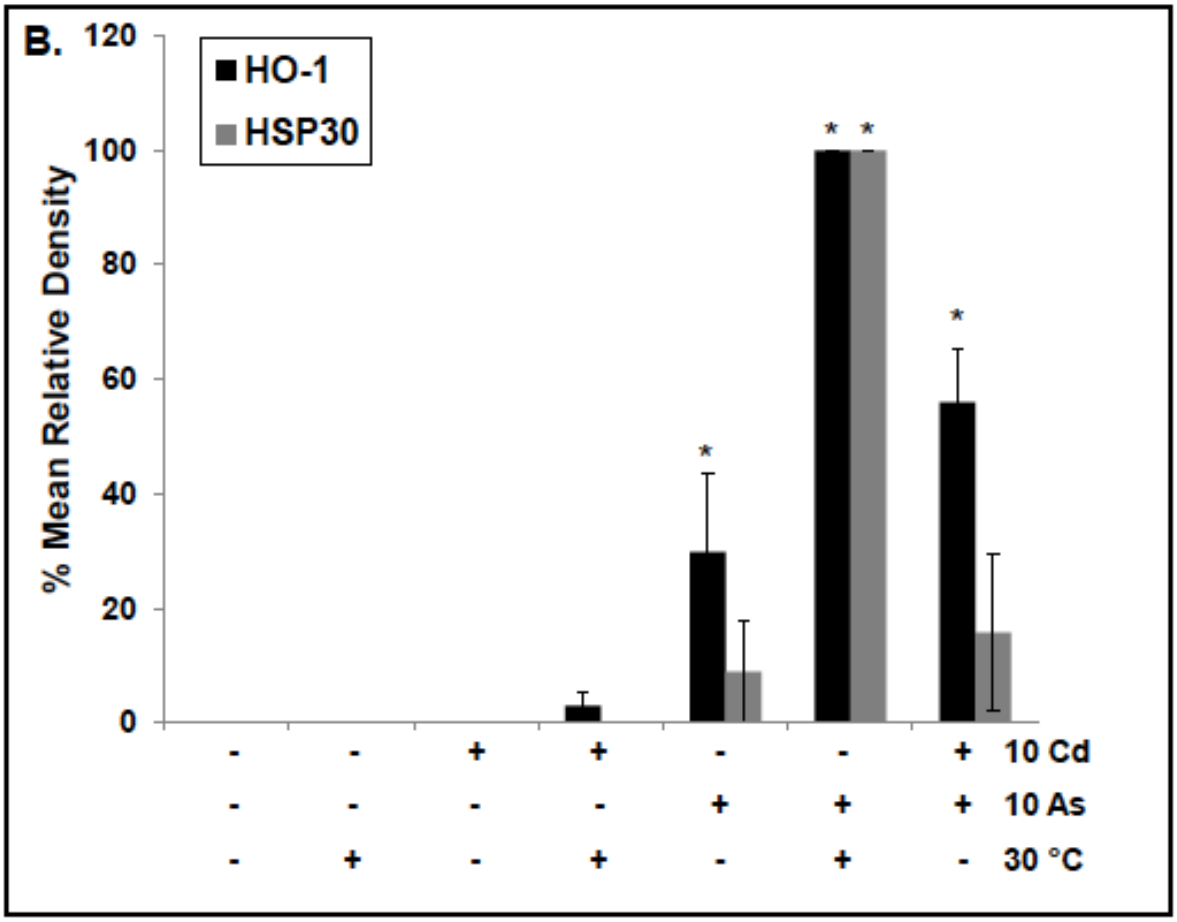
B.
HO-1
HSP30
% Mean Relative Density
120
100
80
60
40
20
0
* * * *
- - + + - - + 10 Cd
- - - - + + + 10 As
- + - + - + - 30 °C

that HO-1 and HSP30 were detectable at 5 μM MG132, peaked at 20 μM with reduced levels at 30 μM (Fig. 20A). Densitometric analysis indicated that HO-1 reduced levels at 30 μM. Densitometric analysis indicated that HO-1 accumulation at 5 μM was 33% of the maximal density, while 10 and 30 μM were 65 and 53%, respectively. Accumulation of HSP30 induced by 5 μM MG132 was 59% of the maximum value, while the relative densities for 10 and 30 μM MG132 treatments were 87 and 68%, respectively (Fig 20B). In time course studies employing 30 μM MG132, minimal HO-1 and HSP30 accumulation was detected at 8 h followed by increasing relative levels in a time-dependent manner up to 48 h (Fig. 21A). Densitometric analysis determined the relative levels of HO-1 accumulation at 8, 12, and 24 h to be 29, 66 and 87%, respectively, of the maximum density. For HSP30, the same time points exhibited relative densities of 16, 45, 76%, respectively, compared to maximal values (Fig. 21B). In cells recovering from MG132 treatment, HO-1 and HSP30 accumulation decayed gradually over 48 h (Fig. 22).

3.8. Localization of MG132-induced HO-1 and HSP30 accumulation, and the effect of a concurrent mild shock shock on MG132-induced accumulation of HO-1 and HSP30

Subsequently, immunocytochemistry and laser scanning confocal microscopy were employed to examine the effect of MG132 on HO-1 and HSP30 localization. HO-1 and HSP30 were detected in approximately 65 and 75% of cells, respectively (Fig. 23). The MG132-treated A6 cells generally displayed an intact F-actin cytoskeleton although membrane ruffling (white arrows) was observed occasionally.

Finally, the effect of a mild heat shock in combination with MG132 on HO-1 and HSP30 accumulation was determined. HO-1 accumulation was induced by 10 μM MG132

Figure 20. Effect of different concentrations of MG132 on HO-1 and HSP30 accumulation. A) Cells were incubated with 0, 5, 10, 20, or 30 μM MG132 at 22 °C for 24 h. Following the different treatments, total protein was isolated and subjected to immunoblot analysis using anti-HO-1, anti-HSP30, and anti-actin antibodies. B) Densitometric analysis of the band intensity for HO-1 (black; panel B) and HSP30 (grey; panel B) employed Image J software. The results were expressed as a percentage of the maximum band intensity acquired for each protein in each trial (20 μM MG132 for both HO-1 and HSP30). Vertical error bars denote the standard error. A one-way ANOVA with a Tukey's Multiple Comparisons post-test was used to determine significance. Significant differences between the control cells and treated cells are indicated as * ($p < 0.05$). The data are representative of 3 separate experiments.

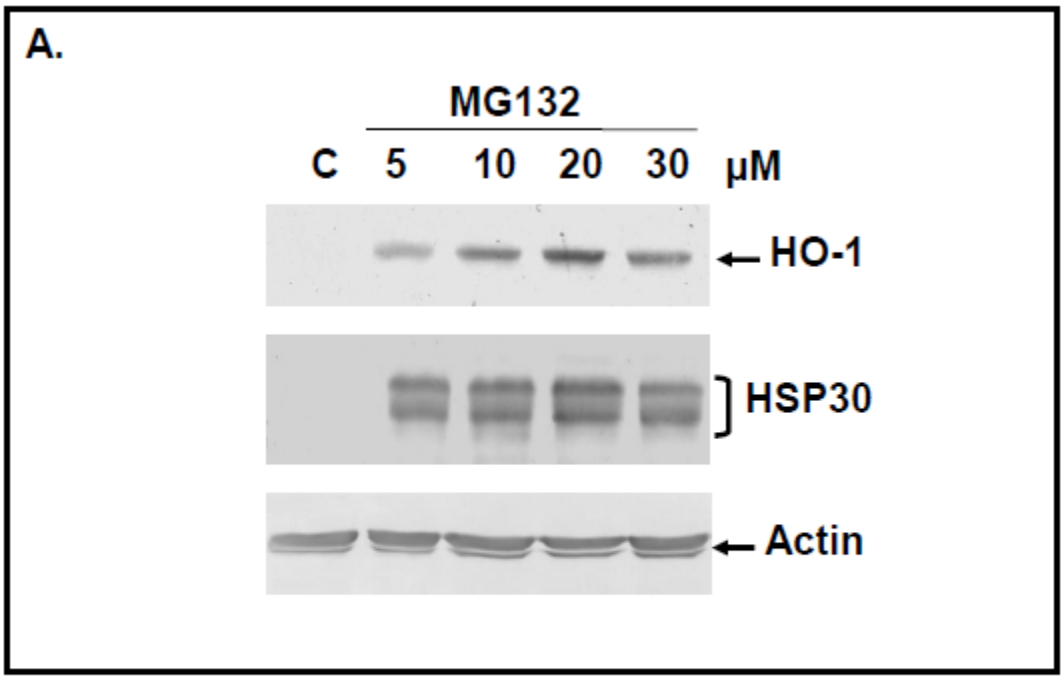
A.
MG132
C
5
10
20
30
μM
HO-1
HSP30
Actin

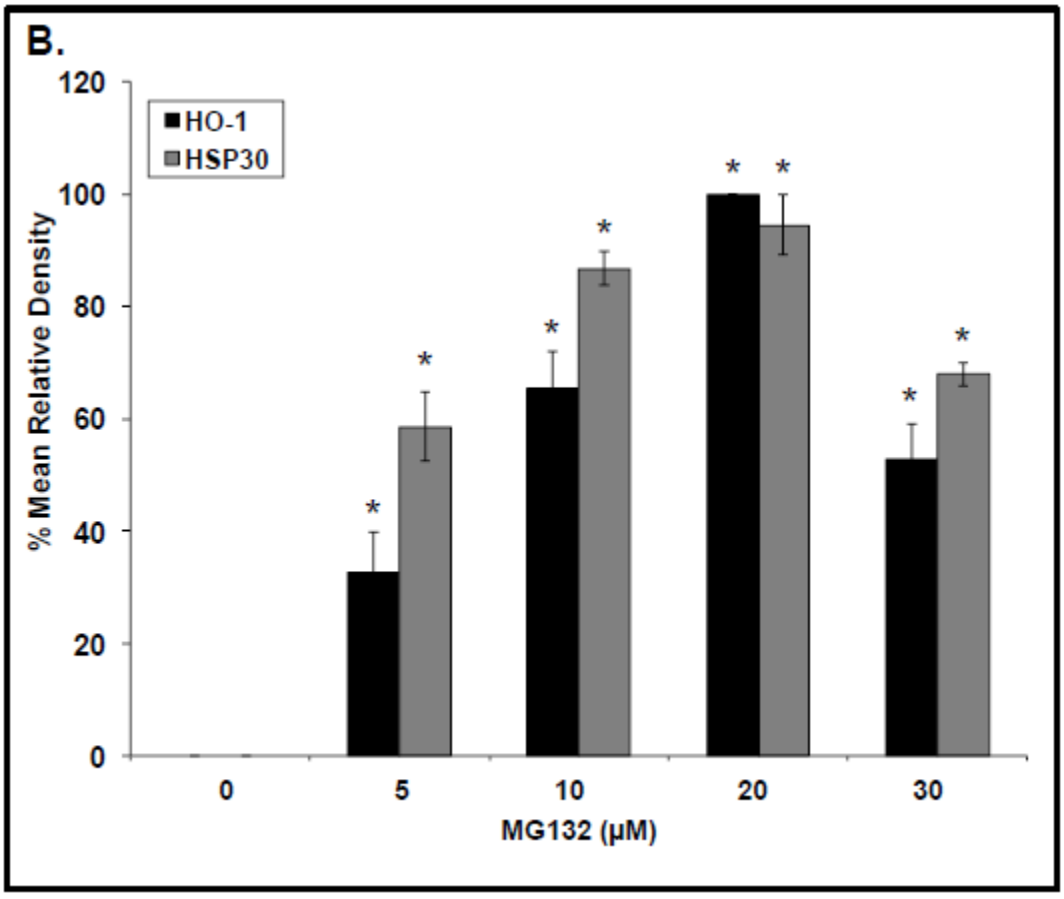
B.
HO-1
HSP30
% Mean Relative Density
120
100
80
60
40
20
0
0
5
10
20
30
MG132 (μM)

Figure 21. Time course of MG132-induced HO-1 and HSP30 accumulation. A) Cells were incubated with 30 μM of MG132 at 22°C for 0, 4, 8, 12, 24, or 48 h. After treatment, total protein was isolated, quantified and subjected to immunoblot analysis as detailed in Materials and methods. B) Densitometric analysis of the band intensity for HO-1 (black; panel B) and HSP30 (grey; panel B) employed Image J software. The results were expressed as a percentage of the maximum band intensity acquired for each protein in each trial (48 h for both HO-1 and HSP30). Vertical error bars denote the standard error. A one-way ANOVA with a Tukey's Multiple Comparisons post-test was used to determine significance. Significant differences between the control cells and treated cells are indicated as * ($p < 0.05$). The data are representative of 3 separate experiments.

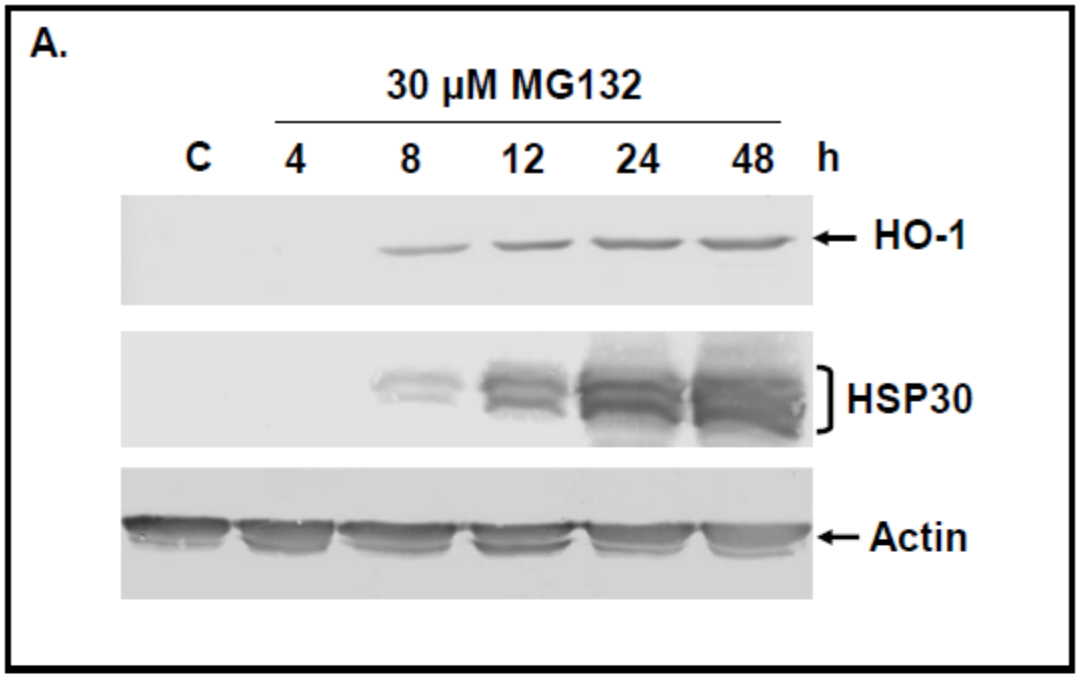
A.
30 μM MG132
C
4
8
12
24
48
h
HO-1
HSP30
Actin

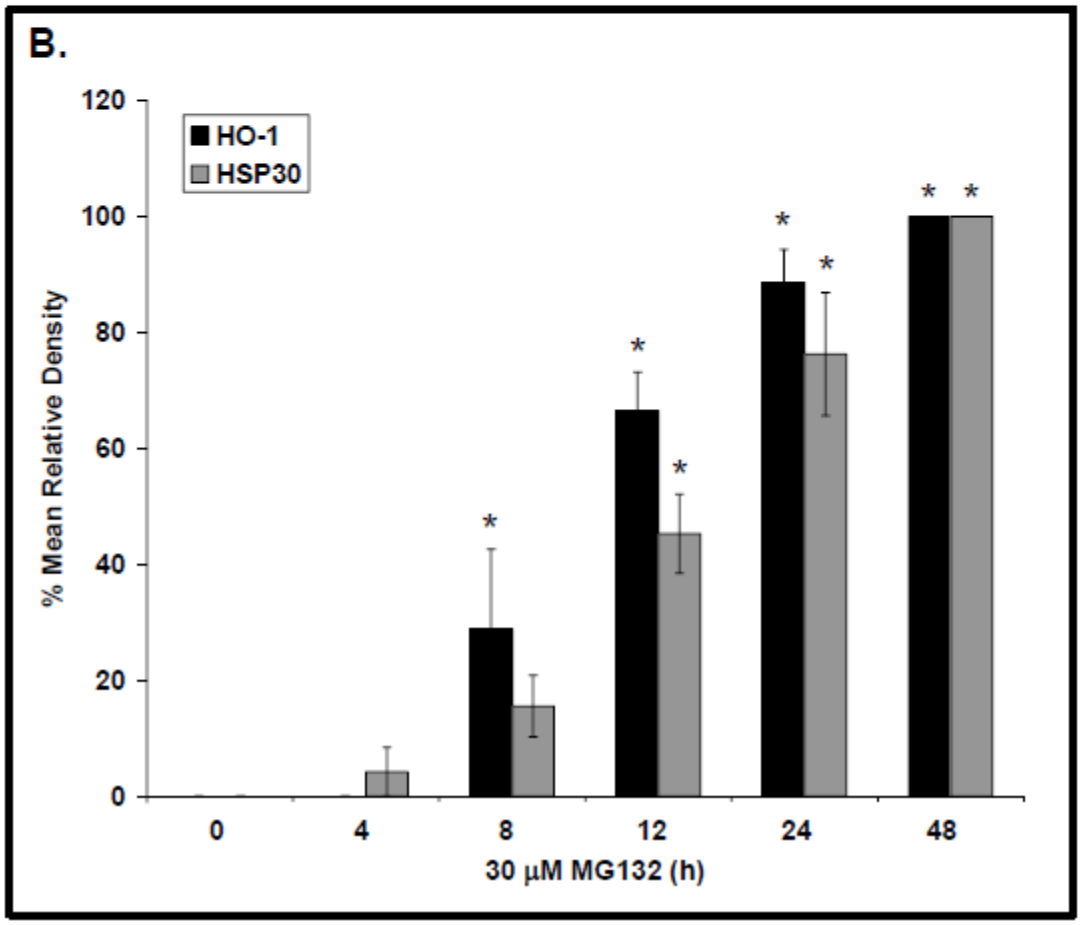
B.
HO-1
HSP30
% Mean Relative Density
120
100
80
60
40
20
0
0
4
8
12
24
48
30 μM MG132 (h)

Figure 22. HO-1 and HSP30 accumulation during recovery from MG132 treatment. A6 cells were maintained at 22 °C (C) or subjected to a 24 h 30 μM MG132 (MG) treatment, then allowed to recover for 0 to 48 h in fresh media at 22 °C. Following treatment, total protein was isolated and subjected to immunoblot analysis as detailed in Materials and methods. Results are representative of two experiments.

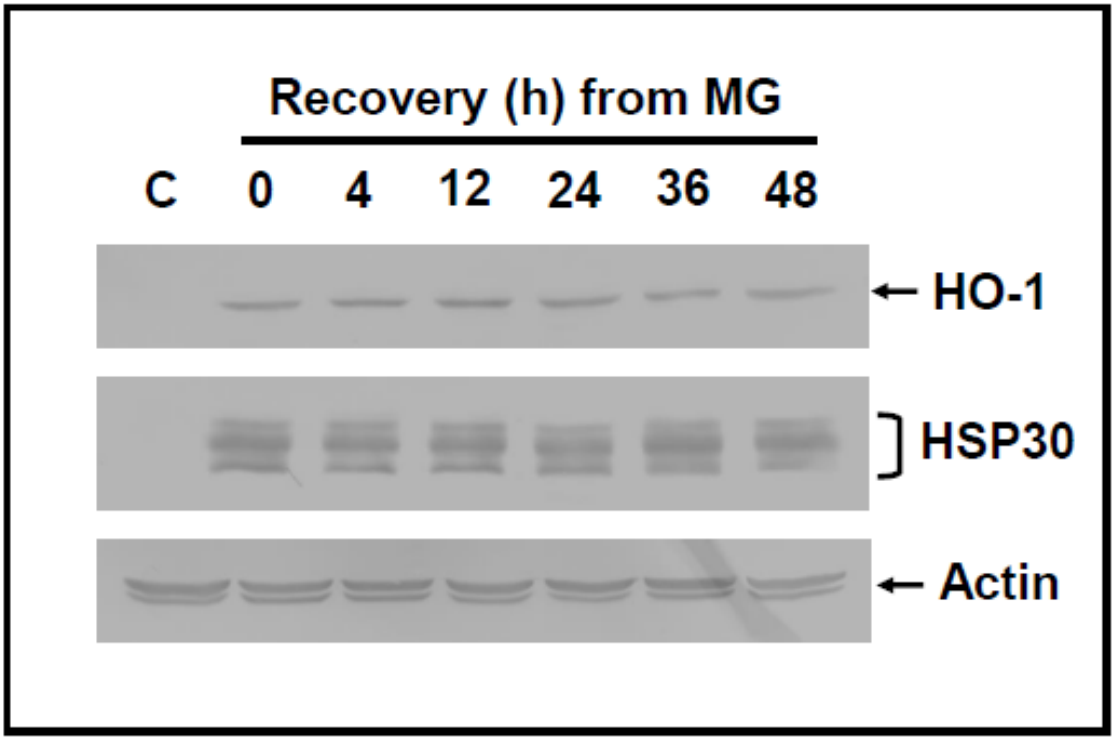
Recovery (h) from MG
C
0
4
12
24
36
48
HO-1
HSP30
Actin

Figure 23. Effect of MG132 on the localization of HO-1 and HSP30 in A6 cells. Cells were cultured on base-washed glass coverslips, and then either maintained at 22 °C (Control) or treated with 20 μM MG132 at 22 °C for 24 h. Actin and nuclei staining were done directly with phalloidin conjugated to TRITC (red) and DAPI (blue), respectively. HO-1 was detected with rabbit anti-HO-1 antibody, and a secondary antibody conjugated to Alexa-488 (green). HSP30 was detected with rabbit anti-HSP30 antibody, and a secondary antibody conjugated to Alexa-488 (green). The columns, from left to right, show the fluorescence detection channels for actin, HO-1 or HSP30, and combined actin, nuclei (DAPI), and HO-1 or HSP30, respectively, as indicated. The LSCM procedure was followed as outlined in the Materials and methods. White arrows indicate ruffling of F-actin cytoskeleton in MG132 treated cells. The 20 μm scale bars are indicated at the bottom right corner of each panel.

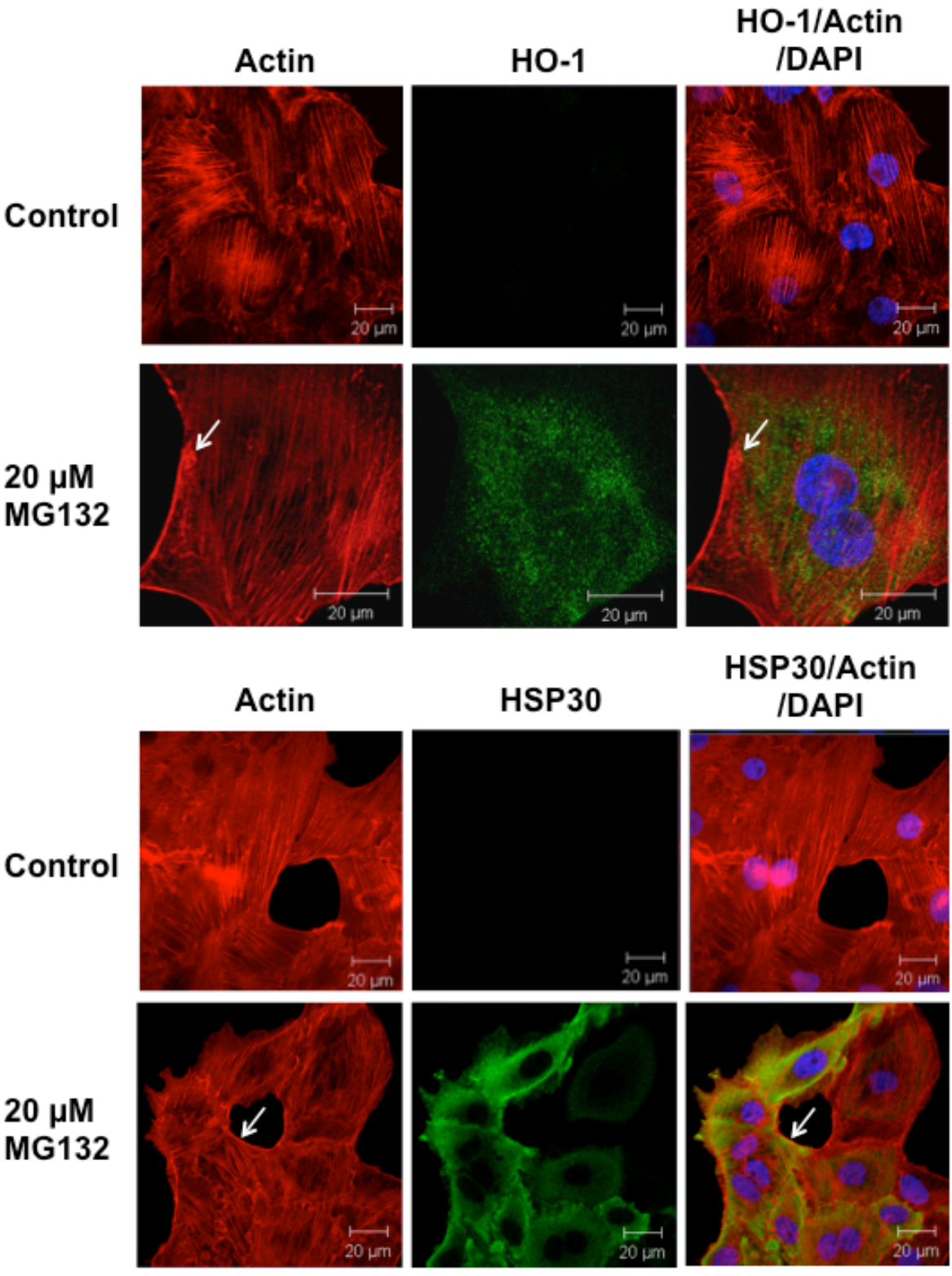
Actin
HO-1
HO-1/Actin /DAPI
Control
20 μM MG132
Actin
HSP30
HSP30/Actin /DAPI
Control
20 μM MG132
20 μm

alone while HSP30 accumulation was not detected at this concentration (Fig. 24). However, when cells were treated concurrently with MG132 and a mild heat shock of 30 °C, an increase in the relative levels of both HO-1 and HSP30 accumulation was observed.

Figure 24. Effect of MG132 on HO-1 and HSP30 accumulation with or without a mild heat shock. A) Cells were maintained at 22 °C (C), or incubated with 10 μM MG132 at either 22 or 30 °C. After treatment, total protein was isolated and subjected to immunoblot analysis as detailed in Materials and methods. B) Densitometric analysis of the band intensity for HO-1 (black; panel B) and HSP30 (grey; panel B) utilized Image J software. The results were expressed as a percentage of the maximum band intensity acquired for each protein in each trial (MG132 plus 30 °C for both HO-1 and HSP30). Vertical error bars denote the standard error. A one-way ANOVA with a Tukey's Multiple Comparisons post-test was used to determine significance. Significant differences between the control cells and treated cells are indicated as * ($p < 0.05$). The data are representative of 3 separate experiments.

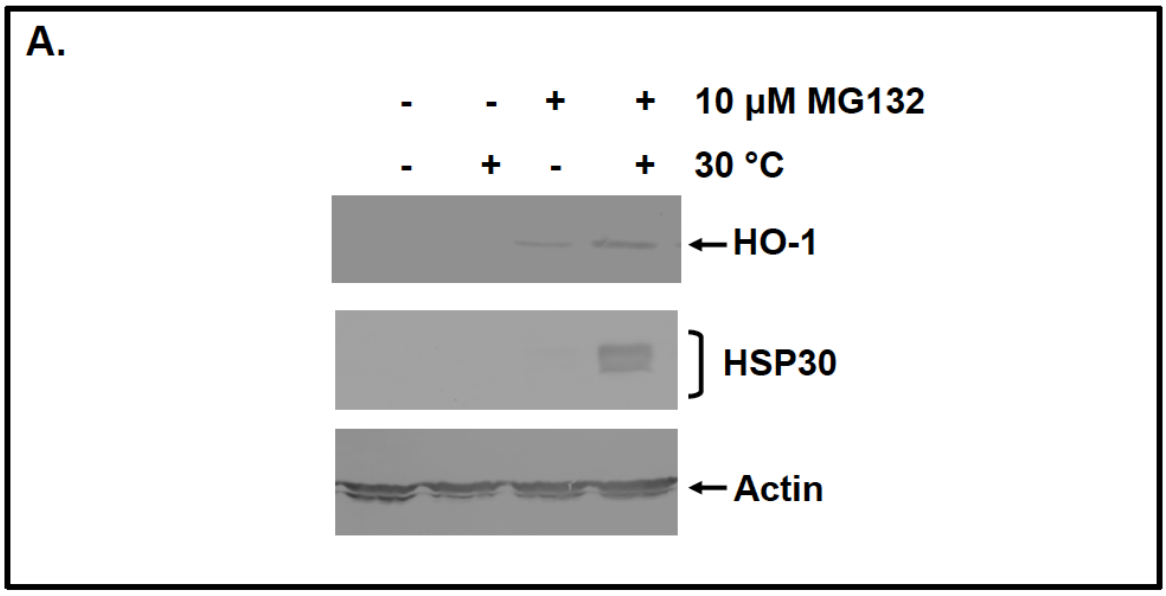
A.
- - + + 10 μM MG132
- + - + 30 °C
HO-1
HSP30
Actin

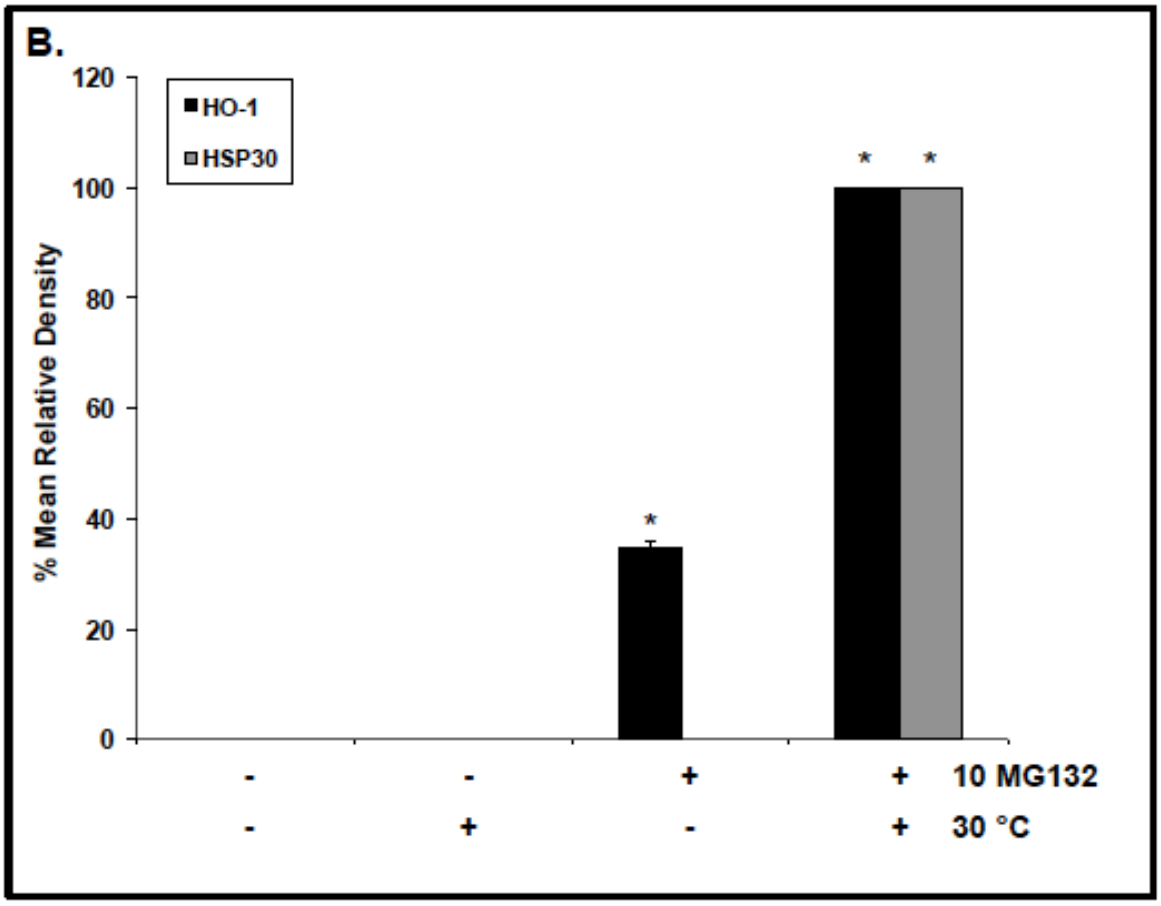
B.
HO-1
HSP30
% Mean Relative Density
120
100
80
60
40
20
0
*
*
*
- - + + 10 MG132
- + - + 30 °C

4. Discussion

The present study has demonstrated, for the first time in *Xenopus laevis,* that treatment with cadmium chloride, sodium arsenite or the proteasomal inhibitor, MG132, induced the accumulation of heme oxygenase-1 (HO-1). Furthermore, the pattern of HO-1 accumulation was compared to HSP30, a member of the small heat shock protein family that has been studied extensively in our laboratory (Young et al., 2009; Heikkila, 2010; Young and Heikkila, 2010; Khan et al., 2012; Khamis and Heikkila, 2013; Khan and Heikkila, 2014).

DNA sequence analysis indicated that the putative *Xenopus laevis* HO-1 cDNA encoded a bona fide HO-1 protein. Amino acid sequence comparison determined that *Xenopus* HO-1 shared identity with HO-1 from other organisms including *Xenopus tropicalis*, chicken, human, alligator and zebrafish. For example, the coding region of HO-1 shared identities of 91% with *X. tropicalis*, 63% with chicken, 59% with human and 45% with zebrafish. However, when a conserved region corresponding to residues P129-R186 of *X. laevis* HO-1 was compared, the percent identity ranged from 100 to 69% in the aforementioned organisms. This region included 4 of the 8 heme binding pocket residues integral for HO-1 function. *X. laevis* HO-1 was compared to the *X. laevis* HO-2 amino acid sequence and determined to share less identity (53%) than with HO-1 from all of the selected species examined except zebrafish. This phenomenon was also reported with rat HO-1 and HO-2, which shared only 43% sequence identity (Rotenberg and Maines, 1990).
Initial immunoblot studies determined that HO-1 accumulation in *X. laevis* A6 cells was not enhanced in response to a 30, 33 or 35 °C heat shock. This finding was in contrast to HSP30, which was strongly induced in the present and previous studies from our laboratory (Krone et

al., 1992; Heikkila, 2010; Khamis and Heikkila, 2013). A lack of heat-inducibility with respect to HO-1 accumulation was also reported in a variety of cell lines, including human alveolar macrophages, hepatoma, glioma, HeLa, fibroblast, erythroblast, and HL60 leukemia (Yoshida et al., 1988; Keyse and Tyrrell, 1989; Taketani et al., 1989; Mitani et al., 1990; Okinaga et al., 1996). Additionally, heat shock induced a decrease in *ho-1* gene expression in spleen and kidney tissue of European sea bass (Hachfi et al., 2012). In contrast to the aforementioned studies, thermal stress enhanced HO-1 accumulation *in vivo* in rat liver, kidney and heart and in European sea bass liver, as well as in murine Sertoli cells, human fibroblasts, and in rat and human hepatoma cell lines (Taketani et al., 1988; Keyse and Tyrrell, 1989; Mitani et al., 1990; Raju and Maines, 1994; Lee et al., 1996; Hachfi et al., 2012; Li et al., 2014). The mechanism(s) responsible for the differences in the heat inducibility of HO-1 accumulation in different cells is not known. Interestingly, studies with a human erythroid cell line revealed that the HSE of the *ho-1* gene was repressed, possibly by transcription factors interacting with a downstream purine-rich region (Okinaga et al., 2006). Unfortunately, the regulatory regions of the *Xenopus laevis ho-1* gene have not been isolated and sequenced. However, the *Xenopus tropicalis* sequence is available (Genbank gene ID: 100488303). By comparing the *Xenopus tropicalis* gene with the available human homolog, it was determined that there is a HSE present in the *X. tropicalis* gene. Given that *X. laevis* and *X. tropicalis* share a 91% amino acid identity, it is possible that the genes are also highly conserved and that the *X. laevis* HO-1 promoter also has a HSE. Thus, it would be of interest to determine if a similar repression mechanism, as described above, occurs during heat shock.

In the present study, treatment of A6 cells with sodium arsenite or cadmium chloride induced both HO-1 and HSP30 accumulation. Previously, sodium arsenite was reported to induce HO-1 in a chicken hepatoma cell line, as well as in the human cell lines, HeLa and HL60 (Taketani et al., 1989; Elbirt et al., 1998; Ryter et al., 2006). Additionally, cadmium chloride induced HO-1 accumulation in soybean plants, fish, and mammalian systems (Taketani et al., 1989; Alam et al., 2000; Balestrasse et al., 2006; Ryter et al., 2006; Søfteland et al., 2010; Williams and Gallagher, 2013). Treatment of *Xenopus* A6 cells with iron sulphate or lead nitrate weakly induced HO-1 but not HSP30 accumulation while zinc sulphate and copper sulphate had no detectable effect on either protein compared to control. An examination of the scientific literature revealed variation in the extent of HO-1 accumulation in a particular tissue/cell type to various metals. For example, in human colon adenocarcinoma cells, it was reported that zinc, but not copper or iron, induced HO-1 accumulation (Smith and Loo, 2012). However, copper and iron were reported to induce HO-1 accumulation in rat liver while copper induced HO-1 in human liver cell lines (Song and Freedman, 2005; Hait-Darshan et al., 2009; Mizukami et al., 2010). Additionally, lead induced HO-1 accumulation in rat kidney, and in rat astrocytes by causing oxidative stress (Vargas et al., 2003; Cabell et al., 2004). The reasons for these differential effects on HO-1 accumulation by these different heavy metals are not known.

In A6 cells treated with sodium arsenite, cadmium chloride or MG132, concentration- and time-dependent increases in HO-1 levels were observed. For example, peak HO-1 accumulation occurred at 10 μM sodium arsenite with slightly decreased levels at higher concentrations of 20 to 50 μM. In time course studies using 30 μM sodium arsenite, the relative levels of HO-1 increased with time from 8 h to 48 h. Concentration- and time-

dependent increases in the relative levels of HO-1 were also observed in avian and mammalian cells. For example, in chick embryo liver cells, treatment with 10 μM sodium arsenite for 24 h induced the highest relative amount of HO-1 (Sardana et al., 1982). In rat astrocytes, peak HO-1 levels occurred with 50 μM sodium arsenite although high relative levels of HO-1 were detected with 20 μM (Fauconneau et al., 2002). Finally, in human epidermal keratinocytes treated with 30 μM arsenite, HO-1 accumulation was detected at 4 h while maximum accumulation was observed at 8 h (Cooper et al., 2007).

In *Xenopus* A6 cells treated with cadmium chloride, enhanced HO-1 levels were detected at 50 μM with maximal amounts at 100 μM. In time course experiments, cadmium chloride-induced HO-1 accumulation was first detected at 8 h and continued to increase up to 48 h. In primary Atlantic cod hepatic cells, enhanced *ho-1* gene expression was detected at 1 and 10 μM with peak levels at 100 μM cadmium chloride (Søfteland et al., 2010). However, in chick embryo liver cells the highest relative level of HO-1 accumulation was observed with only 2 μM cadmium chloride (Sardana et al., 1982). In time course studies with rat hepatocytes, enhanced HO-1 levels were detected after 4 h of cadmium chloride treatment and continued to increase up to the longest time point, 24 h (Badisa et al., 2008).

The induction of HO-1 accumulation in A6 cells in response to the proteasomal inhibitor, MG132, was detectable at 5 μM and peaked at 20 μM. In time course studies using 30 μM MG132, enhanced HO-1 accumulation was detected at 8 h and increased up to 48 h. In mammalian tissue culture systems, high relative levels of HO-1 were induced by relatively lower concentrations of MG132 and shorter time points compared to *Xenopus* A6 cells. For example, high levels of HO-1 accumulation were observed in mouse astrocytes with only 1

μM MG132 for 2 h (Chen and Regan, 2005; Cui et al., 2013). Also, 3 μM MG132 induced HO-1 accumulation in murine macrophages within 3 h and peaked at 12 h (Wu et al., 2004). Sodium arsenite-, cadmium chloride- or proteasomal inhibitor-induced accumulation of HO-1 was reported to act through the MARE/Nrf2 system (Fig. 25A, 25B; Alam et al., 2000; Wu et al., 2004; Yamamoto et al., 2010; Wang et al., 2013). While the *Xenopus laevis ho-1* gene promoter has not been isolated, a Nrf2-binding MARE sequence as well as NF-κB and AP-1 binding elements were detected in the promoter region of the *Xenopus tropicalis ho-1* gene (Genbank gene ID: 100488303). As mentioned previously, Nrf2 is a transcription factor bound to Keap1 in the cytosol under non-stress conditions. In response to redox-dependent stimuli, cysteine residues of Keap1 are modified, leading to the dissociation of Keap1 from Nrf2, which can then translocate to the nucleus and induce the expression of HO-1 (Li et al., 2008; Balogun et al., 2003). Additionally, the thiol-rich transcriptional repressor of the *ho-1* gene, Bach1, is inactivated by pro-oxidants when cysteine residues in its DNA binding domain are oxidized (Ishikawa et al., 2005; Reichard et al., 2007). At least three of these cysteine residues are conserved among human, mouse, and *Xenopus* Bach1 (Ogawa et al., 2001). The *ho-1* gene can be activated by Nrf2 once Bach1 is no longer bound to the promoter and translocates out of the nucleus (Reichard et al., 2007; Paine et al., 2010). In mammalian cells, the Bach1 repressor was inactivated by arsenite, which attacks sulfhydryl groups of cellular components including cysteine residues (Del Razo et al., 2001; Samuel et al., 2005; Reichard et al., 2008). In addition, cadmium was found to induce nuclear export of Bach1, the repressor of the *ho-1* gene (Suzuki et al., 2003). Additionally, both sodium arsenite and cadmium chloride were reported to cause oxidative damage to cellular proteins as cadmium was found to react with vicinal thiol groups (Waisberg et al., 2003; Galazyn-

Figure 25. Potential mechanisms of stress-induced HO-1 accumulation in *Xenopus* cells. A) Sodium arsenite and cadmium chloride have been reported to cause oxidative damage to cellular components including proteins. Arsenite and cadmium may induce HO-1 accumulation through the MARE/Nrf2 and p38 MAPK pathways. Furthermore, cadmium chloride-induced HO-1 may involve the cadmium response element (CdRE), as well as the transcription factors HSF1 and pescadillo. B) MG132 has been reported to induce HO-1 accumulation through the MARE/Nrf2 and p38 MAPK pathways. Additionally, proteasomal inhibition may increase the stability of Nrf2, allowing it to bind and activate the *ho-1* gene. C) Increased temperatures may induce higher HO-1 accumulation by allowing increased uptake of chemicals and by inducing further protein damage.

A.

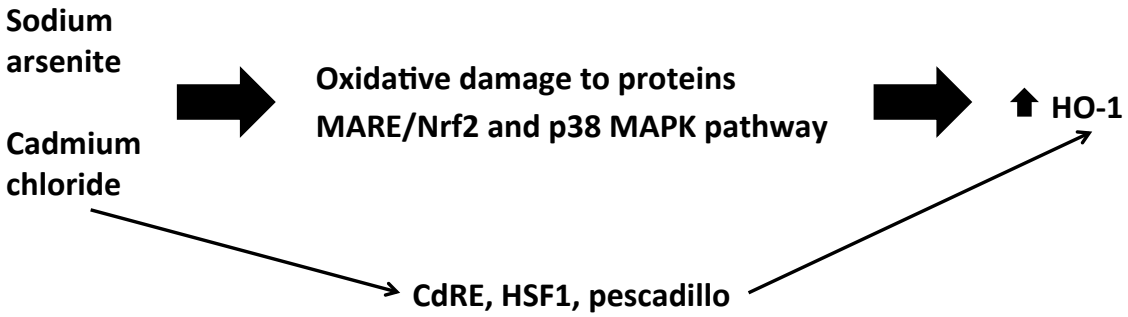
Sodium arsenite
Cadmium chloride
Oxidative damage to proteins
MARE/Nrf2 and p38 MAPK pathway
HO-1
CdRE, HSF1, pescadillo

B.

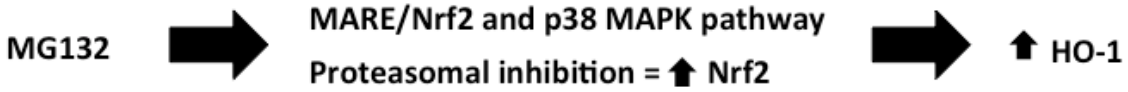
MG132
MARE/Nrf2 and p38 MAPK pathway
Proteasomal inhibition = Nrf2
HO-1

C.

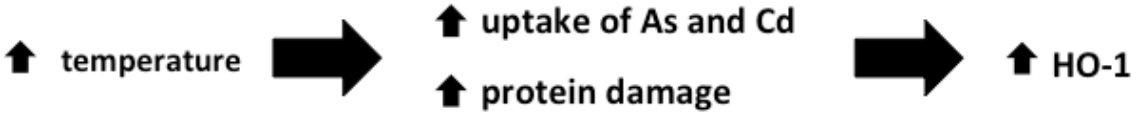
temperature
uptake of As and Cd
protein damage
HO-1

Sidorczuk et al., 2009). Furthermore, cadmium chloride induced a 6- and 9-fold increase in H_2O_2 and $O_2^{\bullet-}$, respectively, in soybean plants (Balestrasse et al., 2006). This oxidative stress likely contributes to cadmium chloride-induced HO-1 accumulation. A previous study with mouse hepatoma cells suggested that cadmium-induced HO-1 accumulation might occur through stabilization of Nrf2, a *ho-1* gene transcription factor, by increasing the half-life of Nrf2 from 13 min to 100 min (Stewart et al., 2003).

Another possibility for the upregulation of HO-1 accumulation by cadmium chloride, which was first described in HeLa cells, involves the binding of transcription factors to the *cis*-acting cadmium-responsive element (CdRE) found in the regulatory region of *ho-1* genes (Fig. 25A; Takeda et al., 1995). As the *Xenopus laevis ho-1* gene sequence was not available, the *Xenopus tropicalis ho-1* gene promoter was searched for the potential CdRE sequence, TGCTAGAT (Sikorski et al., 2006; Koizumi et al., 2007). The sequence, AGCTAGAA, was found, which has a 6-nucleotide core that was identical to human CdRE. This core sequence was essential for metal-induced binding of transcription factor complexes in HeLa cells (Koizumi et al., 2007). Given the finding of a putative CdRE in *X. tropicalis*, it is possible that a comparable enhancer is also present in the promoter of the *Xenopus laevis ho-1* gene. In human renal epithelial cells, the transcription factor pescadillo was found to interact specifically with the CdRE (Sikorski et al., 2006). Overexpression of pescadillo increased the transcriptional activity of the human *ho-1* gene promoter. Interestingly, in HeLa cells it was determined that HSF1 may participate in mediating the transcriptional activation of the *ho-1* gene (Koizumi et al., 2007). In this latter study, it was suggested that in cadmium-treated HeLa cells, pescadillo binding to CdRE or the presence of other transcription factors binding to adjacent regulatory elements may interact with HSF1

resulting in an enhanced expression of the *ho-1* gene. It is not known whether these possible mechanism(s) for cadmium-induced *ho-1* gene activation extend to *Xenopus*. However, the involvement of pescadillo should be examined in the future due to the existence of a homolog in *Xenopus laevis* (Gessert et al., 2007).

It is possible that upregulation of HO-1 by MG132 may also be regulated at the level of protein stability as it is a proteasomal inhibitor (Fig. 25B). Proteasomal inhibitors enhanced the expression of Nrf2, likely due to the prevention of its on-going degradation under non-stress conditions (Stewart et al., 2003). Specifically, MG132 elevated the relative levels of Nrf2 in PC12 rat adrenal pheochromocytoma cells (Martin et al., 2004). Given the above-mentioned findings in mammalian cells, it is possible that *Xenopus laevis* HO-1 accumulation induced by sodium arsenite, cadmium chloride or MG132 may occur by means of similar mechanisms.

In general, treatment of A6 cells with sodium arsenite, cadmium chloride or MG132 in dose response and time course studies produced a pattern of HSP30 accumulation that was similar to HO-1 as well as previous studies of stress-induced HSP30 accumulation in our laboratory (Voyer and Heikkila, 2008; Woolfson and Heikkila, 2009; Young and Heikkila, 2010; Brunt et al., 2012). Also, in these previous studies, induction of *hsp30* gene expression by sodium arsenite, cadmium chloride and MG132 was regulated at least in part at the level of transcription since KNK437, a HSF1 inhibitor, repressed the accumulation of HSP30 and HSP70. HSF1 is triggered by the accumulation of non-native or misfolded proteins within the cell, and all of the stressors employed in this study lead to the accumulation of unfolded or damaged protein as mentioned previously (Morimoto, 1998; Pirkkala et al., 2001; Voellmy, 2004; Morimoto, 2008; Heikkila, 2010). In the current study, the effect of these stressors on

the relative levels of the cytoskeletal protein actin was examined and found to remain relatively constant. These findings agree with previous analyses in our laboratory detailing the effect of various stressors on relative actin levels (Woolfson and Heikkila, 2009; Young and Heikkila, 2010; Brunt et al., 2012; Khamis and Heikkila, 2013).

In A6 cells recovering from sodium arsenite treatment, the relative levels of HO-1 and HSP30 increased up to 12 h before gradually declining to 40-50% of peak levels at 48 h. This enhanced accumulation of HO-1 and HSP30 at 12 h of recovery was inhibited by cycloheximide, a translational inhibitor, suggesting that this transient increase was due to *de novo* protein synthesis. Persistence of enhanced HO-1 accumulation during recovery from sodium arsenite was also observed in human and murine skin cells (Caltabiano et al., 1986). A6 cells recovering from cadmium chloride exhibited an increase in HO-1 and HSP30 accumulation up to 24 h recovery, followed by a decrease. In previous studies, A6 cells that were allowed to recover from a 200 μM cadmium chloride treatment displayed an increase in HSP30 accumulation from 12 to 48 h after stressor removal, with decreased levels at 72 h recovery (Woolfson and Heikkila, 2009). Additionally, an increase in HSP accumulation during recovery from cadmium stress was demonstrated in rat hepatoma cells and rat liver tissue (Goering et al, 1993; Ovelgönne et al., 1995). The persistence of enhanced HO-1 and HSP30 accumulation may be due to the continued actions of the metals on the Nrf-2 and HSF1 pathways within the A6 cell. In contrast, MG132-induced HO-1 and HSP30 accumulation remained relatively constant after fresh media was added until 48 h. Similar findings were made in a previous study examining the effect of MG132-induced HSP30 accumulation in A6 cells after removal of MG132 from the media (Young and Heikkila, 2010). Extended accumulation of HSPs during recovery from the effects of a proteasomal

inhibitor was demonstrated in rat neonatal cardiomyocytes and Chinese hamster ovary cells (Stangl et al., 2002; Kovacs et al., 2006). This prolonged accumulation of HO-1 and HSP30 during recovery may be due to MG132's long half-life, allowing it to continue to inhibit the proteasome (Lee and Goldberg, 1998). Cells may also require additional time to degrade the accumulated ubiquitinated protein by means of the ubiquitin proteasome system, which was inhibited by MG132.

Additionally, the present study determined that incubation of A6 cells with relatively low concentrations (10 μM) of sodium arsenite or cadmium chloride plus a concurrent mild heat shock (30 °C) enhanced the relative levels of HO-1 accumulation compared to the different stressors individually. These results were in contrast to other studies, which demonstrated a heat shock-induced reduction in HO-1 accumulation. For example, in human Hep3B hepatoma cells, in which HO-1 was heat-inducible, the simultaneous treatment of cells with sodium arsenite and a relatively high heat shock temperature (42.5 °C) induced lower levels of HO-1 than observed with sodium arsenite alone (Chou et al., 2005). Also, in a human erythroblastic cell line, it was determined that a 42 °C heat shock inhibited the cadmium-induced activation of the heme oxygenase-1 promoter (Okinaga et al., 1996). Unfortunately, the effect of mild heat shock temperatures plus sodium arsenite or cadmium chloride was not tested in these studies, and heat shock treatment of A6 cells beyond 35 °C leads to cell death. Previously, it was reported that cellular uptake of both sodium arsenite and cadmium chloride increased with elevated temperatures in mammals and fish (McGeachy and Dixon, 1989; Souza et al., 1997; Saydam et al., 2003). Thus, it is possible that the mild heat shock may enhance the uptake of sodium arsenite or cadmium chloride into

A6 cells which may in turn increase their ability to activate the Nrf2 pathway leading *ho-1* gene expression as previously discussed (Fig. 25C).

Mild heat shock also enhanced the MG132-induced accumulation of HO-1 accumulation in A6 cells. At this time, it is not known whether the uptake of MG132, which is dissolved in DMSO, increases with temperature. If this did occur then the enhanced inhibitory action of MG132 on proteasomal degradation may have enhanced the stability of Nrf2 ultimately leading to increased HO-1 accumulation compared to control temperatures. It is also tenable that the mild heat shock may have increased the amount of oxidative stress in A6 cells, which could further activate the Nrf2 pathway.

In the previous sets of experiments, treatment of A6 cells with mild heat shock plus sodium arsenite or MG132 enhanced the accumulation of HSP30. These findings agree with previous studies in our laboratory (Young et al., 2009; Young and Heikkila, 2010; Brunt et al., 2012; Khamis and Heikkila, 2013). Also, treatment of A6 cells with 10 μM cadmium chloride plus a mild heat shock occasionally resulted in enhanced HSP30 accumulation. A low relative level of HSP30 accumulation in A6 cells induced by these stress conditions was reported previously in our laboratory (Khamis and Heikkila, 2013). However, higher concentrations of cadmium chloride plus mild heat were found to produce a high relative level of HSP30 accumulation (Woolfson and Heikkila, 2009). As suggested in these earlier studies, heat shock plus sodium arsenite, cadmium chloride or MG132 may have augmented the extent of protein denaturation, misfolding and ubiquitinated protein leading to HSF1 activation.

Immunocytochemical analysis confirmed the lack of HO-1 accumulation in response to heat shock treatment, whereas HO-1 was detected in response to sodium arsenite,

cadmium chloride and MG132 treatment primarily in the perinuclear region in a punctate pattern. Interestingly, larger HO-1 antibody staining structures were detected in about 20% of cells treated with sodium arsenite treatment. This finding was of interest given that, although it lacks an ER-targeting sequence, HO-1 is anchored to the endoplasmic reticulum by a single C-terminal transmembrane region, and it faces the cytosol in macrophages *in vivo* (Gottlieb et al., 2012; Ryter et al., 2006). However, previous studies reported that stress-induced immunoglobulin-binding protein (BiP), another ER protein, formed larger BiP antibody staining structures with a similar localization pattern (Khan et al., 2012). While HO-1 is primarily an ER protein, it was shown in various mammalian systems to translocate to the nucleus and/or mitochondria in response to hypoxia stress or in tumours (Converso et al., 2006; Slebos et al., 2007; Lin et al., 2007; Gandini et al., 2012; Namba et al., 2014). Interestingly, a recent study determined that NADPH cytochrome P450 reductase can inhibit the translocation of HO-1 to the nucleus and promote oligomerization of HO-1 into higher ordered complexes also containing biliverdin reductase (Huber et al., 2009; Linnenbaum et al., 2012). It is possible that a similar phenomenon may occur with *Xenopus* HO-1 in A6 cells. Treatment of *Xenopus* A6 cells with sodium arsenite, cadmium chloride or MG132 also induced the accumulation of HSP30 primarily in the cytoplasm in a punctate pattern as observed previously in our laboratory (Gellalchew and Heikkila, 2005; Voyer and Heikkila, 2008; Woolfson and Heikkila, 2009; Young and Heikkila, 2010). The HSP30 granular pattern was most likely due to stress-induced multimeric complexes that may be required for the binding of HSP30 to unfolded protein (Ohan et al., 1998; MacRae, 2000; Fernando and Heikkila, 2000; Van Montfort et al., 2001; Fernando et al., 2003). In some cells treated with heat shock, sodium arsenite, cadmium chloride, or MG132 there was observed membrane

ruffling and F-actin cytoskeletal disorganization. This phenomenon has previously been reported in A6 cells and mammalian cultured cells (Mills and Ferm, 1989; Li and Chou, 1992; Wang et al., 1996, Gellalchew and Heikkila, 2005; Woolfson and Heikkila, 2009, Templeton and Liu, 2013).

In summary, the present study determined for the first time in an amphibian cell line that HO-1 accumulation was induced by sodium arsenite, cadmium chloride and the proteasomal inhibitor, MG132, but not heat shock. Additional basic information regarding stress-induced HO-1 accumulation is of importance given that it has been implicated in a variety of diseases and conditions that are associated with oxidative stress, including Alzheimer's disease, diabetes, atherosclerosis, and myocardial infarction (Takahashi et al., 2000; Juan et al., 2001; Turkseven et al., 2005; Liu et al., 2005). Furthermore, some of these diseases are also associated with proteasomal inhibition. Additionally, aquatic organisms, such as amphibians, are quite susceptible to the deleterious effects of toxicants such as sodium arsenite and cadmium chloride. Thus, HO-1 may be of value as a biomarker for studies involving environmental contamination by cadmium chloride, sodium arsenite or other agents. The present study has also shown that HO-1 accumulation by these metals was enhanced by mild heat shock. This last finding is of importance given the global rise in temperature over the last number of decades and its potential effect on aquatic organisms, especially those in contaminated lakes or rivers.

Given the findings of the present study, future studies could examine in more detail the mechanism(s) involved in sodium arsenite-, cadmium chloride-, and MG132-induced accumulation of HO-1 in *Xenopu*s A6 cells. There are various pathways that have been implicated in the induction of HO-1 in response to different stressors. Sodium arsenite,

cadmium chloride, and proteasomal inhibitors were reported to induce HO-1 through the Keap1/Nrf2 system in a variety of mammalian systems (Alam et al., 2000; Wu et al., 2004; Yamamoto et al., 2010; Wang et al., 2013). Additionally, the p38 MAPK inhibitor SB203580 was found to greatly reduce HO-1 accumulation in murine macrophages in response to MG132, suggesting a role in HO-1 accumulation (Wu et al., 2004). Additionally, SB203580 was reported to block Nrf-2 translocation to nuclei, thereby inhibiting *Ginkgo biloba* extract-induced HO-1 accumulation in human aortic endothelial cells, and implicating p38 in *ho-1* induction (Chen et al., 2011). Thus, SB203580 could be employed to determine if sodium arsenite, cadmium chloride and MG132 likewise induce HO-1 accumulation as a result of p38 phosphorylation and the p38 MAPK pathway in *X. laevis* A6 cells. Future studies could also examine the pattern of stress-induced HO-1 accumulation in *Xenopus* embryos. Previously, constitutive levels of HO-1 mRNA were detected in *Xenopus laevis* egg with increasingly higher amounts after the midblastula stage of development (Shi et al., 2008). However, there is no information available on the effect of various stressors, like sodium arsenite or cadmium chloride on *ho-1* gene expression during *Xenopus* embryogenesis.

References

Abdulle, R., Mohindra, A., Fernando, P., and Heikkila, J.J. 2002. *Xenopus* small heat shock proteins, Hsp30C and Hsp30D, maintain heat- and chemically denatured luciferase in a folding-competent state. Cell Stress Chaperones. 7, 6-16.

Acunzo, J., Katsogiannoum, M., and Rocchi, P. 2012. Small heat shock proteins HSP27 (BspB1), αB-crystallin (HspB5) and HSP22 (HspB8) as regulators of cell death. Int. J. Biochem. Cell. Biol. 44, 1622-1631.

Akerfelt, M., Troullet, D., Mezger, V., and Sistonen, L. 2007. Heat shock factors at a crossroad between stress and development. Ann. N. Y. Acad. Sci. 1113, 15-27.

Alam, J. and Cook, J. 2007. How many transcription factors does it take to turn on the heme oxygenase-1 gene? Am. J. Respir. Cell. Mol. Biol. 36, 166-174.

Alam, J., Wicks, C., Stewart, D., Gong, P., Touchard, C., Otterbein, S., Choi, A.M.K., Burow, M.E., and Tou, J. 2000. Mechanism of heme oxygenase-1 gene activation by cadmium in MCF-7 mammary epithelial cells: role of p38 kinase and Nrf2 transcription factor. J. Biol. Chem. 275, 27694-27702.

Allen, S.P., Polazzi, J.O., Gierse, J.K., and Easton, A.M. 1992. Two novel heat shock genes encoding proteins produced in response to heterologous protein expression in *Escherichia coli*. J. Bacteriol. 174, 6938-6947.

Arrigo, A.P., Garrido, C., Fromentin, A., Bonnotte, B., Favre, N., Moutet, M., Mehlen, P., and Solary, E. 1998. Heat shock protein 27 enhances the tumorgenicity of immunogenic rat colon carcinoma cell clones. Cancer Res. 58, 5495-5499.

Awasthi, N. and Wagner, B.J. 2005. Upregulation of heat shock protein expression by proteasome inhibition: an antiapoptotic mechanism in the lens. Invest. Ophthalmol. Vis. Sci. 46, 2082-2091.

Badisa, V.L., Latinwo, L.M., Odewumi, C.O., Ikediobi, C.O., Badisa, R.B., Brooks-Walter, A., Lambert, A.T., and Nwoga, J. Cytotoxicity and stress gene microarray analysis in cadmium-exposed CRL-1439 normal rat liver cells. Int. J. Mol. Med. 22, 213-219.

Barbier, O., Jacquillet, G., Tauc, M., Poujeol, P., Cougnon, M. 2004. Acute study of interaction among cadmium, calcium, and zinc transport along the rat nephron *in vivo*. Am. J. Physiol. Renal. Physiol. 287, 1067-1075.

Balestrasse, K.B., Noriega, G.O., Batlle, A., and Tomaro, M.L. 2006. Heme oxygenase activity and oxidative stress signalling in soybean leaves. Plant Sci. 170, 339-346.

Balogun, E., Hoque, M., Gong, P., Killeen, E., Green, C.J. Foresti, R., Alam, J., and Motterlini, R. 2003. Curcumin activates the haem oxygenase-1 gene via regulation of Nrf2 and the antioxidant-responsive element. Biochem. J. 371, 887-895.

Bauman, J.B. Liu, J., and Klassen, C.D. 1993. Production of metallothionein and heat-shock proteins in response to metals. Fundam. Appl. Toxicol. 21, 15-22.

Becker, J. and Craig, E.A. 1994. Heat-shock proteins as molecular chaperones. Eur. J. Biochem. 219, 11-23.

Bhattacharjee, H., Rosen, B.P, and Mukhopadhyay, R. 2009. Aquaglyceroporins and metalloid transport: implications in human disease. Handb. Exp. Pharmacol. 190, 309-325.

Bienz, M. 1984. Developmental control of the heat shock response in *Xenopus*. Proc. Natl. Acad. Sci. USA 81, 3138-3142.

Bode, A.M., and Dong, Z. 2002. The paradox of arsenic: molecular mechanisms of cell transformation and chemotherapeutic effects. Crit. Rev. Oncol. Hematol. 42, 5-24.

Bonham, R.T, Fine, M.R., Pollock, F.M., and Shelden, E.A. 2003. Hsp27, Hsp70, and metallothionein in MDCK and LLC-PK1 renal epithelial cells: effects of prolonged exposure to cadmium. Toxicol. Appl. Pharmacol. 191, 63-73.

Boston, R.S., Viitanen, P.V., and Vierling, E. 1996. Molecular chaperones and protein folding in plants. Plant Mol. Biol. 32, 191-222.

Brouard, S., Otterbein, L.E., Anrather, J., Tobiasch, E., Bach, F.H., Choi, A.M., and Soares, M.P. 2000. Carbon monoxide generated by heme oxygenase 1 suppresses endothelial cell apoptosis. J. Exp. Med. 192, 1015-1026.

Browne, S., Ferrante, R., and Beal, M.F. 1999. Oxidative stress in Huntington's disease. Brain Pathol. 9, 147–163.

Brunt, J., Khan, S., and Heikkila, J.J. 2012. Sodium arsenite and cadmium chloride induction of proteasomal inhibition and HSP accumulation in *Xenopus laevis* A6 kidney epithelial cells. Comp. Biochem. Physiol. C. Toxicol. Pharmacol. 55, 307-317.

Bush, K.T., Goldberg, A.L., and Nigam, S.K. 1997. Proteasome inhibition leads to a heat shock response, induction of endoplasmic reticulum chaperones, and thermotolerance. J. Biol. Chem. 272, 9086-9092.

Cabell, L., Ferguson, C., Luginbill, D., Kern, M., Weingart, A., and Audesirk, G. 2004. Differential induction of heme oxygenase and other stress proteins in cultured hippocampal astrocytes and neurons by inorganic lead. Toxicol. Appl. Pharmacol. 198, 49-60.

Calabrese, V., Scapagnini, C., Colimbrita. C., Ravagna, A., Pennisi, G., and Stella, A. M. G. 2003. Redox regulation of heat shock protein expression in aging and neurodegenerative disorders associated with oxidative stress: a nutritional approach. Amino Acids. 25, 437-444.

Calabrese, V., Bates, T.E., Mancuso, C., Cornelius, C., Ventimiglia, B., Cambria, M.T., Di Renzo, L., De Lorenzo, A., and Dinkova-Kostova, A.T. 2008. Curcumin and the cellular stress response in free radical-related diseases. Mol. Nutr. Food. Res. 52, 1062-1073.

Caltabiano, M.M., Koestler, T.P., Poste, G., and Greig, R.G. 1986. Induction of 32- and 34-kDa stress proteins by sodium arsenite, heavy metals, and thiol-reactive agents. J. Biol. Chem. 261, 13381-13386.

Chen, Y.C., Lin-Shiau, S.Y., and Lin, J.K. 1998. Involvement of reactive oxygen species and caspase 3 activation in arsenite-induced apoptosis. J. Cell Physiol. 177, 324-333.

Chen, J. and Regan, R.F. 2005. Increasing expression of heme oxygenase-1 by proteasome inhibition protects astrocytes from heme-mediated oxidative injury. Curr. Neurovasc. Res. 2, 189-196.

Chen, J.S., Huang, P.H., Wang, C.H., Lin, F.Y., Tsai, H.Y., Wu, T.C., Lin, S.J., and Chen, J.W. 2011. Nrf-2 mediated heme oxygenase-1 expression, an antioxidant-independent mechanism, contributes to anti-atherogenesis and vascular protective effects of *Ginkgo biloba* extract. Atherosclerosis. 214, 301-309.

Choi, A.M. and Alam, J. 1996. Heme oxygenase-1: function, regulation, and implication of a novel stress-inducible protein in oxidant-induced lung injury. Am. J. Respir. Cell Mol. Biol. 15, 9-19.

Chora, S., McDonagh B., Sheehan, D., Starita-Geribaldi, M., Romeo, M., and Bebianno, M.J. 2008. Ubiquitination and carbonylation as markers of oxidative-stress in *Ruditapes decussates*. Mar. Environ. Res. 66, 95-97.

Chou, Y.H., Ho, F.M., Liu, D.Z., Lin, S.Y., Tsai, L.H., Chen, C.H., Ho, Y.S., Hung, L.F., and Liang, Y.C. 2005. The possible role of heat shock factor-1 in the negative regulation of heme oxygenase-1. Int. J. Biochem. Cell Biol. 37, 604-615.

Chou, I.N. 1989. Distinct cytoskeletal injuries induced by As, Cd, Co, Cr and Ni compounds. Biomed. Environ. Sci. 2, 358-365.

Ciechanover, A., Heller, H., Elias, S., Haas, A.L., and Hershko, A. 1980. ATP-dependent conjugation of reticulocyte proteins with the polypeptide required for protein degradation. Proc. Natl. Acad. Sci. USA 77, 1365–1368.

Cui, W., Bai, Y., Luo, P., Miao, L., and Cai, L. 2013. Preventive and therapeutic effects of MG132 by activating Nrf2-ARE signalling pathway on oxidative stress-induced cardiovascular and renal injury. Oxid. Med. Cell Longev. doi: 10.1155/2013/306073.

Collino, M., Pini, A., Mugelli, N., Mastroianni, R., Bani, D., Fantozzi, R., Papucci, L., Fazi, M., and Masini, E. 2013. Beneficial effect of prolonged heme oxygenase-1 activation in a rat model of chronic heart failure. Dis. Model Mech. 6, 1012-1020.

Converso, D.P., Taillé, C., Carreras, M.C., Jaitovich, A. Poderoso, J.J., and Boczkowski, J. 2006. HO-1 is located in liver mitochondria and modulates mitochondrial heme content and metabolism. FASEB J. 20, 1236-1238.

Cooper, K.L., Liu, K.J., and Hudson, L.G. 2007. Contributions of reactive oxygen species and mitogen-activated protein kinase signalling in arsenite-stimulated hemeoxygenase-1 production. Toxicol. Appl. Pharmacol. 218, 119-127.

Darasch, S., Mosser, D.D., Bols, N.C., and Heikkila, J.J. 1988. Heat shock gene expression in *Xenopus laevis* A6 cells in response to heat shock and sodium arsenite treatments. Biochem. Cell Biol. 66, 862-870.

Del Razo, L.M., Quintanilla-Vega, B., Brambila-Colombres, E., Calderon-Aranda, E.S., Manno M., and Albores, A. 2001. Stress proteins induced by arsenic. Toxicol. Appl. Pharmacol. 177, 132-148.

Deshane, J., Chen, S., Caballero, S., Grochot-Przeczek, A., Was, H., Li Calzi, S., Lach, R., Hock, T.D., Chen, B., Hill-Kapturczak, N., Siegal, G.P., Dulak, J., Jozkowicz, A., Grant, M.B., and Agarwal, A. 2007. Stromal cell-derived factor 1 promotes angiogenesis via a heme oxygenase 1-dependent mechanism. J. Exp. Med. 204, 605-618.

Elbirt K.K., Whitmarsh A.J., Davis R.J., and Bonkovsky H.L. 1998. Mechanism of sodium arsenite mediated induction of heme oxygenase-1 in hepatoma cells. Role of mitogen-activated protein kinases. J. Biol. Chem. 273, 8922-8931.

Endo, T. 2002. Transport of cadmium across the apical membrane of epithelial cell lines. Comp. Biochem. Physiol. C Toxicol. Pharmacol. 131, 223-229.

Ewing, J.F. and Maines, M.D. 1997. Histochemical localization of heme oxygenase-2 protein and mRNA expression in rat brain. Brain Res. Brain Res. Protoc. 1, 165-174.

Fang, J., Sawa, T., Akaike, T., Akuta, T., Sahoo, S.K., Khaled, G., Hamada, A., and Maeda, H. 2004. *In vivo* antitumor activity of pegylated zinc protoporphyrin: targeted inhibition of heme oxygenase in solid tumor. Cancer Res. 63, 3567-3574.

Fauconneau, B., Petegnief, V., Sanfeliu, C., Piriou, A., and Planas, A. M. 2002. Induction of heat shock proteins (HSPs) by sodium arsenite in cultured astrocytes and reduction of hydrogen peroxide-induced cell death. J. Neurochem. 83, 1338-1348.

Fernando, P., and Heikkila, J.J. 2000. Functional characterization of *Xenopus* small heat shock protein, Hsp30C : the carboxyl end is required for stability and chaperone activity. Cell Stress Chaperones 5, 148-159.

Fernando, P., Megeney, L.A. and Heikkila, J.J. 2003. Phosphorylation-dependent structural alterations in the small hsp30 chaperone are associated with cellular recovery. Exp. Cell Res. 286, 175-185.

Ferris, C.D., Jaffrey, S.R., Sawa, A., Takahashi, M., Brady, S.D., Barrow, R.K., Tysoe, S.A., Wolosker, H., Baranano, D.E., Dore, S., Poss, K.D., and Snyder, S.H. 1999. Haem oxygenase-1 prevents cell death by regulating cellular iron. Nat. Cell. Biol. 1, 152-157.

Figueiredo-Pereira, M.E., and Cohen, G. 1999. The ubiquitin/proteasome pathway: friend or foe in zinc-, cadmium-, and H_2O_2-induced neuronal oxidative stress. Mol. Biol. Rep. 26, 65-69.

Fort, D.J., Stover, E.L., Bantle, J.A., Dumont, J.N., and Finch, R.A. 2001. Evaluation of reproductive toxicity assay using *Xenopus laevis*: boric acid, cadmium and ethylene glycol monomethyl ether. J. Appl. Toxicol. 21, 41-52.

Galazyn-Sidorczuk, M., Brzoska, M.M., Jurczuk, M., and Moniuszko-Jakoniuk, J. 2009.

Oxidative damage to proteins and DNA in rats exposed to cadmium and/or ethanol. Chem. Biol. Interac. 180, 31-38.

Gandini, N.A., Fermento, M.E., Salomón, D.G., Blasco, J., Patel, V., Gutkind, J.S., Molinolo, A.A., Facchinetti, and M.M., and Curino, A.C. 2012. Nuclear localization of heme oxygenase-1 is associated with tumor progression of head and neck squamous cell carcinomas. Exp. Mol. Pathol. 93, 237-245.

Garrido, C., Paul, C., Seigneuric, R., and Kampinga, H.H. 2012. The small heat shock proteins family: the long forgotten chaperones. Int. J. Biochem. Cell Biol. Review. 44, 1588-1592.

Gauley, J., and Heikkila, J.J. 2006. Examination of the expression of the heat shock protein gene, hsp110, in *Xenopus laevis* cultured cells and embryos. Comp. Biochem. Physiol. A Mol. Integr. Physiol. 145, 225-234.

Gellalchew, M and Heikkila, J.J. 2005. Intracellular localization of *Xenopus* small heat shock protein, hsp30, in A6 kidney epithelial cells. Cell. Biol. Int. 29, 221-227.

Gessert, S., Maurus, D., Rössner, A., and Kühl, M. Pescadillo is required for *Xenopus laevis* eye development and neural crest migration. Dev. Biol. 310, 99-112.

Goering, P.L., Fisher, B.R., and Kish, C.L. 1993. Stress protein synthesis induced in rat liver by cadmium precedes hepatotoxicity. Toxicol. Appl. Pharmacol. 122, 139-148.

Gong, P., Hu, B., and Cederbaum, A.I. 2004. Diallyl sulfide induces heme oxygenase-1 through MAPK pathway. Arch. Biochem. Biophys. 432, 252–260.

González-Reyes, S., Guzmán-Beltrán, S., Medina-Campos, O.N., and Pedraza-Chaverri, J. 2013. Curcumin pretreatment induces Nrf2 and an antioxidant response and prevents

hemin-induced toxicity in primary cultures of cerebellar granule neurons of rats. Oxid. Med. Cell Longev. doi: 10.1155/2013/801418.

Gottlieb, Y., Truman, M., Cohen, L.A., Leichtmann-Bardoogo, Y., and Meyron-Holtz, E.G. 2012. Endoplasmic reticulum anchored heme-oxygenase 1 faces the cytosol. Haematologica 97, 1489-1493.

Guille, M. 1999. Microinjection into *Xenopus* oocytes and embryos. Methods Mol. Biol. 127, 111-123.

Hachfi, L., Simide, R., Richard, S., Couvray, S., Coupe, S., Gaillard, S., Pierre, S., Grillasca, J.P., and Prevot-D'Alvise, N. 2012. Effect of water temperature increase on HO-1 expression in European sea bass (*Dicentrarchus labrax L.*) tissues. Cell. Mol. Biol. (Noisy-le-grand). Suppl. 58, OL1752-1756.

Hait-Darshan, R., Babushkin, T., and Malik, Z. Regulation of heme synthesis and proteasomal activity by copper: possible implications for Wilson's disease. J. Environ. Pathol. Toxicol. Oncol. 28, 209-221.

Hanneken, A., Lin, F.F., Johnson, J., and Maher, P. 2006. Flavonoids protect human retinal pigment epithelial cells from oxidative-stress-induced death. Invest. Opthalmol. Vis. Sci. 47, 3164-3177.

Hara, E., Takahashi, K., Tominaga, T., Kumabe, T., Kayama, T., Suzuki, H., Fujita, H., Yoshimoto, T., Shirato, K., and Shibahara, S. 1996. Expression of heme oxygenase and inducible nitric oxide synthase mRNA in human brain tumors. Biochem. Biophys. Res. Commun. 224, 153–158.

Hartsfield, C.L., Alam, J. and Choi, A.M. 1998. Transcriptional regulation of the heme oxygenase 1 gene by pyrrolidine dithiocarbamate. FASEB J. 12, 1675-1682.

Hartsfield, C.L., Alam, J., and Choi, A.M. 1999. Differential signaling pathways of HO-1 gene expression in pulmonary and systemic vascular cells. Am. J. Physiol. 277, L1133-L1141.

Heikkila, J.J. 2004. Regulation and function of small heat shock protein genes during amphibian development. J. Cell. Biochem. 93, 672-680.

Heikkila, J.J. 2010. Heat shock protein gene expression and function in amphibian model systems. Comp. Biochem. Physiol. A. Mol. Integr. Physiol. 156, 19-33.

Heikkila, J.J., Kaldis, A., and Abdulle, R. 2006. Analysis of molecular chaperones using a *Xenopus* oocyte protein refolding assay. Methods Mol. Biol. 322, 213-222.

Hendrick, J.P. and Hartl, F.U. 1993. Molecular chaperone functions of heat-shock proteins. Annu. Rev. Biochem. 62, 349-384.

Hirai, K., Sasahira, T., Ohmori, H., Fujii, K., and Kuniyasu, H. 2007. Inhibition of heme oxygenase-1 by zinc protoporphyrin IX reduces tumor growth of LL/2 lung cancer in C57BL mice. Int. J. Cancer. 120, 500-505.

Hill-Kapturczak, N., Thamilselvan, V., Liu, F., Nick, H.S., and Agarwal, A. 2001. Mechanism of heme oxygenase-1 gene induction by curcumin in human renal proximal tubule cells. Am. J. Physiol. Renal Physiol. 281, 851-859.

Hershko, A., Ciechanover, A., Heller, H., Haas, A.L., and Rose, I.A. 1980. Proposed role of ATP in protein breakdown: conjugation of proteins with multiple chains of the polypeptide of ATP-dependent proteolysis. Proc. Natl. Acad. Sci. USA 77, 1783–1786.

Hershko, A. and Ciechanover, A. 1998. The ubiquitin system. Annu. Rev. Biochem. 67, 425-479.

Hock, T.D., Nick, H.S., and Agarwal, A. 2004. Upstream stimulatory factors, USF1 and USF2, bind to the human haem oxygenase-1 proximal promoter *in vivo* and regulate its transcription. Biochem. J. 383(Pt 2), 209-218.

Hough, R., Pratt, G., and Rechsteiner, M. 1987. Purification of two high molecular weight proteases from rabbit reticulocyte lysate. J. Biol. Chem. 262, 8303–8313.

Huber, III, W.J. Scruggs, B.A., and Backes, W.L. 2009. C-terminal membrane spanning region of human heme oxygenase-1 mediates a time-dependent complex formation with cytochrome P450 reductase. Biochemistry 48, 190-197.

Immenschuh, S. and Ramadori, G. 2000. Gene regulation of heme oxygenase-1 as a therapeutic target. Biochem. Pharmacol. 60, 1121-1128.

Ishikawa, M., Numazawa, S., and Yoshida, T. 2005. Redox regulation of the transcriptional repressor Bach1. Free Radic. Biol. Med. 38, 1344-1352.

Iyer. J.K., Shi, L., Shankar, A.H., and Sullivan, D.J. Jr. 2003. Zinc protoporphyrin IX binds heme crystals to inhibit the process of crystallization in *Plasmodium falciparum*. Mol. Med. 9, 175-182.

Joseph, P., Muchnok, T.K., Klishis, M.L., Roberts, J.R., Antonini, J.M., Whong, W.Z., and Ong, T. 2001. Cadmium-induced cell transformation and tumourigenesis are associated with transcriptional activation of *c-fos*, *c-jun*, and *c-myc* proto-oncogenes: role of cellular calcium and reactive oxygen species. Toxicol. Sci. 61, 295-303.

Jozefczak, M., Remans, T., Vangronsveld, J., and Cuypers, A. 2012. Glutathione is a key player in metal-induced oxidative stress defenses. Int. J. Mol. Sci. 13, 3145-3175.

Juan, S.H., Lee, T.S., Tseng, K.W., Liou, J.Y., Shyue, S.K., Wu, K.K., and Chau, L.Y. 2001. Adenovirus-mediated heme oxygenase-1 gene transfer inhibits the development of atherosclerosis in apolipoprotein E-deficient mice. Circulation 104, 1519-1525.

Katschinski, D.M. 2004. On heat and cells and proteins. News Physiol. Sci. 19, 11-15.

Keyse, S.M. and Tyrrell, R. M. 1989. Heme oxygenase is the major 32-kDa stress protein induced in human skin fibroblasts by UVA radiation, hydrogen peroxide and sodium arsenite. Proc. Natl. Acad. Sci. USA 86, 99-103.

Khamis, I. and Heikkila, J.J. 2013. Enhanced HSP30 and HSP70 accumulation in *Xenopus* cells subjected to concurrent sodium arsenite and cadmium chloride stress. Comp. Biochem. Physiol. C Toxicol. Pharmacol. 158, 165-172.

Khan, S., Rammeloo, A.W., and Heikkila, J.J. 2012. Withaferin A induces proteasome inhibition, endoplasmic reticulum stress, the heat shock response and acquisition of thermotolerance. PLOS ONE. 7, e50547. doi: 10.1371/journal/pone.0050547.

Khan, S. and Heikkila, J.J. 2014. Distinct patterns of HSP30 and HSP70 degradation in *Xenopus laevis* A6 cells recovering from thermal stress. Comp. Biochem. Physiol. A. Molec. Integr. Biol. 168, 1-10.

Khan, S. and Heikkila, J.J. 2011. Curcumin-induced inhibition of proteasomal activity, enhanced HSP accumulation and the acquisition of thermotolerance in *Xenopus laevis* A6 cells. Comp. Biochem. Physiol. A. Mol. Integr. Physiol. 158, 566-576.

Kim, Y.K., and Jang, S.K. 2002. Continuous heat shock enhances translational initiation directed by internal ribosomal entry site. Biochem. Biophys. Res. Commun. 297, 224-231.

Kim, Y.M., Pae, H.O., Park, J.E., Lee, Y.C, Woo, J.M., Kim, N.H., Choi, Y.K., Lee, B.S., Kim, S.R., and Chung, H.T. 2011. Heme oxygenase in the regulation of vascular biology: from molecular mechanisms to therapeutic opportunities. Antioxid. Redox. Signal. 1, 137-167.

Kirkby, K.A. and Adin, C.A. 2006. Products of heme oxygenase and their potential therapeutic applications. Am. J. Physiol. Renal Physiol. 290, 563-571.

Kirkpatrick, D.S., Dale, K.V., Catania, J.M., and Gandolfi, A.J. 2003. Low-level arsenite causes accumulation of ubiquitinated proteins in rabbit renal cortical slices and HEK293 cells. Toxicol. Appl. Pharmacol. 186, 101-109.

Koegl, M., Hoppe, T., Schlenker S., Ulrich, H.D, Mayer, T.U., and Jentsch, S. 1999. A novel ubiquitination factor, E4, is involved in multiubiquitin chain assembly. Cell 96, 635- 644.

Koizumi, S., Gong, P., Suzuki, K., and Murata, M. 2007. Cadmium-responsive element of the human heme oxygenase-1 gene mediates heat shock factor 1-dependent transcriptional activation. J. Biol. Chem. 282, 8715-8723.

Kovacs, I., Lentini, K.M., Ingano, L.M., and Kovacs, D.M. 2006. Presenilin 1 forms aggresomal deposits in response to heat shock. J. Mol. Neurosci. 29, 9–19.

Krasny, H.C. and Holbrook, D.J. Jr. 1978. Effects of cadmium on heme oxygenase and hemoproteins in smooth and rough endoplasmic reticulum of rat liver. Biochem. Pharmacol. 27, 364-366.

Krone, P.H., Snow, A., Ali, A., Pasternak, J.J., and Heikkila, J.J. 1992. Comparison of the regulatory and structural regions of the *Xenopus laevis* small heat shock protein encoding gene family. Gene 110, 159-166.

Kwok, S.C. 2013. Zinc protoporphyrin up-regulates heme oxygenase-1 in PC-3 cells via the stress response pathway. Int. J. Cell Biol. 2013, 162094.

Le Goff, P., Le Drean, Y., Le Person, C., Le Jossic-Corcos, C., Ainouche, A., and Michel, D. 2004. Intracellular trafficking of heat shock factor 2. Exp. Cell Res. 294, 480-493.

Lang, L., Miskovic, D., Fernando, P., and Heikkila, J.J. 1999. Spatial pattern of constitutive and heat shock-induced expression of the small heat shock protein gene family, Hsp30, in *Xenopus laevis* tailbud embryos. Dev. Genet. 25, 365-374.

Lau, A., Whitman, S.A., Jaramillo, M.C., and Zhang, D.D. 2012. Arsenic-mediated activation of the Nrf2-Keap1 antioxidant pathway. J. Biochem. Molecular Toxicology. 27, 99-105.

Lee, D.H., and Goldberg, A.L. 1998. Proteasome inhibitors: valuable new tools for cell biologists. Trends Cell Biol. 8, 397-403.

Lee, P.J., Alam, J., Wiegand, G.W., and Choi, A.M.K. 1996. Overexpression of heme oygenase-1 in human pulmonary epithelial cells results in cell growth arrest and increased resistance to hyperoxia. Proc. Natl. Acad. Sci. USA 93, 10393-10398.

Li, W., and Chou, I.N. 1992. Effects of sodium arsenite on the cytoskeleton and cellular glutathione levels in cultured cells. Toxicol. Appl. Pharmacol. 114, 132-139.

Li, L., Yang, H., Chen, D., Cui, C., and Dou, Q.P. 2008a. Disulfiram promotes the conversion of carcinogenic cadmium to a proteasome inhibitor with pro-apoptotic activity in human cancer cells. Toxicol. Appl. Pharmacol. 229, 206-214.

Li, W., Yu, S., Liu, T., Kim, J., Blank, V., Li, H., and Kong, A.N.T. 2008b. Heterodimerization with small Maf proteins enhances nuclear retention of Nrf2 via masking the NESzip motif. Biochim. Biophys. Acta. 1783, 1847-1856.

Liang, P., Amons, R., Clegg, J.S., and MacRae, T.H. 1997. Molecular characterization of a small heat shock/α-crystallin protein in encysted *Artemia* embryos. J. Biol. Chem. 272, 19051- 19058.

Lin, Q., Weis, S., Yang, G., Weng, Y.H., Helston, R., Rish, K., Smith, A., Bordner, J., Polte, T., Gaunitz, F., and Dennery, P.A. Heme oxygenase-1 protein localizes to the nucleus and activates transcription factors important in oxidative stress. J. Biol. Chem. 282, 20621-20633.

Linder, B., Jin, Z., Freeman, J.H., and Rubin, C.S. 1996. Molecular characterization of a novel, developmentally regulated small embryonic chaperone from *Caenorhabditis elegans*. J. Biol. Chem. 271, 30158-30166.

Linnenbaum, M., Busker, M., Kraehling, J.R., Behrends, S. 2012. Heme oxygenase isoforms differ in their subcellular trafficking during hypoxia and are differentially modulated by cytochrome P450 reductase. PLOS ONE. 7, e35483. doi: 10.1371/journal.pone.0035483.

Liu, X., Wei, J., Peng, D.H., Layne, M.D., and Yet, S.F. 2005. Absence of heme oxygenase-1 exacerbates myocardial ischemia/reperfusion injury in diabetic mice. Diabetes. 54, 778-784.

Liu, J., Kadiiska, M.B., Liu, Y., Lu, T., Qu, W., and Waalkes, M.P. 2001. Stress-related gene expression in mice treated with inorganic arsenicals. Toxicol. Sci. 61, 314-320.

Loumbourdis, N.S. 2005. Hepatoxic and nephrotoxic effects of cadmium in the frog *Rana ridibunda*. Arch. Toxicol. 79, 434-440.

Lundgren, J., Masson, P., Mirzaei, Z., and Young, P. 2005. Identification and characterization of a *Drosophila* proteasome regulatory network. Mol. Cell. Biol. 25, 4662-4675.

MacRae, T.H. 2000. Structure and function of small heat shock/α-crystallin proteins: Established concepts and emerging ideas. Cell Mol. Life Sci. 57, 899-913.

Maines. M.D. 1988. Heme oxygenase: function, multiplicity, regulatory mechanisms, and clinical applications. FASEB J. 2, 2557-2568.

Maines, M.D. 1997. The heme oxygenase system: a regulator of second messenger gases. Annu. Rev. Pharmacol. Toxicol. 37, 517-554.

Maines M.D. and Abrahamsson, P.A. 1996. Expression of heme oxygenase-1 (HSP32) in human prostate: normal, hyperplastic, and tumor tissue distribution. Urology 47, 727–733.

Martin, D., Rojo, A.I., Salinas, M., Diaz, R., Gallardo, G., Alam, J., Ruiz de Galarreta, C.M., and Cuadrado, A. 2004. Regulation of heme oxygenase-1 expression through the phosphatidylinositol 3-kinase/Akt pathway and the Nrf2 transcription factor in response to the antioxidant phytochemical carnosol. J. Biol. Chem. 279, 8919-8929.

Masliah, E., Rockenstein, E., Veinbergs, I., Mallory, M., Hashimoto, M., Takeda, A., Sagara, Y., Sisk, A., and Mucke, L. 2000. Dopaminergic loss and inclusion body formation in alpha-synuclein mice: implications for neurodegenerative disorders. Science. 287, 1265–1269.

McCoubrey, W.K. Jr., Huang, T.J., and Maines, M.D. 1997. Isolation and characterization of a cDNA from the rat brain that encodes hemoprotein heme oxygenase-3. Eur. J. Biochem. 247, 725-732.

McDonagh, B. and Sheehan, D. 2006. Redox proteomics in the blue mussel *Mytilus edulis*: Carbonylation is not a pre-requisite for ubiquitination in acute free radical mediated oxidative stress. Aquat. Toxicol. 79, 325-333.

McGeachy, S.M. and Dixon, D.G. 1989. The impact of temperature on the acute toxicity of arsenate and arsenite to rainbow trout (*Salmo gairdneri*). Exotoxicol. Environ. Saf. 17, 86-93.

Medina-Diaz, I.M., Estrada-Muniz, E., Reyes-Hernandez, O.D., Ramirez, P., Vega, L., and Elizondo, G. 2009. Arsenite and its metabolites, MMAIII and DMA III, modify CYP3A4, PXR and RXR alpha expression in the small intestine of CYP3A4 transgenic mice. Toxicol. Appl. Pharmacol. 239, 162-168.

Mendez-Armenta, M. and Rios, C. 2007. Cadmium neurotoxicity. Environ. Toxicol. Pharmacol. 23, 350-358.

Michaud, S., Marin, R., and Tanguay, R.M. 1997. Regulation of heat shock gene induction and expression during *Drosophila* development. Cell. Mol. Life Sci. 53, 104-113.

Mills, J.W. and Ferm, V.H. 1989. Effect of cadmium on F-actin and microtubules of Madin-Darby canine kidney cells. Toxicol. Appl. Pharmacol. 101, 245-254.

Mitani, K., Fujita, H., Sassa, S., and Kappas, A. 1990. Activation of heme oxygenase and heat shock protein 70 genes by stress in human hepatoma cells. Biochem. Biophys. Res. Commun. 166, 1429-1434.

Mizukami, S., Ichimura, R., Kemmochi, S., Wang, L., Taniai, E., Mitsumori, K., and Shibutani, M. 2010. Tumor promotion by copper-overloading and its enhancement by excess iron accumulation involving oxidative stress responses in the early stage of a rat two-stage hepatocarcinogenesis model. Chem. Biol. Interact. 185, 189-201.

Morimoto, R.I. 1998. Regulation of the heat shock transcriptional response: Cross talk between a family of heat shock factors, molecular chaperones, and negative regulators. Genes Dev. 12, 3788-3796.

Morimoto, R.I. 2008. Proteotoxic stress and inducible chaperone networks in neurodegenerative diseases and aging. Genes Dev. 22, 1427-1438.

Morita, T., Mitsialis, S.A., Koike, H., Liu, Y.. and Kourembanas, S. 1997. Carbon monoxide controls the proliferation of hypoxic smooth muscle cells. J. Biol. Chem. 272, 32804-32809.

Motterlini, R., Forestry, R., Bassi, R., Calabrese, V., Clark, J.F., and Green, C.J. 2000. Endothelial heme oxygenase-1 induction by hypoxia. Modulation by inducible nitric-oxide synthase and S-nitrosothiols. J. Biol. Chem. 275, 13613-13620.

Mouchet, F., Baudrimont, M., Gonzalez, P., Cuenot, Y., Bourdineaud, J.P., Boudou, A., and Gauthier, L. 2006. Genotoxic and stress inductive potential of cadmium *in Xenopus laevis* larvae. Aquat. Toxicol. 78, 157-166.

Mymrikov, E., Seit-Nebi, A.S., and Gusev, N.B. 2011. Large potentials of small heat shock proteins. Physiol. Rev. 91, 1123-1159.

Naito, Y., Takagi, T., Uchiyama, K., and Yoshikawa, T. 2011. Heme oxygenase-1: a novel therapeutic target for gastrointestinal diseases. J. Clin. Biochem. Nutr. 48, 126-133.

Nakai, A., Tanabe, M., Kawazoe, Y., Inazawa, J., Morimoto, R.I., and Nagata, K. 1997. HSF4, a new member of the human heat shock factor family which lacks properties of a transcriptional activator. Mol Cell Biol. 17, 469-481.

Namba, F., Go, H., Murphy, J.A., La, P., Yang, G., Sengupta, S., Fernando, A.P., Yohannes, M., Biswas, C., Wehrli, S.L. and Dennery, P.A. 2014. Expression level and subcellular localization of heme oxygenase-1 modulates its cytoprotective properties in response to lung injury: a mouse model. PLOS ONE. 9, e90936. doi: 10.1371/journal.pone.0090936.

Noonan, E.J., Place, R.F., Giardina, C., and Hightower, L.E. 2007. Hsp70B' regulation and function. Cell Stress Chaperones 12, 242-253.

Ohan, N.W., Tam, Y., Fernando, P., and Heikkila, J.J. 1998. Characterization of a novel group of basic small heat shock proteins in *Xenopus laevis* A6 kidney epithelial cells. Biochem. Cell Biol. 76, 665-671.

Okinaga, S., Takahashi, K., Takeda, K., Yoshizawa, M., Fujita, H., Sasaki, H., and Shibahara, S. 1996. Regulation of human heme oxygenase-1 gene expression under thermal stress. Blood. 87, 5074-5084.

Othumpangat, S. Kashon, M., and Joseph, P. 2005. Eukaryotic translation initiation factor 4E is a cellular target for toxicity and death due to exposure to cadmium chloride. J. Biol. Chem. 280, 25162-25169.

Otterbein, L.E., Kolls, J.K., Mantell, L.L., Cook, J.L., Alam, J., and Choi, A.M. 1999. Exogenous administration of heme oxygenase-1 by gene transfer provides protection against hyperoxia induced lung injury. J. Clin. Invest. 103, 1047-1054.

Ogawa, K., Sun, J., Taketani, S., Nakajima, O., Nishitani, C., Sassa, S., Hayashi, N.,

Yamamoto, M., Shibahara, S., Fujita, H., and Igarashi, K. 2001. Heme mediates derepression of Maf recognition element through direct binding to transcription repressor Bach1. EMBO J. 20, 2835-43.

Oguro T., Hayashi, M, Nakajo, S., Numazawa, S., and Yoshida, T. 1998. The expression of hemeoxygenase-1 gene responded to oxidative stress produced by phorone, a glutathione depletor, in the rat liver; the relevance to activation of *c-jun* n-terminal kinase. J. Pharmacol. Exp. Ther. 287, 773-778.

Ovelgönne, J.H., Bitorina, M., and Van Wijk, R. 1995. Stressor-specific activation of heat shock genes in H35 rat hepatoma cells. Toxicol. Appl. Pharmacol. 135, 100-109.

Ovsenek, N., Heikkila, J.J. 1990. DNA sequence-specific binding activity of the heat shock transcription factor is heat-inducible before midblastula transition of early *Xenopus* development. Development. 110, 427-433.

Paine, A., Eiz-Vesper, B., Blasczyk, R., and Immenschuh, S. 2010. Signaling to heme oxygenase-1 and its anti-inflammatory therapeutic potential. Biochem. Pharmacol. 80, 1895-1903.

Panahian, N., Yoshiura, M., and Maines, M.D. 1999. Overexpression of heme oxygenase-1 is neuroprotective in a model of permanent middle cerebral artery occlusion in transgenic mice. J. Neurochem. 72, 1187-1203.

Pappolla, M.A., Chyan, Y.J., Omar, R.A., Hsiao, K., Perry, G., Smith, M.A. and Bozner, P. 1998. Evidence of oxidative stress and *in vivo* neurotoxicity of beta-amyloid in a transgenic mouse model of Alzheimer's disease: a chronic oxidative paradigm for testing antioxidant therapies in vivo. Am. J. Pathol. 152, 871-877.

Park, W.H. and Kim, S.H. 2012. MG132, a proteasome inhibitor, induces human pulmonary fibroblast cell death via increasing ROS levels and GSH depletion. Oncol. Rep. 27, 1284-1291.

Parsell, D.A., and Lindquist, S. 1993. The function of heat-shock proteins in stress tolerance: degradation and reactivation of damaged proteins. Annu. Rev. Genet. 27, 437-496.

Pedersen, T.V. and Bjerregaard, P. 2000. Cadmium influx and efflux across perfused gills of the shore crab, *Carcinus maenas*. Aquat. Toxicol. 48, 223-231.

Pirkkila, L., Nykanen, P., and Sistonen, L. 2001. Roles of the heat shock transcription factors in regulation of the heat shock response and beyond. FASEB J. 15, 1118-1131.

Poss, K.D. and Tonegawa, S. 1997. Reduced stress defense in heme oxygenase 1-deficient cells. Proc. Natl. Acad. Sci. USA 94, 10925-10930.

Pritts, T.A., Hungness, E.S., Hershko, D.D., Robb, B.W., Sun, X., Luo, G.J., Fischer, J.E., Wong, H.R., and Hasselgren, P.O. 2002. Proteasome inhibitors induce heat shock response and increase IL-6 expression in human intestinal epithelial cells. Am. J. Physiol. Regul. Integr. Comp. Physiol. 282, 1016-1026.

Rafferty, K.A. Jr. 1975. Epithelial cells: growth in culture of normal and neoplastic forms. Adv. Can. Res. 21, 249-272.

Rafferty, K.A. Jr. and Sherwin, R.W. 1969. The length of secondary chromosomal constrictions in normal individuals and in a nucleolar mutant of *Xenopus laevis*. Cytogenetics 8, 427-438.

Raju, V.S., and Maines, M.D. 1994. Coordinated expression and mechanism of induction of HSP32 (heme oxygenase-1) mRNA by hyperthermia in rat organs. Biochim. Biophys. Acta. 1217, 273-280.

Raju, V.S., McCoubrey, W.K, and Maines, M.D. 1997. Regulation of heme oxygenase-2 by glucocorticoids in neonatal rat brain: characterization of a functional glucocorticoid response element. Biochim. Biophys. Acta. 1351, 89–104.

Rallu, M., Loones, M., Lallemand, Y., Morimoto, R., Morange, M., and Mezger, V. 1997. Function and regulation of heat shock factor 2 during mouse embryogenesis. Proc. Natl. Acad. Sci. USA 94, 2392-2397.

Rea, M.A., Gregg, J.P., Qin, Q., Phillips, M.A., and Rice, R.H. 2003. Global alteration of gene expression in human keratinocytes by inorganic arsenic. Carcinogenesis 24, 747-756.

Reichard, J.F., Motz, G.T., and Puga, A. 2007. Heme oxygenase-1 induction by Nrf2 requires inactivation of the transcriptional repressor Bach1. Nucleic Acids Res. 35, 7074-7086.

Reichard, J.F., Sartor, M.A., and Puga, A. 2008. BACH1 is a specific repressor of HMOX1 that is inactivated by arsenite. J. Biol. Chem. 283, 22363-22370.

Ritossa, F. 1962. A new puffing pattern induced by temperature shock and DNP in *Drosophila.* Experientia 18, 571–573.

Ross, C.A., and Pickart, C.M. 2004. The ubiquitin-proteasome pathway in Parkinson's disease and other neurodegenerative diseases. Trends Cell Biol. 14, 703-711.

Rotenberg, M.O. and Maines, M.D. 1990. Isolation, characterization, and expression in *Escherichia coli* of a cDNA encoding rat heme oxygenase-2. J. Biol. Chem. 265, 7501-7506.

Ryter, S., Kvam, E., and Tyrrell, R.M. 1999. Heme oxygenase activity determination by high performance liquid chromatography. Methods Enzymol. 300, 322-336.

Ryter, S.W. and Tyrrell, R.M. 2000. The heme synthesis and degradation pathways: role in oxidant sensitivity. Heme oxygenase has both pro- and antioxidant properties. Free Radic. Biol. Med. 28, 289-309.

Ryter, S.W., Alam, J., and Choi, A.M. 2006. Heme oxygenase-1/carbon monoxide: from basic science to therapeutic applications. Physiol. Rev. 86, 583-650.

Sahoo, S.K., Sawa, T., Fang, J., Tanaka, S., Miyamoto, Y., Akaike, T., and Maeda, H. 2002. Pegylated zinc protoporphyrin: A water-soluble heme oxygenase inhibitor with tumor-targeting capacity. Bioconjugate Chem. 13, 1031-1038.

Samuel, S. Kathirvel, R., Jayavelu, T., and Chinnakkannu, P. 2005. Protein oxidative damage in arsenic induced rat brain: influence of DL-alpha-lipoic acid. Toxicol. Lett. 15, 27-34.

Sardana, M.K., Sassa, S., and Kappas, A. 1982. Metal ion-mediated regulation of heme oxygenase induction in cultured avian liver cells. J. Biol. Chem. 257, 4806-4811.

Saydam, N., Steiner, F., Georgiev, O., and Schaffner, W. 2003. Heat and heavy metal stress synergize to mediate transcriptional hyperactivation by metal-responsive transcription factor MTF-1. J. Biol. Chem. 278, 31879-31883.

Schipper, H.M., Liberman, A., and Stopa, E.G. 1998. Neural heme oxygenase-1 expression in idiopathic Parkinson's disease. Exp. Neurol. 150, 60–68.

Shi, J., Mei, W., and Yang, J. 2008. Heme metabolism enzymes are dynamically expressed during *Xenopus* embryonic development. Bio. Cell. 32, 259-263.

Shibahara, S., Yoshida, T., and Kikuchi, G. 1978. Induction of heme oxygenase by hemin in cultured pig alveolar macrophages. Arch. Biochem. Biophys. 188, 243-250.

Sikorski, E.M., Uo, T., Morrison, R.S., and Agarwal, A. 2006. Pescadillo interacts with the cadmium response element of the human heme oxygenase-1 promoter in renal epithelial cells. J. Biol. Chem. 281, 24423-30.

Siow, R.C., Sato, H., and Mann, G.E. 1999. Heme oxygenase-carbon monoxide signalling pathway in atherosclerosis: anti-atherogenic actions of bilirubin and carbon monoxide? Cardiovasc. Res. 41, 385-394.

Slebos, D.J., Ryter, S.W., van der Toorn, M., Liu, F., Guo, F., Baty, C.J., Karlsson, J.M., Watkins, S.C., Kim, H.P., Wang, X., Lee. J.S., Postma, D.S., Kauffman, H.F., and Choi, A.M. 2007. Mitochondrial localization and function of heme oxygenase-1 in cigarette smoke-induced cell death. Am. J. Respir. Cell. Mol. Biol. 36, 409-417.

Smith, M.A., Kutty, R.K., Richey, P.L., Yan, S.D., Stern, D., Chader, G.J., Wiggert, B., Petersen, R.B., and Perry, G. 1994. Heme oxygenase-1 is associated with the neurofibrillary pathology of Alzheimer's disease. Am. J. Pathol. 145, 42–47.

Smith, A.F., and Loo, G. Upregulation of haeme oxygenase-1 by zinc in HCT-116 cells. 2012. Free Radic. Res. 46, 1099-1107.

Søfteland, L., Holen, E., and Olsvik, P.A. 2010. Toxicological application of primary hepatocyte cell cultures of Atlantic cod (*Gadus morhua*)—effects of BNF, PCDD and Cd. Comp. Biochem. Physiol. C Toxicol. Pharmacol. 151, 401-411.

Song, M.O. and Freedman, J.H. 2005. Expression of copper-responsive genes in HepG2 cells. Mol. Cell. Biochem. 279, 141-147.

Souza, V., Bucio, L., and Gutierrez-Ruiz, M.C. 1997. Cadmium uptake by a human hepatic cell line (WRL-68 cells). Toxicology 120, 215-220.

Stangl, K., Gunter, C., Frank, T., Lorenz, M., Meiners, S., Ropke, T., Stelter, L., Moobed, M., Baumann, G., Kloetzel, P.M., and Stangl, V. 2002. Inhibition of the ubiquitin-proteasome pathway induces differential heat-shock protein response in cardiomyocytes and renders early cardiac protection. Biochem. Biophys. Res. Commun. 291, 542-549.

Stewart, D., Killeen, E., Naquin, R., Alam, S., and Alam, J. 2003. Degradation of transcription factor Nrf2 via the ubiquitin-proteasome pathway and stabilization by cadmium. J. Biol. Chem. 278, 2396-2302.

Su, P.F., Hu, Y.J., Ho, I.C., Cheng, Y.M. and Lee, T.C. 2006. Distinct gene expression profiles in immortalized human urothelial cells exposed to inorganic arsenite and its methylated trivalent metabolites. Environ. Health Perspect. 114, 394-403.

Sun, Y. and MacRae, T. H. 2005. Small heat shock proteins: molecular structure and chaperone function. Cell. Mol. Life Sci. 62, 2460-2476.

Suzuki, H., Tashiro, S., Sun, J., Doi, H., Satomi, S., and Igarashi, K. 2003. Cadmium induces nuclear export of Bach1, a transcriptional repressor of heme oxygenase-1 gene. J. Biol. Chem. 278, 49246-49253.

Takahashi, M., Dore, S., Ferris, C.D., Tomita, T., Sawa, A., Wolosker, S.S., and Snyder, S.H. 2000. Amyloid precursor proteins inhibit heme oxygenase activity and augment neurotoxicity in Alzheimer's disease. Neuron 28, 461-473.

Takeda, K., Fujita, H., and Shibahara, S. 1995. Differential control of the metal-mediated activation of the human heme oxygenase-1 and metallothionein IIA genes. Biochem. Boiphys. Res. Commun. 207, 160-167.

Taketani, S., Kohno, H., Yoshinaga, T., and Tokunaga, R. 1988. Induction of heme oxygenase in rat hepatoma cells by exposure to heavy metals and hyperthermia. Biochem. Int. 17, 665-672.

Taketani, S., Kohno, H., Yoshinaga, T., and Tokunaga, R. 1989. The human 32-kDa stress protein induced by exposure to arsenite and cadmium ions is heme oxygenase. FEBS Lett. 245, 173-176.

Tanaka, S., Akaike, T., Fang, J., Beppu, T., Ogawa, M., Tamura, F., Miyamoto, Y., and Maeda, H. 2003. Antiapoptotic effect of haem oxygenase-1 induced by nitric oxide in experimental solid tumour. Br. J. Cancer 88, 902-909.

Templeton, D.M. and Liu, Y. 2013. Effects of cadmium on the actin cytoskeleton in renal mesangial cells. Can. J. Physiol. Pharmacol. 91, 1-7.

Tenhunen, R., Marver, H.S., and Schmid, R. 1968. The enzymatic conversion of heme to bilirubin by microsomal heme oxygenase. Proc. Natl. Acad. Sci. USA 61, 748-755.

Thevenod, F. and Friedmann, J.M. 1999. Cadmium-mediated oxidative stress in kidney proximal tubule cells induces degradation of Na+/K+-ATPase through proteasomal and endo-/lysosomal proteolytic pathways. FASEB J. 13, 1751-1761.

Trakshel, G.M., Ewing, J.F., and Maines, M.D. 1991. Heterogeneity of haem oxygenase 1 and 2 isoenzymes. Rat and primate transcripts for isoenzyme 2 differ in number and size. Biochem. J. 275 (Pt 1), 159-164.

Tonkiss, J., and Calderwood, S.K. 2005. Regulation of heat shock gene transcription in neuronal cells. Int. J. Hyperthermia. 21, 433-444.

Tsou, T.C., Tsai, F.Y., Hseih, Y.W., Li, L.A., Yeh, S.C., and Chang, L.W. 2005. Arsenite induces endothelial cytotoxicity by down-regulation of vascular endothelial nitric oxide synthase. Toxicol. Appl. Pharmacol. 208, 277-284.

Turkseven, S., Kruger, A., Mingone, C.J., Kaminski, P., Inaba, M., Rodella, L.F., Ikehara, S., Wolin, M.S., and Abraham, N.G. 2005. Antioxidant mechanism of heme oxygenase-1 involves an increase in superoxide dismutase and catalase in experimental diabetes. Am. J. Physiol. Heart Circ. Physiol. 289, H701-707.

Turner, C.P., Panter, S.S., and Sharp, F.R. 1999. Anti-oxidants prevent focal rat brain injury as assessed by induction of heat shock proteins (HSP70, HO-1/HSP32, HSP47) following subarachnoid injections of lysed blood. Brain Res. Mol. Brain. Res. 65, 87-102.

Uppu, R.M., Murthy, S., Pryor, W., and Narasimham, P.L. 2010. Free Radicals and Antioxidant Protocols, Methods in Molecular Biology. Humana Press Chapter 17, 285-307.

Van Montfort, R.L., Basha, E., Friedrich, K.L., Slingsby, C., and Vierling, E. 2001. Crystal structure and assembly of a eukaryotic small heat shock protein. Nat. Struct. Biol. 8, 1025-1030.

Vargas, H., Castillo, C., Posadas, F., and Escalante, B. 2003. Acute lead exposure induces renal haeme oxygenase-1 and decreases urinary Na+ excretion. Hum. Exp. Toxicol. 22, 237-44.

Voellmy, R. 2004. On mechanisms that control heat shock transcription factor activity in metazoan cells. Cell Stress Chaperones. 9, 122-133.

Voyer, J. and Heikkila, J.J. 2008. Comparison of the effect of heat shock factor inhibitor, KNK437, on heat shock- and chemical stress-induced hsp30 gene expression in *Xenopus laevis* A6 cells. Comp. Biochem. Physiol. A Mol. Integr. Physiol. 151, 253-261.

Waisberg, M., Pius, J., Hale, B., and Beyersmann, D. 2003. Molecular and cellular mechanisms of cadmium carcinogenesis. Toxicology 192, 95-117.

Walcott, S.E. and Heikkila, J.J. 2010. Celastrol can inhibit proteasome activity and upregulate the expression of heat shock protein genes, *hsp30* and *hsp70*, in *Xenopus laevis* A6 cells. Comp. Biochem. Physiol. A. Mol. Integr. Physiol. 156, 285-293.

Wang, Z., Chin, T.A., and Templeton, D.M. 1996. Calcium-independent effects of cadmium on actin assembly in mesangial and vascular smooth muscle cells. Cell Motil. Cytoskeleton 33, 208-222.

Wang, Y., Gu, Y., Qin, G., Zhong, L., and Meng, Y. 2013. Curcumin ameliorates the permability of the blood-brain barrier during hypoxia by upregulating heme oxygenase-1 expression in brain microvascular endothelial cells. J. Mol. Neurosci. 51, 344-351.

Was, H., Cichon, T., Smolarczyk, R., Rudnicka, D., Stopa, M., Chevalier, C., Leger, J.J., Lackowska, B., Grochot, A., Bojkowska, K., Ratajska, A., Kieda, C., Szala, S., Dulak, J., and Jozkowicz, A. 2006. Overexpression of heme oxygenase-1 in murine melanoma: increased proliferation and viability of tumor cells, decreased survival of mice. Am. J. Pathol. 169, 2181-2198.

Waters, E.R., Lee, G.J., Vierling, E. 1996. Evolution, structure and function of the small heat shock proteins in plants. J. Exp. Bot. 47, 325-338.

Wilkinson, K.D., Urban, M.K., and Haas, A.L. 1980. Ubiquitin is the ATP-dependent proteolysis factor I of rabbit reticulocytes. J. Biol. Chem. 255, 7529–7532.

Williams, C.R, and Gallagher, E.P. 2013. Effects of cadmium on olfactory mediated behaviors and molecular biomarkers in coho salmon (*Oncorhynchus kisutch*). Aquat. Toxicol. 140-141, 295-302.

Wotton, D., Freeman, K., and Shore, D. 1996. Multimerization of Hsp42p, a novel heat shock protein of *Saccharomyces cerevisiae*, is dependent on a conserved carboxyl- terminal sequence. J. Biol. Chem. 271, 2717-2723.

Woolfson, J.P. and Heikkila, J.J. 2009. Examination of cadmium-induced expression of the small heat shock protein gene, *hsp30*, in *Xenopus laevis* A6 kidney epithelial cells. Comp. Biochem. Physiol. A Mol. Integr. Physiol. 152, 91-99.

Wu, W.T., Chi, K.H., Ho, F.M., Tsao, W.C., and Lin, W.W. 2004. Proteasome inhibitors up-regulate haem oxygenase-1 gene expression: requirement of p38 MAPK (mitogen-activated protein kinase) activation but not of NF-kappaB (nuclear factor kappaB) inhibition. Biochem. J. 379, 587-593.

Yachie, A., Niida, Y., Wada, T., Igarashi, N., Kaneda, H., Toma, T., Ohta, K., Kasahara, Y., and Koizumi, S. 1999. Oxidative stress causes enhanced endothelial cell injury in human heme oxygenase-1 deficiency. J. Clin. Invest. 103, 129-135.

Yamamoto, N., Izumi, Y., Matsuo, T., Wakita, S., Kume, T., Takada-Takatori, Y., Sawada, H., and Akaike, A. 2010. Elevation of heme oxygenase-1 by proteasome inhibition afforbs dopaminergic neuroprotection. J. Neurosci. Res. 88, 1934-1942.

Yang, G., Nguyen, X., Ou, J., Rekulapelli, P., Stevenson, D.K., and Dennery, P.A. 2001. Unique effects of zinc protoporphyrin on HO-1 induction and apoptosis. Blood 97, 1306-1313.

Yang, H., Landis-Piwowar, K.R., Chen, D., Milacic, V., and Dou, Q.P. 2008. Natural compounds with proteasome inhibitory activity for cancer prevention and treatment. Curr. Protein Pept. Sci. 9, 227 - 239.

Yang, Y., Kitagaki, J., Wang, H., Hou, D., and Perantoni, A.O. 2009. Targeting the ubiquitin-proteasome system for cancer therapy. Cancer Sci. 100, 24-28.

Yoshida, T., Biro, P., Cohen, T., Muller, R.M., and Shibahara, S. 1988. Human heme oxygenase cDNA and induction of its mRNA by hemin. Eur. J. Biochem. 171, 457-461.

Young, J.T.F. and Heikkila, J.J. 2010. Proteasome inhibition induces *hsp30* and *hsp70* gene expression as well as the acquisition of thermotolerance in *Xenopus laevis* A6 cells. Cell Stress and Chaperones 15, 323-334.

Young, J.T.F., Gauley, J., and Heikkila, J.J. 2009. Simultaneous exposure of *Xenopus* A6 kidney epithelial cells to concurrent mild sodium arsenite and heat stress results in enhanced *hsp30* and *hsp70* gene expression and the acquisition of thermotolerance. Comp. Biochem. Physiol. A. Mol. Int. Physiol. 153, 417-424.

Yu, X., Hong, S., and Faustman, E.M. 2008. Cadmium-induced activation of stress signaling pathways, disruption of ubiquitin-dependent protein degradation and apoptosis in primary rat Sertoli cell-gonocyte cocultures. Toxicol. Sci. 104, 385-396.

Yu, X., Robinson, J.F., Sidhu, J.S., Hong, S., and Faustman, E.M. 2010. A system-based comparison of gene expression reveals alterations in oxidative stress, disruption of

ubiquitin-proteasome system and altered cell cycle regulation after exposure to cadmium and methylmercury in mouse embryonic fibroblast. Toxicol. Sci. 114, 356-377.

Yu, X., Robinson, J.F., Sidhu, J.S., Hong, S., and Faustman, E.M. 2010. A system-based comparison of gene expression reveals alterations in oxidative stress, disruption of ubiquitin-proteasome system and altered cell cycle regulation after exposure to cadmium and methylmercury in mouse embryonic fibroblast. Toxicol. Sci. 114, 356-377.

Yu, X., Sidhu, J.S., Hong, S., Robinson, J.F., Ponce, R.A., and Faustman, E.M. 2011. Cadmium induced p53-dependent activation of stress signaling, accumulation of ubiquitinated proteins, and apoptosis in mouse embryonic fibroblast cells. Toxicol. Sci. 120, 403-412.

Zhong, M., Orosz, A., and Wu, C. 1998. Direct sensing of heat and oxidation by *Drosophila* heat shock transcription factor. Mol. Cell. 1, 101-108.